Differential Quantitative Proteomics of Platelets and Extracellular Vesicles in Patients with Diabetes Mellitus

Dissertation

for the acquisition of the academic degree

Doctor rerum naturalium (Dr. rer. nat.)

at the

Faculty of Mathematics, Informatics and Natural Science

Department of Chemistry

University of Hamburg

Submitted by

Rosa Haghiri Limoudehi, M. Sc.

From Rasht, Iran

Hamburg

2023

Supervisor: Prof. Dr. Hartmut Schlüter

Co-supervisor: Dr. Hannah Voß

Evaluators for the Dissertation:

Prof. Dr. Hartmut Schlüter

PD Dr. Markus Perbandt

In the Presence of the Committee Members:

Prof. Dr. Hartmut Schlüter

Prof. Dr. Ralph Holl

Prof. Dr. Dr. Christian Betzel

Date of Disputation:

01.03.2024

This study was conducted and analyzed from April 2021 to December 2023 in the laboratories of Prof. Dr. Hartmut Schlüter and Prof. Dr. Dr. Thomas Renné at the Institute for Clinical Chemistry and Laboratory Medicine, University Medical Centre Eppendorf, Hamburg (UKE), under the supervision of Prof. Dr. Hartmut Schlüter in the Mass Spectrometry Proteomics Group.

List of Posters

1. The International Society on Thrombosis and Haemostasis (ISTH) 2022: Differential quantitative proteomics of platelets in patients with diabetes mellitus

2. The International Society on Thrombosis and Haemostasis (ISTH) 2022: Hyperglycaemia enhances platelet degranulation and microparticle shedding: a novel mechanism underlying thrombotic complications in diabetes

Table of Contents

List of Abbreviations

A2M	Alpha-2-macroglobulin
ACN	Acetonitrile
ADP	Adenosine diphosphate
AGEs	Advanced glycation end products
Akt	Protein kinase B
AmbiCA	Ammonium hydrogen carbonate
ANOVA	One-way analysis of variance
ANXA1	Annexin A1
AP-2	Adaptor protein complex 2
ApoER2	ApoE receptor 2
APP	Amyloid precursor protein
ATP2C1	ATPase secretory pathway Ca^{2+} transporting 1
BIN2	Bridging integrator 2
CAD	Coronary artery disease
cAMP	Cyclic adenosine monophosphate
CapZ beta	F-actin-capping protein subunit beta
CDG	Congenital disorders of glycosylation
CFH	Complement factor H
cGMP	Cyclic guanosine monophosphate
CHC1	Clathrin heavy chain 1
CID	Collision-induced dissociation
CRP	Collagen-related peptide
CVDs	Cardiovascular diseases

List of Abbreviations

CVX	Convulxin
Da	Dalton
DAB2	Adapter protein disabled-2
Dab2-pSer24	Dab2-serine 24 phosphorylation
Dab2-pSer723	Dab2-serine 723 phosphorylation
DB	Digestion buffer
DC	Direct current
DDA	Data-Dependent Acquisition
DIA	Data-Independent Acquisition
DKA	Diabetic ketoacidosis
DKD	Diabetic kidney disease
DM	Diabetes mellitus
DMSO	Dimethyl sulfoxide
DN	Diabetic nephropathy
DR	Diabetic retinopathy
DTT	Dithiothreitol
ECM	Extracellular matrix
eGFR	Estimated glomerular filtration rate
EGTA	Ethylene glycol bis(beta-aminoethyl ether)-N,N,N',N'-tetraacetic acid
EI	Electron ionization
ER	Endoplasmic reticulum
ESI	Electrospray ionization
ETD	Electron transfer dissociation
EThcD	Electron-transfer/higher-energy collision dissociation
EVs	Extracellular vesicles
EXOC3	Exocyst complex component 3

List of Abbreviations

EXOC3L2	EXOC3-like 2
EXOC3L4	EXOC3-like protein 4
FA	Formic acid
FASP	Filter-aided sample preparation
GNAS	Guanine nucleotide-binding protein G(s) subunit alpha isoforms Xlas
GP9	Platelet glycoprotein IX
GPCRs	G-protein-coupled receptors
GPIb-IX-V	Glycoprotein Ib-IX-V-receptor
GPIbβ	Platelet glycoprotein Ibβ
GPVI	Glycoprotein VI
GRK5	G protein-coupled receptor kinase 5
GSK3	Glycogen synthase kinase 3
GTP	Guanosine triphosphate
GUCY1A3	Guanylate cyclase soluble subunit alpha-3
GWAS	Genome-wide association studies
GYG1	Elevated levels of glycogenin-1
H_2O_2	Hydrogen peroxide
HbA1c	Hemoglobin A1c
HCD	Higher-energy C-trap dissociation
HCL	Hydrochloric acid
HDL	High-density lipoprotein
HEPES	4-(2-hydroxyethyl)-1-piperazineethanesulfonic acid
HNPs	Human neutrophil peptides
IAA	Iodoacetamide
IL-1β	Interleukin-1 beta

List of Abbreviations

IL-6	Interleukin-6
KCl	Potassium Chloride
KO	Knockout
LC-MS/MS	Liquid chromatography tandem mass spectrometry
LDL	Low-density lipoprotein
LFQ	Label-Free Quantification
LW/BW	Liver weight-to-body weight ratio
m/z	mass-to-charge ratios
$MgCl_2$	Magnesium chloride
mGPDH	Glycerol-3-phosphate dehydrogenase, mitochondrial
MI	Myocardial infarction
MICOS	Mitochondrial contact site and cristae organizing system
MIF	Macrophage migration inhibitory factor
MINK1	Misshapen/Nck-interacting kinase (NIK)–related kinase 1
MKs	Megakaryocytes
MPV	Mean platelet volume
MS	Mass spectrometry
MSCs	Mesenchymal stem cells
MVs	Microvesicles
NaCl	Sodium chloride
NaH_2PO_4	Sodium Dihydrogen Phosphate
NaOH	Sodium hydroxide
NF-κB p65	Transcription factor p65
NH_4HCO_3	Ammonium bicarbonate
NO	Nitric oxide
NOX1	NADPH oxidase 1

List of Abbreviations

NOX2	NADPH oxidase 2
OGTT	Oral glucose tolerance test
PA	Phosphatidic acid
PAD	Peripheral artery disease
PAI-1	Plasminogen activator inhibitor-1
PAR4	Protease-activated receptor 4
PBP	Platelet basic protein
PBS	Phosphate buffered saline
PDE3A	cGMP-inhibited 3',5'-cyclic phosphodiesterase A
PDEVs	Platelet-derived EVs
PDI	Protein disulfide isomerase
PDIA3	Protein disulfide-isomerase A3
PEDF	Pigment epithelium-derived factor
PF4	Platelet factor 4
PFA	Paraformaldehyde
PFP	Platelet-free plasma
PGE1	Prostaglandin E1
PGRN	Progranulin
PI3K	Phosphoinositide 3-kinase
PKC	Protein Kinase C
PKCα	Protein Kinase C α
PKD	Protein kinase D
PLT-Exos	Platelet-derived exosomes
PPP	Platelet-poor plasma
PRP	Platelet-rich plasma
PRRs	Pattern recognition receptors

List of Abbreviations

PS	Phosphatidylserine
PTB	Phosphotyrosine-binding domain
PTMs	Post-translational modifications
PVDF	Polyvinylidene difluoride
R^2	R-squared
Rac1	Ras-related C3 botulinum toxin substrate 1
Rac2	Ras-related C3 botulinum toxin substrate 2
RC	Rhodocytin
rHDL	Reconstituted HDL
RIPA	Radioimmunoprecipitation assay
ROCK	Rho-associated coiled-coil containing kinase
ROS	Reactive oxygen species
rPGRN	Recombinant human PGRN
SDC	Sodium deoxycholate
SDS	Sodium dodecyl sulfate
SDS-PAGE	SDS-polyacrylamide gel electrophoresis
sGC	Soluble guanylyl cyclase
SH3	Src homology 3
siRNA	Small-interfering RNA
SIRT2	Sirtuin-2
SP3	Single-Pot, Solid-Phase, Sample-preparation
SRE	Splicing regulatory element
T1DM	Type 1 diabetes mellitus
T2DM	Type 2 diabetes mellitus
TG	Triglyceride
TGRL	Triglyceride-rich lipoproteins

List of Abbreviations

TNF-α	Tumor necrosis factor-alpha
VLDLR	Very low-density lipoprotein receptor
vWF	von Willebrand factor
WT	Wild-type
XLαs	Extra-large α-subunit

Abstract

Diabetes mellitus (DM) is a metabolic disorder characterized by insufficient regulation of glucose levels in the bloodstream. The prevalence of diabetes is increasing globally and is associated with various complications, including an increased risk of cardiovascular diseases (CVDs). Platelet dysfunction is a key factor in the development of these complications. Platelets release extracellular vesicles (EVs), which play a role in inflammation, thrombosis, and the transmission of biological information. In diabetes, platelet-EVs can promote endothelial dysfunction and contribute to the progression of diabetic complications. By extracting platelet proteins and studying their proteome, as well as the proteome of plasma-derived EVs, valuable insights can be gained into the molecular mechanisms that underlie platelet hyperactivity, thrombus formation, and complications related to diabetes. A proper protein extraction method is essential for reliable platelet proteomics research. The SDS-SP3 method was chosen due to its cost-effectiveness and high data reproducibility for extracting platelet proteins. The platelet proteome changes in individuals with diabetes compared to healthy controls, with distinct patterns observed in different age groups. In young individuals with diabetes, a significant downregulation of GUCY1A3 and GNAS compared to controls was observed. These downregulated proteins, which are involved in ion channel function in the vascular endothelium, may contribute to platelet hyperactivity and increase the risk of thrombus formation in this group. On the other hand, the upregulation of C6 and C8G suggests enhanced complement activation in young-aged diabetes, potentially leading to increased platelet aggregation. In middle-aged individuals with diabetes, PF4, F12, and A2M are significantly upregulated and are involved in fibrin clot formation. The upregulation of PF4 and F12 may increase platelet activation and elevate the risk of CVDs in this group. However, the upregulation of A2M may act as a compensatory mechanism to reduce platelet activation. In old-aged individuals with diabetes, the downregulation of GMPPA and ALG5, which are involved in N-glycan precursor biosynthesis, may increase the risk of thrombus formation. The analysis of plasma-derived EVs in middle-aged diabetes patients highlighted the presence of dysregulated proteins that may impact platelet function and thrombus formation. Specifically, proteins involved in focal adhesion, including RAC2, ROCK2, and RELN, were significantly downregulated in the EVs

proteome of middle-aged individuals with diabetes compared to controls. The low level of RAC2 may serve as a compensatory mechanism to reduce vascular oxidative stress and inflammation in diabetes patients. Additionally, low levels of ROCK2 and RELN may act as compensatory mechanisms to reduce the risk of thrombus formation in this group. On the other hand, in the EVs proteome of diabetes patients, JAK2, CAPZB, VPS45, and PPBP are significantly upregulated and show enrichment in the hemostasis pathway. Among these proteins, JAK2 and PPBP may enhance platelet activation, thereby increasing the risk of thrombus formation. The study of the platelet membrane fraction proteome indicated a significant downregulation of GPIBB and GP9 in diabetes compared to controls, which may be related to the bleeding complications in diabetes patients. These findings may contribute to the development of novel therapeutic approaches and biomarkers for diabetes patients across various age groups, as well as their related complications.

Zusammenfassung

Diabetes mellitus (DM) ist ein Stoffwechselzustand, der sich durch unzureichende Regulation der Blutzuckerspiegel auszeichnet. Die weltweite Häufigkeit von Diabetes nimmt zu und steht in Verbindung mit verschiedenen Komplikationen, einschließlich eines erhöhten Risikos für kardiovaskuläre Erkrankungen (KVDs). Eine Schlüsselrolle bei der Entwicklung dieser Komplikationen spielt die Dysfunktion der Blutplättchen. Blutplättchen setzen extrazelluläre Vesikel (EVs) frei, die bei Entzündungen, Thrombosen und der Übertragung von biologischer Information eine Rolle spielen. Bei Diabetes wurde beobachtet, dass Plättchen-EVs eine wesentliche Rolle bei der Entwicklung von endothelialer Dysfunktion und der Fortschreitung diabetischer Komplikationen spielen. Durch die Extraktion von Proteinen aus Blutplättchen und die anschließende Analyse ihres Proteoms zusammen mit dem Proteom von plasmaderivierten EVs können signifikante Erkenntnisse über die molekularen Wege gewonnen werden, die der Plättchenüberaktivität, der Thrombusbildung und den mit Diabetes zusammenhängenden Komplikationen zugrunde liegen. Eine geeignete Proteingewinnungstechnik ist entscheidend, um die Zuverlässigkeit der Proteomik-Forschung an Blutplättchen zu gewährleisten. Die SDS-SP3-Methode wurde aufgrund ihrer kostengünstigen Eigenschaften und der hohen Datenreproduzierbarkeit für die Extraktion von Blutplättchenproteinen ausgewählt. Das Proteom der Blutplättchen verändert sich bei Personen mit Diabetes im Vergleich zu gesunden Kontrollpersonen, wobei in verschiedenen Altersgruppen unterschiedliche Muster beobachtet werden. Bei jungen Personen mit Diabetes wurde eine signifikante Herunterregulierung von GUCY1A3 und GNAS im Vergleich zu Kontrollpersonen festgestellt. Diese herunterregulierten Proteine, die an der Ionkanalfunktion in der Gefäßendothelium beteiligt sind, könnten zur übermäßigen Aktivität von Blutplättchen beitragen und das Risiko für die Bildung von Thromben in dieser Gruppe erhöhen. Andererseits deutet die beobachtete Überexpression von C6 und C8G bei jungen Personen mit Diabetes auf eine gesteigerte Aktivierung des Komplementsystems hin, was zu einer verstärkten Aggregation von Blutplättchen führen kann. Bei mittelalten Personen mit Diabetes ist die Expression von PF4, F12 und A2M deutlich erhöht, was auf ihre Beteiligung am Prozess

der Bildung von Fibringerinnseln hinweist. Die Hochregulierung von PF4 und F12 könnte die Aktivierung von Blutplättchen verstärken und das Risiko von kardiovaskulären Erkrankungen in dieser Gruppe erhöhen. Dennoch könnte die Überexpression von A2M als kompensatorischer Mechanismus dienen, um die Aktivierung von Blutplättchen abzuschwächen. Bei älteren Personen mit Diabetes könnte die Herunterregulierung von GMPPA und ALG5, die an der Biosynthese von N-Glykan-Vorläufern beteiligt sind, das Risiko der Thrombusbildung erhöhen. Die Analyse von plasmaderivierten EVs bei Patienten mittleren Alters mit Typ-2-Diabetes ergab das Vorhandensein von dysregulierten Proteinen, die die Plättchenfunktion und die Thrombusbildung beeinflussen könnten. Die proteomische Analyse von EVs bei Personen mittleren Alters mit Diabetes zeigte eine signifikante Herunterregulierung von Proteinen im Zusammenhang mit fokaler Adhäsion, einschließlich RAC2, ROCK2 und RELN, im Vergleich zur Kontrollgruppe. Das geringe Niveau von RAC2 könnte als kompensatorischer Mechanismus dienen, um oxidativen Stress und Entzündungen in den Blutgefäßen von Diabetespatienten zu verringern. Darüber hinaus könnten niedrige levels von ROCK2 und RELN als kompensatorische Mechanismen in dieser Population fungieren, um die Wahrscheinlichkeit von Thrombusbildung zu verringern. Andererseits zeigt das Proteom von EVs bei Diabetespatienten eine deutliche Hochregulierung von JAK2, CAPZB, VPS45 und PPBP, die im Hämostase-Weg angereichert sind. Von diesen Proteinen könnten JAK2 und PPBP das Risiko einer Thrombusbildung erhöhen, indem sie die Plättchenaktivierung verstärken. Die Analyse des Proteoms der Thrombozytenmembranfraktion zeigte eine signifikante Herunterregulierung von GPIBB und GP9 bei Diabetes im Vergleich zu Kontrollen, was mit diabetesbedingten Blutungskomplikationen in Verbindung gebracht werden könnte. Diese Erkenntnisse könnten zur Entwicklung neuer Behandlungsmethoden und Biomarker für Diabetespatienten jeden Alters sowie deren assoziierte Begleiterkrankungen führen.

1. Introduction

1.1. Diabetes

Diabetes is a term used to describe a group of medical conditions that interfere with the body's ability to control blood glucose levels effectively. In 2017, about 425 million had diabetes, a number predicted to reach 629 million by 2045 [1]. The effects of long-term hyperglycemia on the body's tissues and organs include diabetic nephropathy, diabetic retinopathy, coronary heart disease, stroke, and other vascular complications. These complications not only increase the mortality and disability of diabetic patients but also impose a significant financial burden on them. According to previous studies, patients with type 2 diabetes (T2DM) have an increased risk of cardiovascular complications, which further complicates the prognosis of the disease [2]. Both T2DM and type 1 diabetes mellitus (T1DM) are heterogeneous diseases with a wide range of clinical presentations and disease progressions. Although classification is crucial for selecting a form of therapy, some patients cannot be clearly categorized as having type 1 or type 2 diabetes at the time of diagnosis. The traditional beliefs that type 2 diabetes exclusively affects adults and type 1 diabetes only affects children are no longer true, as both diseases can affect people of all ages. Polyuria/polydipsia is the hallmark symptom of type 1 diabetes in children, and diabetic ketoacidosis (DKA) is present in about one-third of cases [3]. The onset of type 1 diabetes in adults may vary more compared to children, and they may not exhibit the classic symptoms seen in children. Patients with T2DM, especially those from ethnic minorities, might exhibit DKA [4].

1.1.1. Etiology

There are several modifiable and non-modifiable risk factors that can influence the likelihood of acquiring diabetes. The main non-modifiable risk factors for diabetes are increasing age, some specific ethnicities, lower socioeconomic circumstances, male gender, history of smoking, history of poor blood glucose management, pancreatic disorders, genetic susceptibility, and a family history of the disease [5]. On the other

hand, modifiable risk factors include smoking, abnormal cholesterol levels, physical inactivity, obesity, and hypertension [6], [7].

In humans, glucose reserves are stored as the polymer glycogen. The liver and muscle tissues have the highest concentrations of glycogen. The peptide hormones insulin and glucagon play a significant role in the regulation of glycogen and, consequently, glucose. Insulin and glucagon are produced by beta cells and alpha cells, respectively, in the pancreatic Islet of Langerhans [8]. In the case of diabetes mellitus (DM), insulin is either absent or not functioning properly, leading to hyperglycemia [9]. Although the exact causes of type 2 diabetes are unknown, patients do not experience autoimmune destruction of cells or have any of the other known causes of diabetes. Patients with T2DM generally tend to be overweight or obese, but not always. Patients who do not meet the traditional weight criteria for obesity or overweight may have an elevated percentage of body fat primarily located in the abdominal area [10]. Genetics and lifestyle have a complicated role in T2DM. There is unambiguous proof that T2DM has a stronger hereditary profile than T1DM. Most patients with the disease have at least one parent who also has type 2 diabetes [11]. To date several polymorphisms have been identified that either increase the incidence or provide protection for T2DM. These genes encode proteins that have a role in a number of DM-related pathways, such as pancreatic development, insulin synthesis, secretion, and development, amyloid accumulation in beta cells, insulin resistance, and gluconeogenesis regulatory dysfunction [12], [13]. The majority of genetic loci linked to T2DM have been detected in populations of European ancestry. A recent meta-analysis of genome-wide association studies (GWAS) of almost 900,000 individuals of European ancestry identified >240 loci impacting T2DM risk [14].

1.1.2. Pathophysiology

In the pathophysiology of T2DM, insulin resistance and insulin secretion deficiencies play a key role [15]. β-cells are prompted to secrete more insulin under conditions of insulin resistance than under conditions in which insulin sensitivity is normal [16]. Hyperglycemia and, subsequently, T2DM are caused by insufficient insulin secretion, especially when there is insulin resistance, glucolipotoxicity, and inflammation associated with obesity [17]. In a prior investigation, the insulin sensitivity index did not

substantially predict incident pre-diabetes or T2DM after accounting for the amount of visceral adipose tissue. It is worth noting that insulin secretion was related to the progression to pre-diabetes or T2DM after a mean of 2.5 years [18]. There are mixed findings for the pathogenesis of T2DM in terms of impaired insulin secretion and insulin resistance. Cross-sectional investigations conducted in Shanghai suggested that patients with T2DM had worse β-cell function than those with pre-diabetes, while insulin sensitivity was similar among the groups [19], [20].

According to the history of T1DM, environmental factors in genetically susceptible individuals are more likely to cause autoimmunity against several islet β-cells antigens, which are driven by T cells [21]. Recent research describes the role of β-cell-associated immunogenicity in addition to the auto-immune component. This role could potentially be linked to genetic or environmental factors. In fact, the susceptibility of islet β-cells causes cell stress and the production of neoantigens, which are targeted by the immune system [22].

1.1.3. Evaluation

Increased serum glucose levels (fasting glucose levels above 126 mg/dL, random glucose levels over 200 mg/dL, or hemoglobin A1c (HbA1c) value greater than 6.5%) either with or without antibodies to insulin and glutamic acid decarboxylase are used in the diagnosis of T1DM. For the early detection of T2DM, fasting glucose levels and HbA1c testing are helpful. A glucose tolerance test can be used to assess both fasting glucose levels and serum reaction to an oral glucose tolerance test (OGTT) if they are borderline. The development of T2DM is usually preceded by prediabetes, which can be diagnosed by impaired fasting blood glucose level (100 to 125 mg/dL) or impaired glucose tolerance (a 2-hour glucose level between 140 and 200 mg/dL after OGTT) [23], [24].

1.1.4. Microvascular and Macrovascular Complications

The root cause of the development of diabetic complications is exposure to a hyperglycemic environment, which triggers or accelerates various metabolic pathways, including the polyol pathway, the Protein Kinase C (PKC) pathway, and the formation of

advanced glycation end products (AGEs) [25]. AGEs, which are a diverse group of compounds, are created through irreversible non-enzymatic reactions between reducing sugars and proteins, lipids, or nucleic acids, a process called glycation [26]. AGEs can either be derived from exogenous sources such as food, or can be synthesized within the body through endogenous processes [27]. AGEs may induce changes in the extracellular matrix (ECM), which is the potential mechanism that could link to the consequences of inflammation-related diabetes, such as atherosclerosis [28]. In addition to atherosclerosis, the buildup of AGEs in the ECM is believed to play a significant role in other complications of diabetes, such as an elevated risk of renal failure and retinopathy [29].

Diabetes can cause higher mortality rates and numerous major complications such as renal issues, cardiovascular diseases (CVDs), blindness, and many other health concerns, that are expensive to manage and so result in decreasing the quality of life [1]. According to epidemiologic research, there is a strong correlation between vascular complications in diabetes [31], [30]. For instance, diabetic retinopathy (DR) is a strong predictor of stroke and CVDs and is highly linked to the risk of developing diabetic kidney disease (DKD) [31]. Although the exact mechanisms of hyperglycemia-induced vascular damage are complex and poorly understood, it is thought that elevated intracellular glucose levels enhance the production of reactive oxygen species (ROS), which changes a number of important downstream pathways such as polyol pathway flux, formation and activation of AGE, activation of PKC, and hexosamine pathway flux [32].

The development of macrovascular and microvascular complications is significantly impacted by the rising prevalence of diabetes and the increase in life years lived with the disease [33]. Typically, microvascular complications develop over several years [34]. Its etiology, development, and progression are considerably influenced by the synergistic effects of smoking, diabetes duration, dyslipidemia (low level of high-density lipoprotein (HDL) and often increased triglycerides), and hypertension. The interaction between genetic and environmental changes (diet, lifestyle) is a feasible mechanism for the development of microvascular complications in diabetes [35]. Cardiovascular outcomes have also been linked to microvascular disorders, particularly DKD and DR. Although DKD diagnosis, lower estimated glomerular filtration rate (eGFR), and higher albuminuria are all linked to the increased risk of CVDs. This indicates that diabetes complications, both macrovascular and microvascular, can occur together [36], [37], [38]. According to research on the co-occurrence of DKD and DR, decreased kidney function

is linked to higher rates of DR in both T1DM and T2DM [39]. Additionally, individual microvascular complications in T2DM patients demonstrate cardiovascular risk better than classic risk factors including blood pressure, HbA1c, and low-density lipoprotein (LDL)-cholesterol [40].

Macrovascular complications bear coronary artery disease (CAD, myocardial infarction, coronary revascularization, angina), cerebrovascular disease (CVD, stroke, transient ischaemic attack, carotid endarterectomy or stenting), peripheral artery disease (PAD, diabetic foot, amputation) and heart failure. Macrovascular complications can lead to various symptoms, such as angina, claudication, dyspnoea or weakness, which can significantly limit patients' physical abilities and their ability to interact with others. As a result, they may be at a higher risk of depression and experience a decline in their overall quality of life. The effect of microvascular complications on quality of life is less precise. In the early stages, retinopathy and nephropathy usually do not cause symptoms or limitations that would have a detrimental impact on quality of life. However, in later stages, such as blindness or end-stage renal disease, they can significantly impair a patient's well-being. Conversely, neuropathy is typically detected only when symptoms are present, which might account for the correlation between neuropathy and worse physical quality of life [41].

1.2. Platelet Development and Function

Platelets are anucleate blood cells (2–4 μm in diameter) [42] derived from mature megakaryocytes. The process of platelet formation can be divided into two stages. The initial stage involves the maturation and development of megakaryocytes (MKs), which takes several days to finish and requires specific growth factors for the MK. This stage involves nuclear proliferation and enlargement of the cytoplasm of the MK, leading to the accumulation of platelet-specific granules, cytoskeletal proteins, and enough membrane to complete the platelet assembly process. On the other hand, the second phase is relatively fast, taking just a few hours to complete. In this phase, MKs produce platelets by reorganizing their cytoplasm into proplatelets. These proplatelets then mature into preplatelets, which further undergo fission processes to form discoid platelets. In humans, it takes approximately five days for MKs to complete polyploidization, mature, and

release platelets [43], [44], [45]. Platelets have multiple functions with an average lifespan of 7–10 days in humans, after which platelets are removed from the bloodstream and are eliminated in the liver [46]. Platelets play a vital role in thrombus formation and hemostasis [47]. The presence of various blood components, including red blood cells, white blood cells, platelets, and plasma constituents, along with the shear force within blood vessels, prevents platelets from flowing in the central flow of the vessel. As a result, platelets are mainly found near the vessel wall. This specific location of platelets allows them to effectively and promptly respond to vascular injuries, thereby playing a crucial role in hemostasis [48]. When the blood vessel walls are damaged, components in the subendothelial extracellular matrix may bind to platelet surface receptors. For example, platelet glycoprotein Ib-IX-V-receptor (GPIb-IX-V) interacts with collagen-bound von Willebrand factor (vWF). This enables the interaction of glycoprotein VI (GPVI) with collagen and thereby the shift of integrins (integrin αIIbβ3 and integrin α2β1) to a high-affinity state [49], [50]. At this point, a structural transformation of platelets leads to the secretion of granule contents, which promotes platelet aggregation and platelet plug formation [51]. Platelets contain 3 types of granules with different functions: 1) α-granules, which are critical to normal platelet function and contain different proteins, growth factors (such as vascular endothelial growth factor, endostatin, thrombospondin-1), chemokines and cytokines including stromal-derived factor 1 α and Interleukin-8 [52], [53]. 2) Platelet δ-granules are critical to hemostasis and contain small molecules such as adenosine diphosphate (ADP), serotonin, polyphosphates, glutamate, and calcium [54]. 3) Platelet lysosomes contain various enzymes (such as α-fucosidase, β-glucoronidase, acid phosphatase, and β-galactosidase), which can lead to the degradation of glycoproteins, glycolipids, and glycosaminoglycans [55], [52]. The heterogeneity of circulating platelets in size, surface receptors, and age stems from differences in the platelet-producing megakaryocytes and environmental conditions of platelets. Therefore, the heterogeneity of circulating platelets can lead to the different responses of individual platelets to the same agonist. Consequently, they may form populations with specific phenotypes and their associated functional attributes [56], [57]. Larger platelets are more dynamic and contain more dense granules, leading to a stronger procoagulant effect and an increased likelihood of blood clots. Therefore, there may be a direct connection between the mean platelet volume (MPV) and the vascular complications associated with T2DM. However, it is important to note that an increase in MPV may also be a result of

thrombotic events caused by the rapid consumption of small platelets and the accelerated production of immature platelets by the bone marrow, known as reticulated platelets [58].

Pathological factors can change normal hemostasis and lead to clot formation and vessel occlusion in either the arteries or veins. Arterial thrombosis is caused by the formation of platelet aggregates around ruptured atherosclerotic plaques and endothelium after injury. Arterial thrombosis can lead to myocardial infarction (MI) and stroke, while venous thrombosis may occur either around an intact endothelial wall or under low shear flow [51], [59]. In addition to the role of platelets in hemostasis and thrombosis, platelets are suggested to have distinct roles in regulating and supporting immune responses and inflammatory reactions [60]. Herein, platelets have pattern recognition receptors (PRRs) that detect various components that enhance during infection. These components can either be pathogen-associated molecular patterns, which are microbial structures, or damage-associated molecular patterns, which are host-derived components. Platelets have distinct types of PRRs, including Toll-like receptors, C-type lectin receptors, and nucleotide-binding oligomerization domain-like receptors [61]. When pathogens or antigens bind to these receptors, it triggers platelet activation, differential release of granules, and interaction with leukocytes. Thus, platelets can perform the dual roles of thrombotic and immune cells [62], [61], [63].

1.3. Platelet Dysfunction in Diabetes

Hyperglycemia

Hyperglycemia is a key contributor to the various vascular abnormalities that lead to diabetic patients having a higher risk of blood clots (prothrombotic state) [64], [65]. Postprandial hyperglycemia, which can occur before a formal diabetes diagnosis, is a metabolic abnormality and an independent risk factor for CVDs in T2DM [66]. The detrimental effects of glucose fluctuations during the postprandial period may occur through mechanisms such as increased oxidative stress and endothelial dysfunction, which can both contribute to the activation of platelets [67], [68]. Santilli et al. suggested that newly diagnosed T2DM patients treated with acarbose, an α-glucosidase inhibitor that reduces postprandial hyperglycemia, experienced a significant decrease in platelet

activation [69]. Additionally, evidence suggests that an acute, short-term hyperglycemia increases platelet activation in T2DM patients, especially when exposed to high-shear stress, which increases the risk of arterial thrombosis. This is partly attributed to the acute enhancement of vWF in the bloodstream [70]. *In vitro* exposure of platelets from healthy individuals to glucose concentrations seen in DM patients resulted in reduced platelet adhesion and a decrease in GPIIIa expression on the platelets, suggesting that hyperglycemia per se decreases the adhesion potential of platelets rather than increasing it. Despite the decrease in GPIIIa levels, there was no notable increase in the soluble form of GPIIIa. This may be attributed to the antigen being better preserved or the significant involvement of GPIIIa derived from the endothelial cells in the intravital conditions [71].

Insulin resistance

Obesity and disruptions in lipid metabolism are important factors in the pathogenesis and development of insulin resistance, followed by T2DM [72]. Moreover, mitochondrial dysfunction can lead to insulin resistance, which can cause metabolic and cardiovascular morbidities [73]. Insulin has a direct influence on platelet functions *via* a functional insulin receptor located on the surface of platelets [74]. The reduced number and sensitivity of insulin receptors on platelets in T2DM patients can lead to platelet hyperactivation [75]. On the other hand, abnormal intracellular insulin signaling through the second messenger system can result in a decrease in platelet sensitivity to insulin [76], [77], [78]. A previous finding indicated that platelet counts, as well as BMI, HbA1c, and triglyceride levels, are all independent predictors of insulin resistance in non-obese patients with T2DM [79]. This statement highlights that the increased activity of platelets in individuals with insulin resistance and obesity cannot be attributed solely to these factors. In addition to these factors, hyperglycemia plays a role by promoting the glycation of platelet proteins (non-enzymatic glycosylation) and increasing their reactivity. Insulin normally acts to counteract platelet activation and thrombus formation. However, platelet reactivity can increase when there is insufficient insulin, which can be due to either insulin resistance or insulin deficiency. Endothelial dysfunction, a common complication of diabetes, can further promote platelet activation by decreasing the release of nitric oxide (NO) from capillary vessel cells. The activation of these events exacerbates blood vessel constriction and facilitates thrombus formation, which results in the

development of atherosclerosis. Therefore, platelet hyperactivity in individuals with insulin resistance and obesity is a complex phenomenon with multiple contributing factors [80], [81].

Oxidative stress

It has been reported that T2DM patients have elevated levels of oxidative stress. This increase in oxidative stress contributes to the activation of platelets and facilitates the response of platelet aggregation [82]. It has been found that oxidative stress can damage mitochondria, which can contribute to an increased risk of thrombosis. Additionally, a basal autophagy process plays an important role in normal platelet activation. In diabetic platelets, there is a substantial induction of mitophagy (above basal autophagy levels), which protects the platelets from apoptosis by removing damaged mitochondria in response to oxidative stress through JNK activation. This, in turn, reduces the risk of thrombosis [83].

Platelet hyperactivity can be triggered by increased oxidative stress, particularly in uncontrolled cases of T2DM, through three distinct mechanisms. The first mechanism involves the increase in the production of F2 isoprostane, a prostaglandin-like compound that serves as a marker of oxidative stress. The increased production of F2 isoprostane may intensify platelet response to agonists. The second mechanism is attributed to a reduction in the activity of endothelial NO synthase, leading to decreased NO production. Finally, the third mechanism involves an increase in the signaling of platelet receptors [81]. Platelet ROS production involves both NADPH oxidase 1 (NOX1) and NADPH oxidase 2 (NOX2) enzymes, but their roles differ. When platelets respond to collagen, NOX1 is the primary source of oxygen radicals, as shown in an *in vitro* study. Conversely, NOX2 is essential for activation by thrombin. Elevated levels of oxidative stress are exhibited by platelets from T2DM patients. This is due to the increased production of ROS, which is partially mediated by NOX2 activation, resulting in increased platelet aggregation [84], [85], [86]. While NOX1 and NOX2 both contribute to the production of ROS in platelets, the precise function of NOX1 in diabetic platelets is not well-established.

Dyslipidemia

T2DM patients are at a high risk of developing dyslipidemia, which involves a rise in triglycerides, an increase in LDL cholesterol, and a decrease in HDL cholesterol [87], [88]. It has been observed that both native HDL and reconstituted HDL (rHDL) can promote cholesterol efflux from platelets and influence platelet function, although the effect of rHDL on platelet cholesterol efflux is stronger than that of native HDL. A previous finding indicated that rHDL decreases platelet aggregation in patients with diabetes, partly by reducing the cholesterol content of platelet membranes [89]. It is well known that triglycerides are transported by triglyceride-rich lipoproteins (TGRL) in the bloodstream, which includes chylomicrons, very low-density lipoproteins, and their remnants [90]. Boulet et al. suggested that healthy platelets, when preincubated with large TGRL from T2DM patients, showed a significant increase in collagen-stimulated or thrombin-stimulated platelet aggregation *via* the activation of the arachidonic acid signaling pathway compared to those exposed to only subthreshold concentrations of collagen or thrombin. This increase in platelet aggregation may play a role in the development of atherothrombosis in T2DM patients. In contrast, large TGRL from healthy blood donors had no effect on platelet aggregation [91].

1.4. Extracellular Vesicles

Extracellular vesicles (EVs), including exosomes, microvesicles (MVs), and apoptotic bodies [92], are released by various cell types, including platelets, and can be found in body fluids, such as plasma [93]. Exosomes are produced through an endocytic process, whereas MVs are generated by budding and blebbing of the plasma membrane. On the other hand, apoptotic bodies are generated during the process of programmed cell death [94]. EVs exhibit distinct characteristics based on their size and cellular origin. Exosomes typically range in size from 40 to 100 nm, while the larger MVs have diameters between 100 and 500 nm. Apoptotic bodies, on the other hand, span from 500 nm to 2 μm. EVs serve as important mediators of cell-to-cell communication and play a role in both protective and pathologic effects within the body [95]. EVs have the ability to influence the target cell in various ways, including: 1) merging with the target cell and transferring their contents, 2) internalizing and releasing their contents through endocytosis, and 3)

binding to the target cell and transmitting signals [96]. By carrying specific cargo such as proteins, growth factors, protease inhibitors, lipids, sugars, adhesion integrins, and nucleic acids, EVs facilitate the transfer of information and molecules between cells, thereby influencing cellular processes and signaling pathways. Additionally, EVs play a role in regulating cellular homeostasis through their involvement in the removal of cellular contents [95].

1.4.1. Platelet-Derived Extracellular Vesicles in Thrombosis and Hemostasis

Platelets have the ability to release EVs under diverse conditions, including activation, shear stress, apoptosis, and storage [97], [98]. The precise proportion of platelet-derived EVs (PDEVs) is a topic of debate and can vary from 30% to 85%, with the majority of studies indicating higher percentages [97]. PDEVs have significant functions in both hemostasis and thrombosis [99]. PDEVs exhibit a procoagulant role, promoting clot formation by reducing clotting time and facilitating the production of thrombin, a crucial enzyme involved in blood coagulation. Additionally, aside from their procoagulant characteristics, PDEVs might possess anticoagulant properties. These differences could be attributed to the presence of various subsets of PDEVs [100]. The presence of negatively charged phospholipids, such as phosphatidylserine and phosphatidylethanolamine, on the surface of PDEVs provides an additional platform for the formation of coagulation cascade complexes [101]. Platelet-derived exosomes (PLT-Exos), the main subtype of EVs released by platelets, play a crucial role in intercellular communication. Studies indicate that the functions of PLT-Exos differ among various donors. In the case of healthy volunteers or mice, PLT-Exos can inhibit platelet aggregation and reduce inflammation in endothelial cells. However, in some patients, PLT-Exos can promote endothelial cell apoptosis and trigger an inflammatory response mediated by neutrophils. It is known that the levels of PLT-Exos increase upon platelet activation and contribute to the progression of atherothrombosis by transporting cargo to recipient cells [102].

1.4.2. Extracellular Vesicles in Diabetes Mellitus

EVs play a role in the pathological changes of insulin resistance, inflammation, and endothelial injury, and are involved in the development of DM and its complications. These complications include diabetic foot, cardiomyopathy, nephropathy, retinopathy, neuropathy, and atherosclerosis [103]. Wu et al. suggested that the protein profiles associated with inflammation in EVs are varied by diabetes status. EVs derived from diabetes patients possess an inflammatory protein cargo that can have functional effects on endothelial cells, leading to alterations in endothelial cell morphology and migration [104]. Increased levels of EVs have been reported in disease states characterized by a prothrombotic tendency, including thrombotic thrombocytopenic purpura. Additionally, individuals with cardiovascular risk factors like DM also exhibit elevated levels of EVs [105].

1.5. A General Overview of Mass Spectrometry

The emergence of genome sequencing and DNA microarray technologies in the 1990s paved the way for the "omics" era of research [106]. While the genome sequence and identified genes offer valuable insights, they provide an incomplete picture of an organism's comprehensive biological complexity. The proteome, on the other hand, exhibits significant diversity across different cells and over time, offering a profound description of biological phenotype. Post-translational modifications (PTMs) further contribute to the diversity of protein species, expanding beyond what is predicted by the genome alone. Mass spectrometry (MS)-based proteomics has wide-ranging applications, from descriptive to quantitative, and plays a pivotal role in systems biology initiatives and biomarker discovery for diagnostics. Recent advancements in MS technologies and sample preparation techniques have enhanced our understanding of the biological complexity across various sample types, including organelles, membranes, biofluids, tissues, and organs [107]. The basic concept of MS is to determine the mass of a molecule, which provides valuable information across various levels and types. Its underlying technique primarily focuses on ionizing molecules, involving the conversion of molecules from a solution to the gas phase. After the generation of ions, they are

focused into a beam and directed towards a collision cell where their dissociation can be induced. Following that, the mass analysis of the intact ions and/or their fragments is performed by evaluating their resulting mass-to-charge ratios (m/z) [108].

1.5.1. Peptide Ionization

Electron ionization (EI) is a preferred method for analyzing small (<1000 Da), nonpolar, and volatile compounds. It is classified as a hard ionization technique. In EI, the compound is ionized by electrons possessing approximately 70 electron volts of energy. The energy level is sufficient to produce reproducible mass spectra with numerous fragments. Due to the high internal energy transferred to the precursor molecules during this ionization process, the resulting mass spectra often do not contain molecular ions of the radical type (M^+) [109]. The absence of molecular weight information represents a major drawback of this method [110]. Currently, soft ionization techniques such as electrospray ionization (ESI) and atmospheric pressure chemical ionization are commonly employed for ionizing organic analytes that are thermally labile and moderately polar [111]. In the current study, ESI was utilized as a soft ionization method.

ESI employs electrical energy to aid in the transfer of ions from a solution to the gas phase, where they can be further analyzed using MS. By utilizing ESI-MS, ionic species present in a solution can be analyzed with heightened sensitivity. Additionally, neutral compounds can be converted into ionic form either in solution or in the gas phase through processes like protonation or cationization (e.g., using metal cations), enabling the study of these neutral compounds using ESI-MS. ESI involves three steps in transferring ionic species from a solution to the gas phase: (1) creating a fine spray of charged droplets, (2) evaporating the solvent, and (3) ejecting ions from the highly charged droplets. The process involves maintaining a high voltage in a capillary tube, generating charged droplets with the same polarity, and enhancing the sample flow rate with nebulizing gas. The charged droplets travel toward the mass spectrometer's analyzer region, where they are continuously reduced in size through solvent evaporation by utilizing an elevated ESI-source temperature and/or introducing a stream of nitrogen drying gas. This process results in an enhanced surface charge density and a decrease in the radius of the droplets. When the electric field strength within the droplets reaches a critical point, ions on the

droplet surface are ejected into the gas phase. These emitted ions are then sampled, accelerated into the mass analyzer, and analyzed for molecular mass and ion intensity measurement (Figure 1) [112], [113]. A notable benefit of employing soft ionization methods is the generation of ions with low internal energy. Consequently, when conducting a single-stage MS experiment, the fragmentation of these ions is minimal or negligible [110].

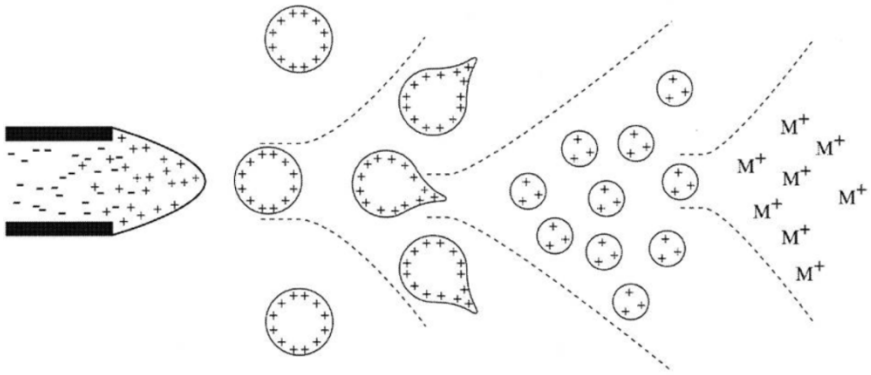

Figure 1: Schematic representation of droplet formation through electrospray ionization source. In the electrospray ionization (ESI) source, a steady flow of sample solution is directed through a capillary made of stainless steel or quartz silica [113].

1.5.2. Peptide Fragmentation

In a typical liquid chromatography tandem mass spectrometry (LC-MS/MS) procedure, the first step is to obtain an initial mass spectrum (MS1) of the intact (precursor) peptide. Next, the targeted precursor ion is isolated and fragmented into smaller fragments. These smaller fragments undergo mass analysis (MS2) to determine their individual masses. This entire process is repeated throughout the duration of the liquid chromatography separation of the peptide mixture [107]. Peptide fragmentation commonly occurs through various methods such as higher-energy C-trap dissociation (HCD), collision-induced dissociation (CID), electron transfer dissociation (ETD), and electron-transfer/higher-energy collision dissociation (EThcD) [114], [107]. In this study, HCD was used for peptide fragmentation. To induce fragmentation using HCD, a gas-filled quadrupole known as the HCD cell is positioned immediately after the C-trap. This arrangement, referred to as the dead-end geometry, is primarily designed to place the HCD cell at a

significant distance from the linear ion trap mass analyzer. The purpose of this configuration is to reduce the flow of gas back into the linear trap. In the HCD cell, ions are fragmented by adjusting the direct current (DC) offset applied to the rod electrodes. This adjustment provides the necessary collision energy to induce fragmentation in a manner similar to that of a conventional collision cell [114].

1.5.3. MS Quantification Methods

Data-Dependent Acquisition (DDA) and Data-Independent Acquisition (DIA) are two distinct MS quantification methods used in the field of proteomics [115]. Among them, LC-MS/MS with DDA is a commonly employed technique in proteomic analysis. Typically, DDA involves an initial MS1 scan to gather precursor m/z information from all peptide peaks, followed by an MS2 scan of selected peaks based on the MS1-scan data. This approach allows for high-purity MS2 scans for individual peptides, but unselected peptide features are missed due to instrument cycle time limitations. In contrast, the DIA method involves fragmenting all precursor ions within a predetermined MS1 m/z isolation window during the MS2 scan. This process is repeated until MS2 spectra are obtained for all the MS1 windows [116].

DDA generates MS2 spectra that target a particular ion, ensuring confidence in the source of observed fragment ions. However, DDA has limited reproducibility and coverage as it only fragments a subset of sample ions. On the other hand, DIA provides chromatographic traces for all detected fragment ions, facilitating the identification of complex samples and isomers. DIA is more reproducible and does not rely on MS1 survey scans, potentially resolving coverage issues by assigning MS2 fragments to any detected MS1 ion [115]. In this study, the DDA method was used as the MS quantification method.

1.5.4. Sequence Identification

Fragment ion spectra are utilized in "bottom-up" proteomics to identify peptide sequences. Methods have been developed to generate and match peptide fragment ion

spectra to their sequences. In the bottom-up proteomic approach, peptides are identified by searching databases for peptide-spectrum matches. Acquired fragment ion spectra are compared to theoretical peptide fragment ion spectra generated from a specified sequence database. The database search is limited to a user-defined precursor mass tolerance. The match between experimental and theoretical spectra is evaluated using multiple scores, such as the number of matching or nonmatching fragments and consecutive fragment ion matches. Some search engines in peptide identification utilize the relative intensities of acquired fragment ion signals. The relative fragment ion intensity pattern obtained from controlled fragmentation conditions can serve as a distinctive "fingerprint" for a given precursor. Community efforts in acquiring and sharing datasets have mapped out proteomes of certain species. Access to experimental fragment ion spectra for entire proteomes is increasing through spectral databases [117].

1.6. Aim of the Study

The hyperactivity of blood platelets in diabetes patients significantly contributes to the development of thrombosis and increases the risk of CVDs. In addition to mitochondrial dysfunction and ER stress, various other factors, including chronic inflammation, oxidative stress, insulin resistance, abnormal lipid metabolism, and endothelial dysfunction, can contribute to platelet dysfunction and CVDs in diabetes patients. In this study, quantitative bottom-up proteomics was utilized as a valuable technique to investigate and characterize the protein composition and changes associated with platelet hyperactivity in diabetes. This study followed the hypothesis that through quantification of protein abundance, insights into the dysregulated pathways and potential therapeutic targets for the development of antiplatelet therapies in diabetes patients will be obtained.

This study had three main objectives. Firstly, it was aimed to examine the proteome profiles of platelets in individuals with diabetes across different age groups (young, middle, and old age) compared to controls. This analysis would provide valuable insights into how age-related changes in the proteome impact platelet function in diabetes patients. This knowledge is important for developing targeted therapies for different age groups in diabetes patients and managing CVDs. Secondly, the focus was on analyzing the proteome of plasma-derived EVs from diabetes patients and controls. This analysis would yield valuable information about proteins that can directly or indirectly trigger platelet activation and their role in diabetes-related complications. Lastly, the focus was on the platelet fraction containing soluble proteins and loosely membrane-associated proteins. This research aimed to expand our understanding of the specific proteins that play crucial roles in platelet function and signaling pathways.

2. Material and Reagents

Table 1 contains the list of chemicals, antibodies, and enzymes used in this study. Table 2 contains the list of instruments and devices used for various analyses and measurements. The list of reusable and disposable items can be found in table 3, while table 4 presents the list of software used for data processing, analysis, and visualization in this study.

Table 1: List of chemicals, antibodies, and enzymes, along with their corresponding manufacturers.

Chemicals, antibodies, and enzymes	Manufacturer
2-Mercaptoethanol	Sigma-Aldrich (St. Louis, Missouri, USA)
2-Propanol	Sigma-Aldrich (St. Louis, Missouri, USA)
30% Acrylamide/Bis Solution, 29:1	BIO-RAD (USA)
4-(2-hydroxyethyl)-1-piperazineethanesulfonic acid (HEPES)	Sigma-Aldrich (St. Louis, Missouri, USA)
Acetonitrile (ACN), LC-MS grade	Merck (Darmstadt, Germany)
Ammonium hydrogen carbonate (AmbiCA)	Sigma-Aldrich (St. Louis, Missouri, USA)
Ammonium persulphate	Roth (Germany)
Anti-Phosphotyrosine Antibody, #05321	Merck Millipore (Darmstadt, Germany)
Brilliant Violet 421™ anti-human CD63 Antibody	Biolegend (California, USA)
Bromophenol Blue	Sigma-Aldrich (St. Louis, Missouri, USA)
Citrate Concentrated Solution	Sigma-Aldrich (St. Louis, Missouri, USA)
Citric acid	Sigma-Aldrich (St. Louis, Missouri, USA)
Collagen Reagens HORM® Suspension (KRH)	Takeda (Linz, Austria)
D-(+) Glucose	Sigma-Aldrich (St. Louis, Missouri, USA)
Dimethyl sulfoxide (DMSO)	Sigma-Aldrich (St. Louis, Missouri, USA)
Dithiothreitol (DTT)	Sigma-Aldrich (St. Louis, Missouri, USA)
Donkey anti-Mouse #926-68022	LI-COR (USA)
Donkey anti-Rabbit #926-32213	LI-COR (USA)

2. Material and Reagents

Ethylene glycol bis(beta-aminoethyl ether)-N,N,N',N'-tetraacetic acid (EGTA)	Sigma-Aldrich (St. Louis, Missouri, USA)
Flow Cytometry Sub-micron Particle Size Reference Kit, Green fluorescent	Thermo Fisher (Waltham, Massachusetts, USA)
Formic acid (FA)	Sigma-Aldrich (St. Louis, Missouri, USA)
Glycerol	Sigma-Aldrich (St. Louis, Missouri, USA)
Glycine	Sigma-Aldrich (St. Louis, Missouri, USA)
Hydrochloric acid (HCL)	Roth (Germany)
Indomethacin	Sigma-Aldrich (St. Louis, Missouri, USA)
Intercept® Blocking Buffer	LI-COR (USA)
Iodoacetamide (IAA)	Sigma-Aldrich (St. Louis, Missouri, USA)
Magnesium chloride ($MgCl_2$)	Sigma-Aldrich (St. Louis, Missouri, USA)
Methanol for LC-MS	Sigma-Aldrich (St. Louis, Missouri, USA)
Methanol for Western blot	J.T.Baker (Poland)
Phosphatase inhibitor cocktails 2 and 3	Sigma-Aldrich (St. Louis, Missouri, USA)
Phosphate buffered saline (PBS)	Thermo Fisher Scientific (UK)
Potassium Chloride (KCl)	Sigma-Aldrich (St. Louis, Missouri, USA)
Powdered milk	Roth (Germany)
Prostaglandin E1 (PGE1)	Sigma-Aldrich (St. Louis, Missouri, USA)
Protease inhibitor, a Roche complete mini tablet	Sigma-Aldrich (St. Louis, Missouri, USA)
ROTI®Histofix	Roth (Germany)
Sera-Mag™ Magnetic carboxylate	(Buckinghamshire, UK)
Sodium chloride (NaCl)	Sigma-Aldrich (St. Louis, Missouri, USA)
Sodium deoxycholate (SDC)	Sigma-Aldrich (St. Louis, Missouri, USA)
Sodium Dihydrogen Phosphate (NaH_2PO_4)	Sigma-Aldrich (St. Louis, Missouri, USA)
Sodium dodecyl sulfate (SDS)	Sigma-Aldrich (St. Louis, Missouri, USA)
Sodium hydroxide (NaOH)	Roth (Germany)
Tetramethylethylenediamine	Bio-Rad (USA)
Thrombin	Sigma-Aldrich (St. Louis, Missouri, USA)
Triethylammonium bicarbonate	Thermo Fisher (Waltham, Massachusetts, USA)
Trisodium citrate dihydrate	Sigma-Aldrich (St. Louis, Missouri, USA)
Triton X-100	Sigma-Aldrich (St. Louis, Missouri, USA)
Trizma ® base	Sigma-Aldrich (St. Louis, Missouri, USA)
Trypsin	Promega (Madison, WI USA)

2. Material and Reagents

Tween	Sigma-Aldrich (St. Louis, Missouri, USA)
Urea	Sigma-Aldrich (St. Louis, Missouri, USA)
VASP (A-11) Antibody, # SC-46668	Santa Cruz (Texas, USA)
Water, LC-MS grade	Merck (Darmstadt, Germany)

Table 2: List of instruments and devices, along with their corresponding manufacturers.

Instruments and devices	**Manufacturer**
100 µm x 20 mm, 100 Å pore size, 5 µm particle size, C18, Nano Viper	Thermo Fisher (Waltham, Massachusetts, USA)
25 cm C18 reversed-phase column (75 µm x 250 mm, 130 Å pore size, 1.7 µm particle size, peptide BEH C18)	NanoEase, Waters (Milford, Massachussets, USA)
490 4+4 aggregometer	Chrono-Log (Havertown, USA)
Analytical scale ALS 120-4	Kern & Sohn GmbH (Balingen-Frommern, Germany)
Centrifuge 5424	Eppendorf (Hamburg, Germany)
ChemiDoc MP Imaging System	BIO-RAD (USA)
Corning™ Stripettor Ultra	Thermo Fisher (Waltham, Massachusetts, USA)
Hybrid quadrupole-orbitrap mass spectrometer (Q Exactive)	Thermo Fisher Scientific (Bremen, Germany)
Incubation/Inactivation Bath 1002	GFL (Germany)
Invitrogen PowerEase 500 Power Supply	Life Technologies (USA)
Magnetic rack	BIO-RAD (USA)
Microplate Reader	Tecan Life Sciences (Männedorf, Switzerland)
Midi CO_2 Incubator, 40 L	Thermo Fisher (Waltham, USA)

2. Material and Reagents

MIKRO 220 Centrifuge	Hettich (Tuttlingen, Germany)
nano-UPLC (Dionex Ultimate 3000 UPLC system)	Thermo Fisher Scientific (Waltham, MA, USA)
NovoCyte Quanteon Flow Cytometer System	Agilent (Santa Clara, USA)
Probe sonicator Sonoplus	Bandelin electronic GmbH & Co. KG (Berlin, Germany)
S140-AT Fixed Angle Rotor	Thermo Fisher (Waltham, Massachusetts, USA)
Sorvall Discovery M120 SE Ultracentrifuge	LabMakelaar Benelux B.V. (Netherlands)
Speedvac	Thermo Fisher (Waltham, Massachusetts, USA)
Thermomixer compact	Eppendorf (Hamburg, Germany)
Tribrid quadrupole-orbitrap-ion trap mass spectrometer (Fusion)	Thermo Fisher Scientific (Bremen, Germany)
Universal 320R Centrifuge	Hettich (Tuttlingen, Germany)

Table 3: List of reusable and disposable items, along with their corresponding manufacturers.

Reusable and disposable items	**Manufacturer**
0.1 µm Sartorius Minisart™ NML Syringe Filters, Sterile	Thermo Fisher (Waltham, Massachusetts, USA)
Amicon Ultra 0.5 ml 30K centrifugal filters	Merck Millipore (Billerica, Massachussets, USA)
BD Plastipak ™ - 3-Piece Syringe	Thermo Fisher (Waltham, Massachusetts, USA)
Immobilon-P Membrane, PVDF	Merck Millipore (Darmstadt, Germany)
Pipette Tips	Sarstedt (Nümbrecht, Germany)
Reaction Tubes	Sarstedt (Nümbrecht, Germany)
Serological Pipettes	Thermo Fisher (Waltham, USA)

2. Material and Reagents

Single-channel microlitre pipette Eppendorf Research® plus, 100 to 1000 µl, blue	Roth (Germany)
S-Monovette® - Sarstedt	Nümbrecht, Germany
Ultracentrifuge tubes	Thermo Fisher (Waltham, Massachusetts, USA)

Table 4: List of softwares and their corresponding manufacturers or developers.

Softwares	**Manufacturer/Developer**
GraphPad Prism 8	(San Diego, CA, USA)
Image J 1.47v	(Wayne Rasband, National Institute of Health, USA)
Magellan	Tecan Life Sciences (Männedorf, Switzerland)
Perseus 2.0.3.0	Max-Planck-Institut (München, Germany)
ProteomeDiscoverer 2.0	Thermo Fisher (Waltham, Massachusetts, USA)
R-Software 4.2.2	(New Zealand)

3. Methods

3.1. Platelet Isolation

Peripheral blood samples were collected from diabetes patients and healthy controls using S-Monovette® - Sarstedt under the approval of Ethik-Kommission der Ärztekammer Hamburg, PU2322. All the samples utilized in this study were processed and analyzed at the laboratories of Prof. Schlüter and Prof. Renné, Institute for Clinical Chemistry and Laboratory Medicine at UKE. Platelet-rich plasma (PRP) was isolated from whole blood through a first centrifugation step at 200 g for 15 minutes. Platelets were then isolated from PRP through a second centrifugation step at 500 g for 15 minutes in the presence of indomethacin (10µM) and PGE1 (100 ng/ml). Once platelets were isolated, they were resuspended in warm modified Tyrode's buffer (136 mM NaCl, 5.5 mM glucose, 1 mM $MgCl_2$, 2.7 mM KCl, 10 mM HEPES, PH 7.4) at 37ºC containing 0.5% w/v citrate, indomethacin (10µM), and PGE1 (100 ng/ml). Following that, they were centrifuged at 500 g for 15 minutes to reduce plasma proteins. Isolated platelets were subsequently resuspended in warm modified Tyrode's buffer at a density of 2×10^8 platelets/ml during the entire study.

3.2. Isolation of Platelet Soluble Proteins Along with Loosely Associated Membrane Proteins

The platelet pellets from diabetes and healthy individuals were mixed with a hypotonic solution containing 100 µl of citrate wash buffer (11 mM glucose, 128 mM NaCl, 4.3 mM NaH_2PO_4, 4.8 mM sodium citrate, 2.4 mM citric acid, pH 6.5) and 900 µl of deionized water. The mixture was then placed on ice for 1 hour. To disrupt cell membranes and large cytoskeletal fragments, the mixture was sonicated twice for five seconds at 20% amplitude. Subsequently, the whole platelet homogenate (W) was centrifuged at 1,500 g for 10 minutes to precipitate any cellular debris. The supernatant (S1) was further centrifuged at 100,000 g for one hour at 4°C to isolate platelet soluble proteins along with loosely associated membrane proteins. The protocol was modified from Donovan et al.'s work and used in the study [118].

3.3. Plasma-Derived Extracellular Vesicles Isolation

Peripheral blood samples were collected from diabetes patients and healthy controls using S-Monovette® - Sarstedt. PRP was isolated from the whole blood by a first centrifugation step at 200 g for 15 minutes. Platelet-poor plasma (PPP) was obtained from PRP through a second centrifugation step at 500 g for 15 minutes, with the presence of indomethacin (10µM) and PGE1 (100 ng/ml). After that, PPP was further centrifuged at 3000 g for 15 minutes to remove any remaining platelets, and then the platelet-free plasma (PFP) was centrifuged at 100,000 g for 4 hours. The EVs pellet was resuspended in 1 ml of modified Tyrode's buffer along with citrate buffer (in a 1:7 ratio) and centrifuged at 100,000 g for 4 hours. The EVs pellet was then resuspended either in 40 µl of modified Tyrode's buffer for flow cytometry and aggregation study or lysed with radioimmunoprecipitation assay (RIPA) buffer (50 mM Tris-HCl, pH 8, 1% v/v Triton X-100, 0.5% w/v sodium deoxycholate, 0.1% w/v sodium dodecyl sulfate, 150 mM NaCl) for the plasma-derived EVs proteomics.

3.4. Counting Plasma-Derived Extracellular Vesicles Using Flow Cytometry

The Brilliant Violet 421™ anti-human CD63 (BioLegend) was used to stain plasma-derived extracellular vesicles for 15 minutes at 37°C in the dark. Following that, samples were fixed with 4% paraformaldehyde (PFA) for 15 minutes at room temperature and diluted with PBS immediately before measurement. To minimize background interference, both PFA and PBS were filtered through a 0.1 µm filter. The samples were then analyzed on a NovoCyte Quanteon Flow Cytometer (Agilent, Santa Clara, CA, USA) with a slow flow rate. Initially, a histogram was used to identify the CD63 positive population of plasma-derived EVs. Subsequently, gating was performed based on the CD63-positive plasma-derived EVs subpopulation (sized between 0.1-1 micrometers, determined by previous measurements using size beads). This gating was carried out using a dot plot, and the selected population was counted. The resulting data are presented as event densities (events/µl).

3.5. Platelet Aggregation Assay

Healthy platelets resuspended in modified Tyrode's buffer containing 5mM glucose at a density of 2 × 10^8 platelets/ml. These platelets (250 µl) were then pre-incubated with 20,000 EVs obtained either from the plasma of diabetes patients or from healthy individuals. The mixture was incubated for 30 minutes at 37°C. Following this, platelets were assayed using a Chrono-Log 490 4+4 aggregometer. After 10 minutes, aggregation was induced using either 0.05 U/ml thrombin or 10 µg/ml collagen. The absorbance of the mixture was measured for a period of 10 minutes in the case of collagen-induced aggregation, or 20 minutes in the case of thrombin-induced aggregation. Control samples were not treated with EVs.

3.6. The Effect of Extracellular Vesicles on Platelets: Phosphotyrosine Immunoblotting

Isolated healthy platelets were prepared and resuspended in modified Tyrode's buffer containing 5mM glucose, achieving a density of 2 x 10^8 platelets/ml. The platelet suspension was then divided into aliquots of 250 µl each. In order to investigate the effects of plasma-derived EVs on platelets, 20,000 plasma-derived diabetes EVs (n=4) or 20,000 plasma-derived control EVs (n=4) with CD63-positive identification (0.1-1 µm) were added to platelet suspension aliquots. An additional aliquot of the platelet suspension without EVs was used as the control group. Subsequently, all samples were incubated at 37°C for 30 minutes. After the incubation period, 1.25 µl of 200 mM EGTA was added to achieve a final concentration of 1 mM. Following this, 250 µl of 2x RIPA lysis buffer, supplemented with protease inhibitor ($^1/_{20}$ of a Roche complete mini tablet) and diluted phosphatase inhibitor cocktails 2 and 3 (1 in 50 dilution), were added to the samples. Notably, as a second control, 20,000 EVs from each donor in 20 µl of modified Tyrode's buffer were mixed with 20 µl of 2x RIPA lysis buffer. Subsequently, all samples were rotated at 4°C for 90 minutes. At the end of the 90 minutes rotation, all aliquots were centrifuged at 2,000 g for 5 minutes. The supernatants were carefully collected, and the protein concentration was determined using the BCA assay. Platelet proteins and EVs proteins were separated using SDS-polyacrylamide gel electrophoresis (SDS-PAGE). Subsequently, they were transferred onto a polyvinylidene difluoride (PVDF) membrane,

and analyzed by immunoblotting for anti-Phosphotyrosine (Millipore), and VASP (Santa Cruz Biotechnologies). The relative phosphorylation of p-Tyr over total VASP (i.e. loading control) was quantified using image analysis software, Image J 1.47v (Wayne Rasband, National Institute of Health, US).

3.7. Statistical Analysis

Statistical analysis was performed using GraphPad Prism 8 (San Diego, CA, USA). The normality test was assessed using the D'Agostino-Pearson omnibus (K2) test. To evaluate whether the variances among the compared groups were statistically equal or significantly different, the Brown-Forsythe test and Bartlett's test were employed. The one-way analysis of variance (ANOVA) is used to determine whether there are any statistically significant differences between the means of three independent groups. To identify which specific groups were significantly different from each other, post hoc multiple comparison tests were performed.

3.8. Sample Preparation and Tryptic Digestion for Mass Spectrometric Analysis

3.8.1. Single-Pot, Solid-Phase, Sample-preparation (SP3) protocol

Following the platelet isolation method previously described. Platelet pellets from diabetes samples and their matched healthy controls were lysed using SDS lysis buffer (0.05M Tris-HCl at pH 7.6 and 2% (v/w) SDS) or SDC lysis buffer (0.05M Tris-HCl at pH 7.6 and 2% (v/w) SDC), while plasma-derived EVs from diabetes patients and their matched controls were lysed with RIPA buffer. Lysed samples were boiled at 95°C for 5 minutes and sonicated three times at 20% using a probe sonicator. Following this, a 0.5 µl solution of 1 M DTT (a final concentration of 10 mM) was added to the sample, which was then incubated for 30 minutes at 60°C on a heating block. Subsequently, a 2 µl solution of 0.5 M IAA (a final concentration of 20 mM) was added to the sample and incubated for 30 minutes at 37°C in the dark. For bead addition, 2 µl of the mixed bead solution was added. Afterwards, the sample was mixed with acetonitrile (ACN, a final

concentration of approximately 70%) and incubated for 18 minutes at room temperature. The sample tube was placed on a magnetic rack to allow the beads to settle for 2 minutes. The beads were washed twice by adding 200 µl of 100% ACN, incubating for 30 seconds, and allowing the beads to settle for 2 minutes on the magnetic rack before removing the supernatant. This washing process was repeated two more times using 200 µl of 70% ethanol for each wash, followed by the removal and discarding of the supernatant. The resulting pellet was then resuspended in 50 µl of 50 mM AmbiCA. Trypsin was added to the sample at a 1:100 ratio (approximately 250 ng), and the sample was incubated overnight at 37°C. Subsequently, 950 µl of ACN (a final acetonitrile concentration of 95%) was added. The sample was then vortexed and incubated for 8 minutes. The sample was washed twice with 200 µl of ACN, discarding the supernatant after each wash. Finally, the peptides were eluted using 20 µl of a 2% DMSO/1% FA solution. The samples were dried in a vacuum centrifuge and resuspended in 0.1% FA to achieve a final protein concentration of 1 µg/µl [119], [120].

3.8.2. Filter-aided sample preparation (FASP) protocol

Following the platelet isolation method previously described. Protein pellets from healthy control samples (platelet) were lysed using SDS lysis buffer (0.05M Tris-HCl at pH 7.6 and 2% (v/w) SDS), boiled at 95°C for 5 minutes and sonicated three times at 20% using a probe sonicator. Up to 30 µl of a protein extract (20 µg) was mixed with 200 µl of UA (8 M urea in 0.1 M Tris–HCl, pH 8.5) in the filter unit and centrifuged at 10,000 g for 10-15 minutes until less than 10 µl of the sample remained in the filter. 200 µl of UA was then added to the filter unit and the centrifugation step was repeated. The flow-through from the collection tube was discarded. Next, 100 µl of IAA (0.05 M iodoacetamide in UA) solution was added and mixed at 600 rpm in a thermo mixer for 1 minute. The filter units were centrifuged at 10,000 g for 10 minutes. 100 µl of UA was added to the filter unit and was centrifuged at 10,000 g for 15 minutes. This step was repeated twice. Afterward, 100 µl of digestion buffer (DB) (0.05 M Tris–HCl, pH 8.5) was added to the filter unit and centrifuged at 10,000 g for 10 minutes. This step was repeated twice as well. Then, 40 µl of DB with trypsin (enzyme-to-protein ratio 1:100) was added, and the mixture was mixed at 600 rpm in a thermomixer for 1 minute. The units were incubated in a humid chamber at 37°C for 1.5-18 hours. Finally, the filter units were transferred to

new collection tubes. The filter units were centrifuged at 10,000 g until the solution completely passed the filter membrane (about 5 minutes). Subsequently, 100 µl of DB was added, and the filter units were centrifuged at 10,000 g. The samples were dried in a vacuum centrifuge and resuspended in 0.1% FA to achieve a final protein concentration of 1 µg/µl [121].

3.8.3. LC-MS/MS in Data Dependent Acquisition Mode

Quadrupole-iontrap-orbitrap mass spectrometer (Orbitrap Fusion)

The platelet proteome or EVs proteome was analyzed using LC-MS/MS, utilizing a quadrupole-ion-trap-orbitrap mass spectrometer (Orbitrap Fusion, Thermo Fisher) coupled to a nano-UPLC. Chromatographic separation of peptides was achieved using a two-buffer system: buffer A containing 0.1% FA in water, and buffer B containing 0.1% FA in ACN. Connected to the UPLC system was a peptide trap (100 µm x 20 mm, 100 Å pore size, 5 µm particle size, C18, Nano Viper, Thermo Fisher) designed for online desalting and purification. This was followed by a 25 cm C18 reversed-phase column (75 µm x 250 mm, 130 Å pore size, 1.7 µm particle size, peptide BEH C18, nanoEase, Waters). The separation of peptides was accomplished by using an 80-minute gradient, linearly increasing ACN concentration from 2% to 30% over a span of 60 minutes. The eluting peptides underwent ionization using a nano-electrospray ionization source (nano-ESI) with a spray voltage set at 1,800. Subsequently, they were transferred into the MS, and analyzed in DDA mode. For each MS1 scan, ions were collected for up to 120 milliseconds or until they reached a charge density of 2×10^5 ions (AGC Target). Fourier-transformation based mass analysis of the data from the orbitrap mass analyzer was conducted, covering a mass range of 400 – 1,300 m/z with a resolution of 120,000 at m/z = 200. Peptides with charge states ranging from 2^+ to 5^+ and an intensity greater than 1,000 were isolated within a 1.6 m/z isolation window in Top Speed mode for 3 seconds for each precursor scan. Subsequently, they underwent fragmentation utilizing HCD with a normalized collision energy of 30%. MS2 scanning was conducted using an ion trap mass analyzer at a rapid scan rate, covering a mass range starting at 120 m/z. Data

accumulation continued for 60 milliseconds or until achieving an AGC target of 1 x 10^5. Already fragmented peptides were excluded for a duration of 30 seconds.

Quadrupole-orbitrap mass spectrometer (QExactive) for the platelet fraction

Regarding platelet fraction, the eluting peptides were analyzed using a Quadrupole Orbitrap hybrid mass spectrometer (QExactive, Thermo Fisher Scientific). Herein, the ions responsible for the top 15 signal intensities per precursor scan (1×10^6 ions, 70,000 Resolution, 240ms fill time) were analyzed by MS/MS (HCD at 25 normalized collision energy, 1×10^5 ions, 17,500 Resolution, 50 ms fill time) in a range of 400–1200 m/z. Additionally, a dynamic precursor exclusion of 20 seconds was applied.

3.8.4. LC-MS/MS data processing and analysis

The LC-MS/MS data obtained through DDA mode were searched against the human SwissProt protein database, which was downloaded from the Uniprot protein database (release December 2018, EMBL, Hinxton, Great Britain). The search was performed using the Sequest search engine integrated into the protein identification software "Proteome Discoverer". The mass tolerances for precursor ions were set at 10 ppm, and for fragment ions, it was set at 0.02 Da. Only peptides with a high level of confidence, determined by a false discovery rate of less than 1% using a decoy database approach, were considered as identified [122]. The relative abundance of proteins was imported into the Perseus statistical analysis software. Perseus software, version 2.0.3.0, was used for further analysis, including profile plots and multi-scatter plots. One outlier from the profile plot of the platelet proteome of middle-aged diabetes patients was identified and excluded for further analysis. Similarly, one outlier from the profile plot of the plasma-derived EVs proteome of a middle-aged healthy individuals was also identified and excluded for further analysis. Additionally, t-tests were used to generate volcano plots and heat maps after performing statistical testing and filtering for valid values using Perseus software.

3.8.5. Pathway and enrichment analysis

The genes, which code for significantly differentially upregulated or downregulated proteins between diabetes and healthy individuals from EVs lysate or platelet lysate, were used for pathway analysis separately. Pathway analysis was performed using EnrichR by choosing BioPlanet2019. Then, clustergram was generated by considering the p-value and adjusted p-value less than 0.05 for the involved pathways.

4. Result

4.1. Platelet Protein Extraction and Analysis: Methods, Protein Yield, and Data Reproducibility

Due to the absence of a nucleus in platelets and the resulting limited levels of protein synthesis, together with the regulation of platelet activity through PTMs, proteomics becomes an invaluable tool for characterizing the fundamental processes that impact platelet homeostasis. Understanding these processes is crucial for determining the roles of platelets in both health and disease [123]. Both reproducible sample preparation and high-yield generation of peptides are the prerequisites for a successful bottom-up proteomics workflow [119], [124]. In the current study, different detergent-based methods were used to extract platelet proteins with the aim of getting insight into selecting a suitable method based on factors such as data reproducibility, protein yield, and cost-effectiveness.

4.1.1. Detergent-based Methods for Platelet Protein Extraction

Human platelet proteins were extracted using three different methods: one SDC-based method and two SDS-based methods. The SDC-based method involved the use of SP3 technique [119], [120], which is represented as SDC-SP3. The SDS-based methods involved the use of FASP [121] and SP3 sample preparation techniques, which are represented as SDS-FASP and SDS-SP3, respectively. Three samples, with technical duplicates in each group, were used to identify proteins from the human platelet lysate. The proteins identified in equivalent samples prepared by the SDC-SP3, SDS-SP3 and SDS-FASP methods were compared using *Venn* diagram to present the total, unique, and shared protein identifications among the experimental groups. The SDS-FASP method for extracting platelet proteins resulted in a greater protein yield (2092 proteins) when compared to the SDC-SP3 (1833 proteins), and SDS-SP3 (1772 proteins) methods (Figure 2).

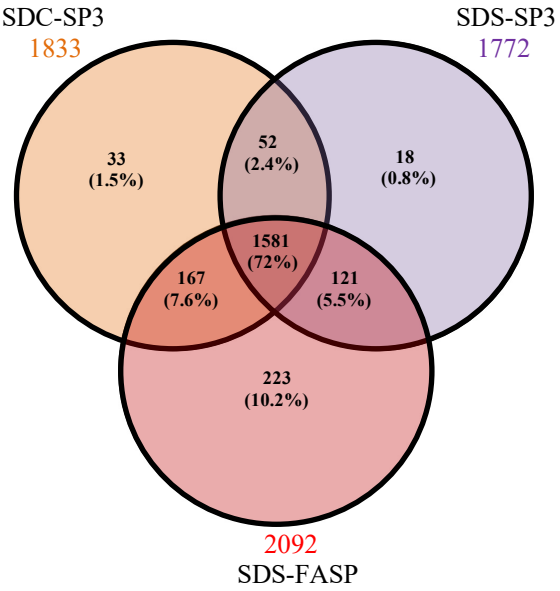

Figure 2: *Venn* diagram visualization of total, unique, and shared protein identifications among the experimental groups (SDC-SP3, SDS-SP3 and SDS-FASP). Among all identified proteins, 2195 proteins were found in at least two samples in at least one method and used further. A total of 1833, 1772, and 2092 proteins were identified in the SDC-SP3, SDS-SP3 and SDS-FASP preparations, respectively. 1581 (72%) proteins were common between SDC-SP3, SDS-SP3 and SDS-FASP extraction methods. Three samples with technical duplicates were used in each group (n=6).

4.1.2. Quantitative Comparison of Identified Proteins from SDC-SP3, SDS-SP3, and SDS-FASP Sample Preparation

Protein yield

All 2195 identified proteins, which were found in at least two samples of all experimental groups (SDC-SP3, SDS-SP3, and SDS-FASP) from the Label-Free Quantification (LFQ) experiment, were transformed to $\log_2$ and then used to create a Profile Plot to visualize the relative abundance of proteins in different samples and groups. The Boxplot in the Profile Plot was utilized to visualize the distribution of protein abundance in each sample and identify potential outliers. Notably, a significantly lower total protein amount was

detected for the SDS-SP3 experimental group, compared to both SDS-FASP and SDC-SP3 groups (Figure 3).

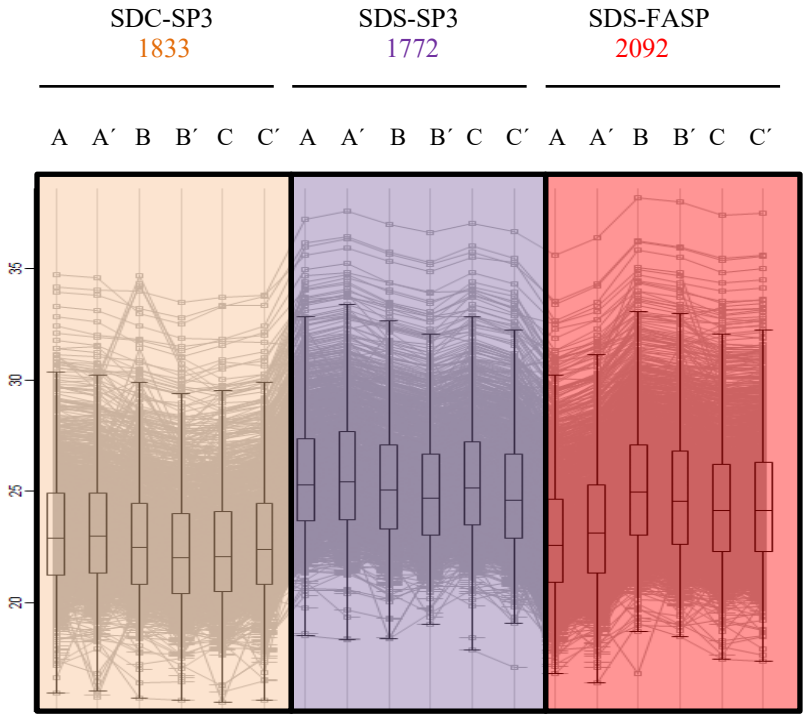

Figure 3: Profile Plot visualization of all 2195 identified proteins, across all analyzed samples, based on the log_2 transformed unnormalized protein abundance from the SDC-SP3, SDS-SP3, and SDS-FASP groups. Each point represents the relative abundance of a protein in the corresponding sample and each horizontal line depicts the trend of a protein abundance identified in the total proteome in different samples and groups. Boxplot indicates the scattering around the mean value of the protein abundance of each sample. Data is displayed from the Perseus database. Three samples with technical duplicates were used in each group (n=6).

Data Reproducibility

The LFQ intensity values of the samples that were processed using the SDS-FASP, SDS-SP3, and SDC-SP3 methods were normalized. To evaluate the quantitative reproducibility of the applied techniques, the Pearson correlation coefficient was calculated. In addition, the abundance of all quantified proteins was plotted by comparing each possible sample pair across all methods of sample preparation. The resulting multi-scatter plot demonstrated a correlation of >80% for all techniques. The mean R-squared (R^2) value in

the SDC-SP3 group was above 0.8, whereas the mean R^2 values in both the SDS-SP3 and SDS-FASP groups were above 0.9 (Figure 4). Taken together, the SDS-SP3 and SDS-FASP groups displayed higher data reproducibility compared to the SDC-SP3 group. Therefore, it can be concluded that protein lysis with SDS, followed by processing with either SP3 or FASP, is a suitable method for the processing of platelet proteins in quantitative bottom-up proteomics. The SDS-SP3 method was selected for subsequent experiments based on its cost-effectiveness in comparison to the SDS-FASP method [125], [120].

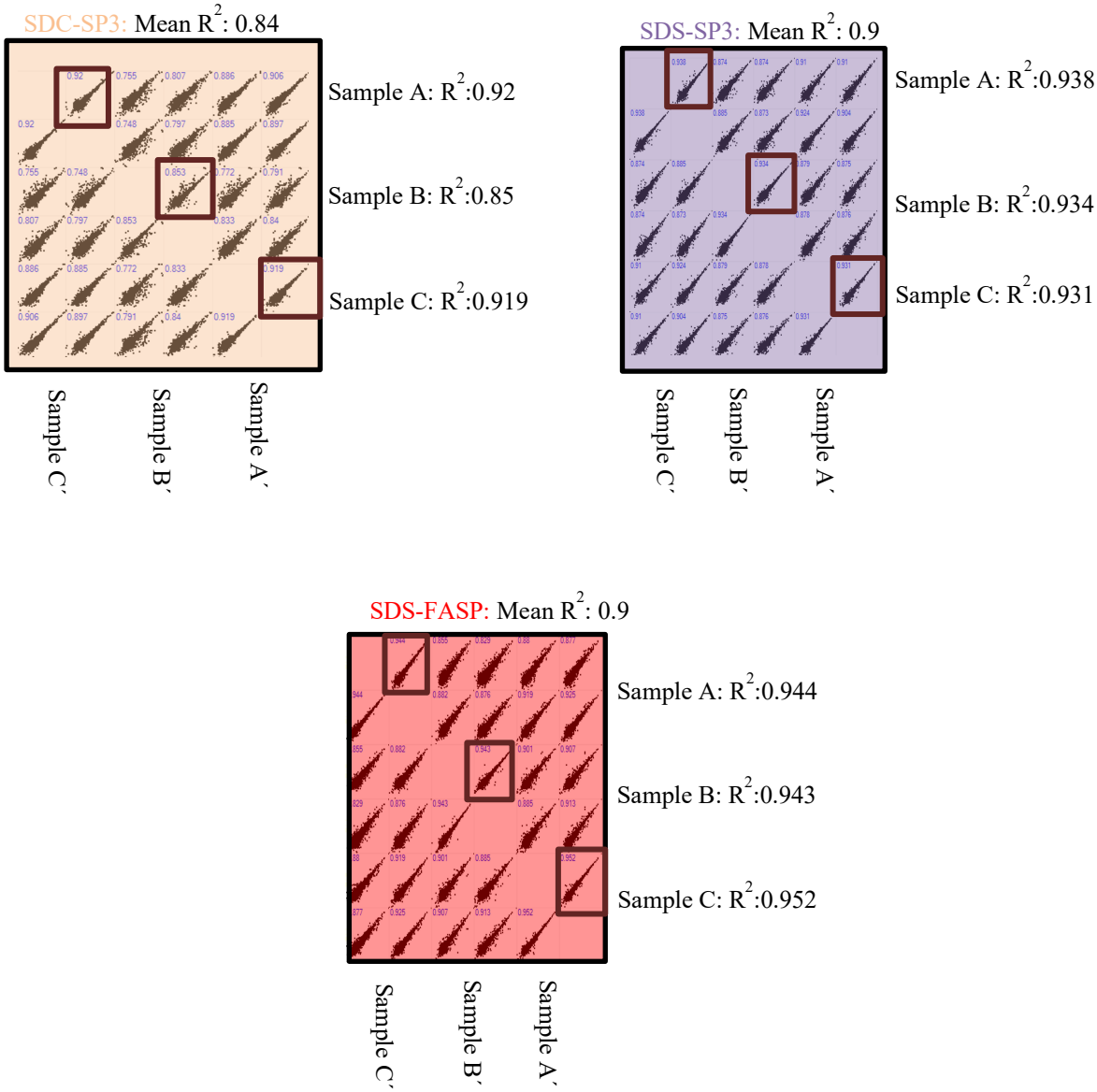

Figure 4: Multi scatter plot comparing the protein intensities obtained by the three experimental groups (SDC-SP3, SDS-SP3, and SDS-FASP) from three samples (A, B, and C) with technical duplicates. Each dot represents a protein. The depicted number

in each of the individual scatter plots is the Pearson correlation value. The R^2 value for each sample is displayed. The correlation between technical replicates is marked in brown. Three samples with technical duplicates were used in each group (n=6).

4.2. Platelet Proteome Changes between Diabetic and Healthy Individuals

Platelets from patients with diabetes have increased reactivity and baseline activation compared to those from healthy individuals [81]. Furthermore, platelets play a key role in hemostasis and thrombosis [126], and their dysfunction in diabetes patients increases the risk of cardiovascular complications [127]. Platelet proteome changes in diabetes can provide valuable insights into the molecular mechanisms that contribute to platelet dysfunction in diabetes [126], [128].

4.2.1. Selection Criteria for Diabetes Patients and Healthy Controls

Peripheral blood samples were collected from 24 diabetes patients and 24 age- and sex-matched healthy controls. The selection of participants was based on their HbA1c levels. Diabetes patients were selected based on HbA1c values > 7.0% (indicative of hyperglycemia), while healthy controls were chosen with HbA1c < 6.0% (indicative of euglycemia). Following that, the samples were classified into three groups based on age: A) Young age (under 55) with 6 diabetic samples and 6 controls. B) Middle age (55-75) with 12 diabetic samples and 12 controls. C) Old age (over 75) with 6 diabetic samples and 6 controls (Table 5).

4. Result

Table 5: Selection criteria for diabetes patients and healthy controls based on HbA1c values.

Sample number	Diabetes mellitus				Controls			
	Age	Sex	HbA1c	Platelet count	Age	Sex	HbA1c	Platelet count
1	49	M	11.1%	$4.20*10^8$	51	M	5.7%	$1.864*10^8$
2	51	M	9.7%	$1.014*10^8$	51	M	5.3%	$1.164*10^8$
3	48	M	8.2%	$1.805*10^8$	43	M	5.3%	$1.513*10^8$
4	42	M	8.0%	$2.487*10^8$	38	M	5.3%	$1.112*10^8$
5	47	M	7.4%	$1.704*10^8$	52	M	5.3%	$3.258*10^8$
6	32	F	7.9%	$1.381*10^8$	33	F	4.7%	$1.006*10^8$
7	73	F	8.8%	$2.126*10^8$	75	F	5.0%	$2.812*10^8$
8	70	M	7.4%	$1.389*10^8$	74	M	5.9%	$1.27*10^8$
9	75	F	7.1%	$1.814*10^8$	75	F	5.7%	$3.392*10^8$
10	58	M	8.2%	$3.688*10^8$	58	M	4.2%	$1.62*10^8$
11	57	F	7.5%	$2.677*10^8$	57	F	5.4%	$2.216*10^8$
12	61	M	7.2%	$1.114*10^8$	62	M	5.5%	$1.322*10^8$
13	65	M	9.3%	$2.217*10^8$	60	M	5.7%	$1.224*10^8$
14	62	F	11.9%	$1.002*10^8$	58	F	5.6%	$1.923*10^8$
15	69	M	7.4%	$1.634*10^8$	65	M	5.5%	$1.335*10^8$
16	61	F	7.3%	$1.362*10^8$	64	F	5.2%	$2.933*10^8$
17	65	M	7.2%	$2.151*10^8$	62	M	5.7%	$2.538*10^8$
18	70	F	7.7%	$2.828*10^8$	70	F	5.9%	$3.117*10^8$
19	84	F	7.5%	$2.308*10^8$	82	F	5.7%	$1.408*10^8$
20	80	M	7.5%	$2.206*10^8$	83	M	5.8%	$1.265*10^8$
21	81	M	7.1%	$1.057*10^8$	81	M	5.7%	$1.041*10^8$
22	78	M	7.5%	$1.033*10^8$	76	M	5.6%	$1.208*10^8$
23	82	M	7.1%	$3.007*10^8$	80	M	5.1%	$1.95*10^8$
24	81	M	7.1%	$3.514*10^8$	79	M	5.3%	$2.076*10^8$

	Age	Sex	Diabetes	Controls
	Middle	woman	6	6
	Middle	man	6	6
	Old	woman	1	1
	Old	man	5	5
	Young	woman	1	1
	Young	man	5	5
Middle age = 55-75				
Old age = over 75				
Young age = under 55				

4.2.2. Workflow Overview

Washed platelets from the peripheral citrated blood of diabetes (HbA1c values > 7.0%) and controls (HbA1c values < 6.0%) were isolated by centrifugation and lysed by ultrasonication in the presence of SDS. Extracted proteins were proteolyzed by trypsin and identified by LC-MS/MS (Figure 5).

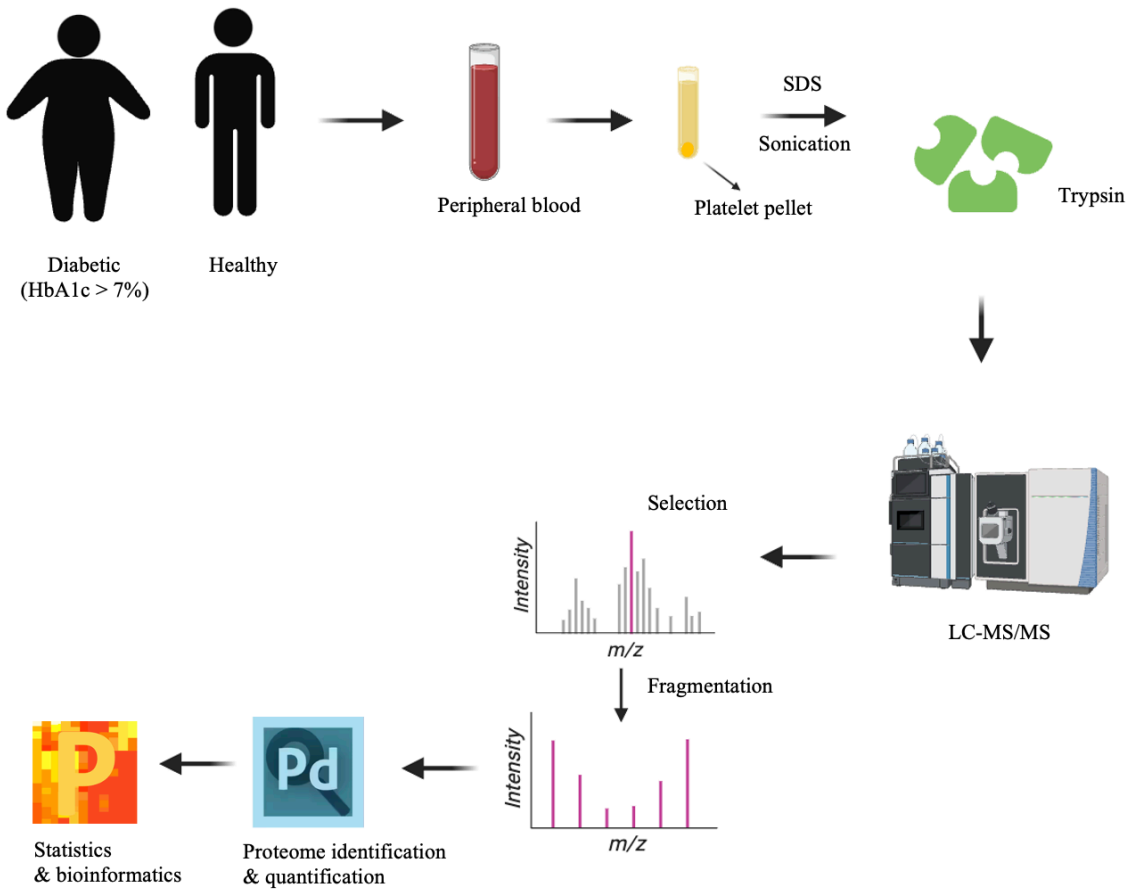

Figure 5: **Overall scheme of platelet proteome profiling by using differential quantitative bottom-up proteomics.** These include the key steps that were undertaken for protein identification and quantification in platelets from diabetic and healthy individuals.

4.2.3. Platelet Proteome Changes in Young Diabetics versus Healthy Controls

In the platelet proteome of young, middle-aged, and old individuals, a total of 2860 proteins were identified. Among the platelet proteome of young individuals, 37 unique proteins were found to be significantly more abundant (at least 1.5-fold) in individuals with diabetes compared to age- and sex-matched healthy controls, meeting the threshold for statistical significance (p-value < 0.05). Meanwhile, 29 unique proteins were found to be significantly less abundant (at least 1.5-fold) in individuals with diabetes compared to controls. A volcano plot was generated to highlight these differences. Among the significantly differentially downregulated genes, KCMF1, GNAS, GUCY1A3, APOOL, PDHA1, and PRDX2, and among the significantly differentially upregulated genes, MIF, C8G, SIRT2, C6, CFH, PDE3A, DAB2, SERPINF1, and INPP5D, may play a role in platelet function (Figure 6A).

102 proteins were identified as significant (p-value < 0.05) and able to clearly separate between diabetes and control in young patients. Out of these, 37 proteins were found to be at least 1.5 times more abundant in diabetes, and 29 proteins were found to be at least 1.5 times less abundant in diabetes, both of which were used for further statistical analysis. The supervised cluster analysis clearly separated diabetes patients from healthy controls and revealed a distinct heatmap pattern for upregulated and downregulated proteins (Figure 6B).

To further elaborate on the function of proteins identified as significantly differentially abundant between young diabetes and healthy controls, pathway analysis was performed, based on the Bioplanet 2019 database. Proteins, up and down-regulated in diabetes were analyzed separately (Figure 6C, and 6D). Ion channel function in vascular endothelium was the only significant enriched term that was identified from the significantly downregulated gene set in young diabetes patients compared to controls. The genes GUCY1A3 and GNAS, which code for "Guanylate cyclase soluble subunit alpha-3" and "Guanine nucleotide-binding protein G(s) subunit alpha isoforms XLas," respectively, were found to be significantly enriched in this term (Figure 6C). In contrast, the terminal pathway of complement was identified as the most significantly enriched term from the significantly upregulated gene set in young diabetes patients compared to controls. The

4. Result

genes C8G and C6, which code for "Complement component C8 gamma chain" and "Complement component C6", respectively, were found to be significantly enriched in this term. Of note, C8G and C6 were the main contributors to the all significantly enriched gene sets (Figure 6D).

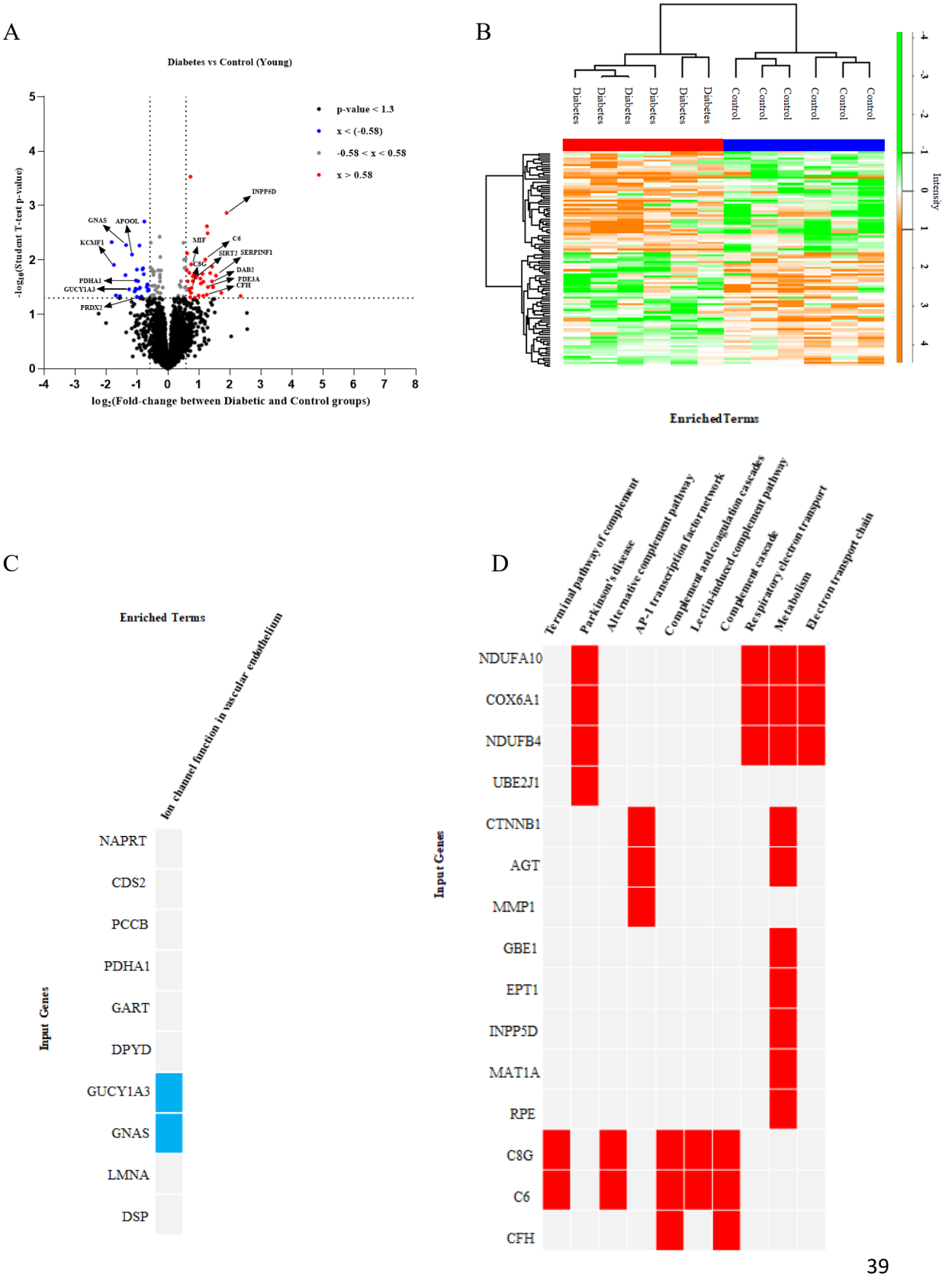

Figure 6: Differentially expressed proteins and altered pathways in the platelet proteome of young individuals with diabetes compared to healthy sex- and age-matched controls. A) The volcano plot shows the two-sided unpaired t-test results for all quantified proteins from the platelet lysate in both diabetic and control groups of the young age group after applying a randomForest-based algorithm for missing data imputation. Each dot indicates a protein. **B)** A heatmap and supervised cluster analysis of proteins extracted from platelets of young individuals with diabetes, compared to healthy sex- and age-matched controls, after applying a randomForest-based imputation strategy. The color intensity in the heatmap represents the relative abundance of proteins detected in each sample. In the heatmap, each column represents a sample, each row represents a protein, and each rectangle indicates the Pearson's correlation coefficient between a pair of data for the relative abundance of a protein in a sample. The value for the correlation coefficient is represented by the intensity of the orange or green color, as indicated on the color scale. **C**) and **D)** To elucidate the biological functions and pathways associated with the significantly differentially expressed proteins between diabetes and control groups, gene set enrichment analysis of the downregulated and upregulated genes in diabetes compared to controls from the whole platelet lysate in the young age group was performed, based on the Bioplanet 2019 database, using EnrichR. Ion channel function in vascular endothelium was the only significant enriched term that was identified from the significantly downregulated gene set in young diabetes patients compared to controls. The genes GUCY1A3 and GNAS were found to be significantly enriched in this term (Figure 6C). The terminal pathway of complement was identified as the most significantly enriched term from the significantly upregulated gene set in young diabetes patients compared to controls. The genes C8G and C6 were found to be significantly enriched in this term (Figure 6D).

4.2.4. Platelet Proteome Changes in Middle-Aged Diabetics versus Healthy Controls

Among the platelet proteome of middle-aged individuals, 42 unique proteins were found to be significantly more abundant (at least 1.5-fold) in individuals with diabetes compared to age- and sex-matched healthy controls, meeting the threshold for statistical significance (p-value < 0.05). Meanwhile, 37 unique proteins were found to be significantly less abundant (at least 1.5-fold) in individuals with diabetes compared to controls. A volcano plot was generated to highlight these differences. Among the significantly differentially downregulated genes, GSK3A, ANXA1, EXOC3L4, VIM, EFNB1, and GRK5, and among the significantly differentially upregulated genes, PF4, PRKD2, F12, C7, and A2M, may play a role in platelet function (Figure 7A).

162 proteins were identified as significant (p-value < 0.05) and able to clearly separate between middle-aged diabetes patients and healthy controls. Out of these, 42 proteins were found to be at least 1.5 times more abundant in diabetes, and 37 proteins were found to be at least 1.5 times less abundant in diabetes, both of which were used for further statistical analysis. The supervised cluster analysis clearly separated diabetes patients from healthy controls and revealed a distinct heatmap pattern for upregulated and downregulated proteins (Figure 7B).

To further elaborate on the function of proteins identified as significantly differentially abundant between middle-aged diabetes and healthy controls, pathway analysis was performed, based on the Bioplanet 2019 database. Proteins, up and down-regulated in diabetes were analyzed separately. Fibrin clot formation (clotting cascade) was identified as the most significantly enriched term from the significantly upregulated gene set in middle-aged diabetes patients compared to controls. The genes F12, A2M, and PF4 which code for "Coagulation factor XII", "Alpha-2-macroglobulin", and "Platelet factor 4", respectively, were found to be significantly enriched in this term. Of note, F12 and A2M were the main contributors to the all significantly enriched gene sets (Figure 7C).

4. Result

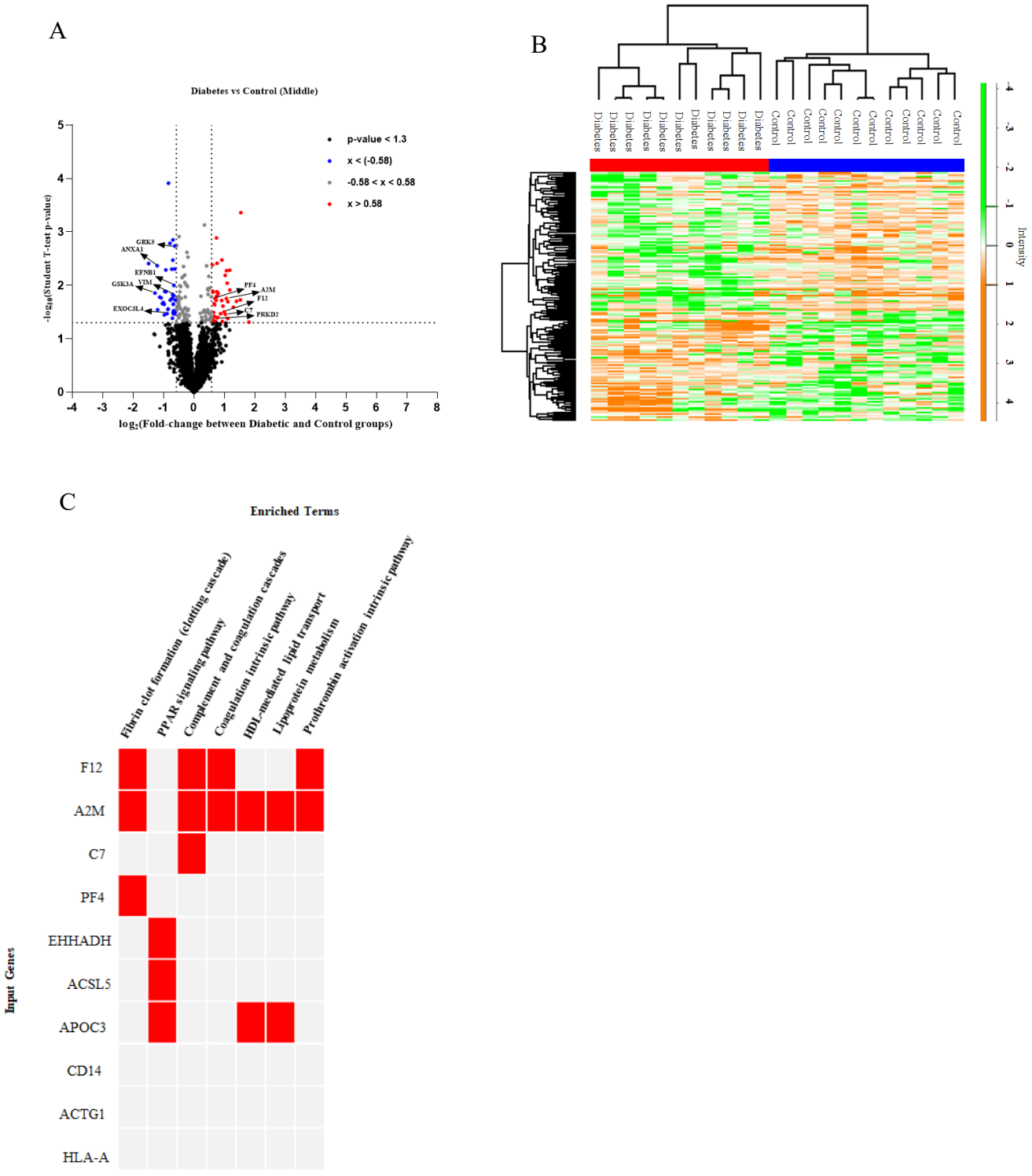

Figure 7: Differentially expressed proteins and altered pathways in the platelet proteome of middle-aged individuals with diabetes compared to healthy sex- and age-matched controls. A) The volcano plot shows the two-sided unpaired t-test results for all quantified proteins from the platelet lysate in both diabetic and control groups of the middle-aged group after applying a randomForest-based algorithm for missing data

imputation. Each dot indicates a protein. **B)** A heatmap and supervised cluster analysis of proteins extracted from platelets of middle-aged individuals with diabetes, compared to healthy sex- and age-matched controls, after applying a randomForest-based imputation strategy. The color intensity in the heatmap represents the relative abundance of proteins detected in each sample. In the heatmap, each column represents a sample, each row represents a protein, and each rectangle indicates the Pearson's correlation coefficient between a pair of data for the relative abundance of a protein in a sample. The value for the correlation coefficient is represented by the intensity of the orange or green color, as indicated on the color scale. **C**) To elucidate the biological functions and pathways associated with the significantly differentially expressed proteins between diabetes and control groups, gene set enrichment analysis of the upregulated genes in diabetes compared to controls from the whole platelet lysate in the middle-aged group was performed, based on the Bioplanet 2019 database, using EnrichR. Fibrin clot formation (clotting cascade) was identified as the most significantly enriched term from the significantly upregulated gene set in middle-aged diabetes patients compared to controls. The genes F12, A2M, and PF4 were found to be significantly enriched in this term. Of note, F12 and A2M were the main contributors to the all significantly enriched gene sets.

4.2.5. Platelet Proteome Changes in Old-Aged Diabetics versus Healthy Controls

Among the platelet proteome of old individuals, 31 unique proteins were found to be significantly more abundant (at least 1.5-fold) in individuals with diabetes compared to age- and sex-matched healthy controls, meeting the threshold for statistical significance (p-value < 0.05). Meanwhile, 23 unique proteins were found to be significantly less abundant (at least 1.5-fold) in individuals with diabetes compared to controls. A volcano plot was generated to highlight these differences. Among the significantly differentially downregulated genes, GMPPA, ALG5, INPPL1, and GYG1, and among the significantly differentially upregulated genes, ATP2C1, SH3GL1, FTH1, and GSK3A may play a role in platelet function (Figure 8A).

113 proteins were identified as significant (p-value < 0.05) and able to clearly separate between old individuals with diabetes and healthy controls. Out of these, 31 proteins were

found to be at least 1.5 times more abundant in diabetes, and 23 proteins were found to be at least 1.5 times less abundant in diabetes, both of which were used for further statistical analysis. The supervised cluster analysis clearly separated diabetes patients from healthy controls and revealed a distinct heatmap pattern for upregulated and downregulated proteins (Figure 8B).

To further elaborate on the function of proteins identified as significantly differentially abundant between old individuals with diabetes and healthy controls, pathway analysis was performed, based on the Bioplanet 2019 database. Proteins, up and down-regulated in diabetes were analyzed separately. N-glycan precursor substrate biosynthesis was identified as the most significantly enriched term from the significantly downregulated gene set in old individuals with diabetes compared to controls. The genes GMPPA and ALG5 which code for Mannose-1-phosphate guanyltransferase alpha", and "Dolichyl-phosphate beta-glucosyltransferase", respectively, were found to be significantly enriched in this term (Figure 8C).

4. Result

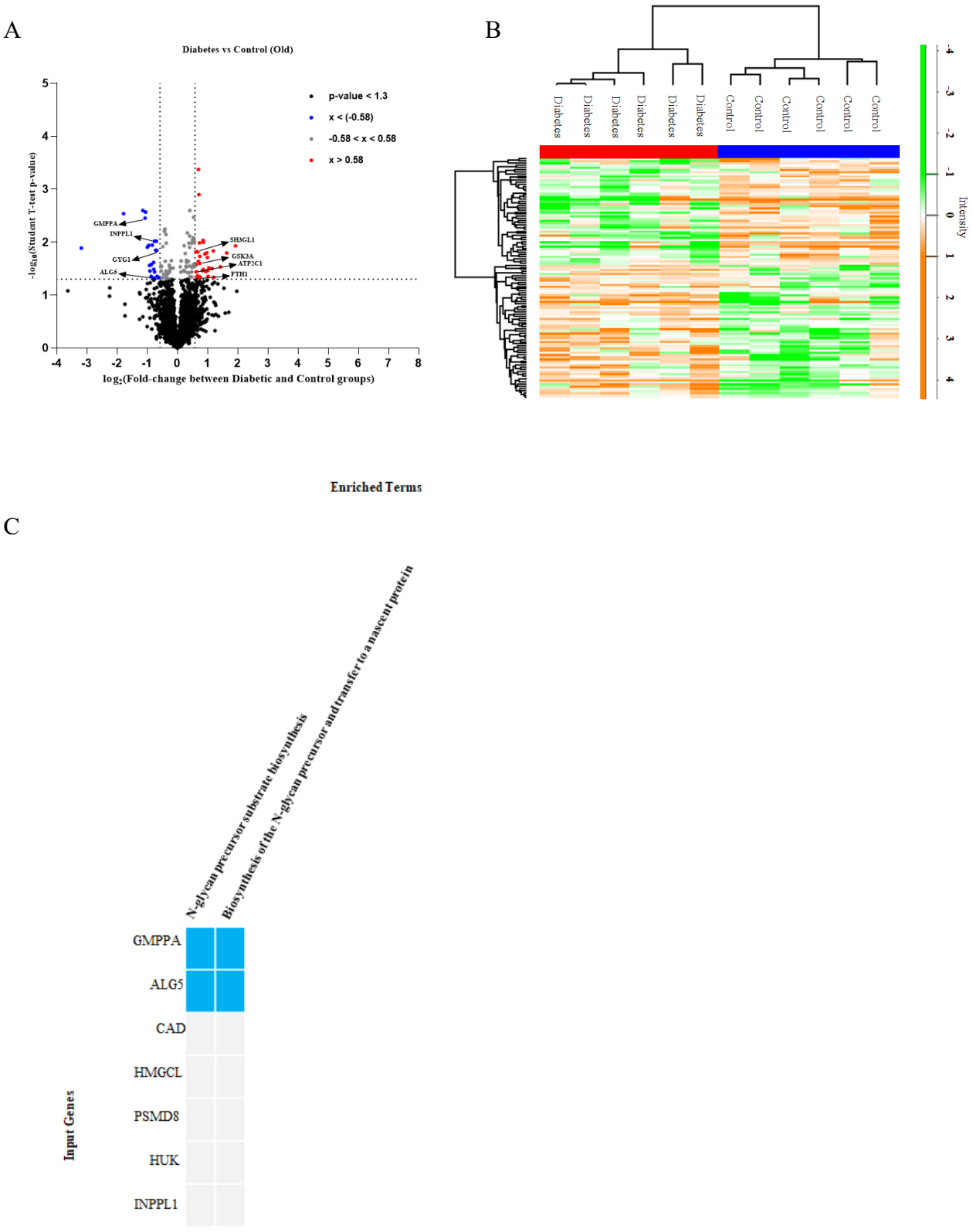

Figure 8: Differentially expressed proteins and altered pathways in the platelet proteome of old-aged diabetes compared to healthy sex- and age-matched controls. A) The volcano plot shows the two-sided unpaired t-test results for all quantified proteins from the platelet lysate in both diabetic and control groups of the old age group after

applying a randomForest-based algorithm for missing data imputation. Each dot indicates a protein. **B)** A heatmap and supervised cluster analysis of proteins extracted from platelets of old individuals with diabetes, compared to healthy sex- and age-matched controls, after applying a randomForest-based imputation strategy. The color intensity in the heatmap represents the relative abundance of proteins detected in each sample. In the heatmap, each column represents a sample, each row represents a protein, and each rectangle indicates the Pearson's correlation coefficient between a pair of data for the relative abundance of a protein in a sample. The value for the correlation coefficient is represented by the intensity of the orange or green color, as indicated on the color scale. **C**) To elucidate the biological functions and pathways associated with the significantly differentially expressed proteins between diabetes and control groups, gene set enrichment analysis of the downregulated genes in diabetes compared to controls from the whole platelet lysate in the old age group was performed, based on the Bioplanet 2019 database, using EnrichR. N-glycan precursor substrate biosynthesis was identified as the most significantly enriched term from the significantly downregulated gene set in old individuals with diabetes compared to controls. The genes GMPPA and ALG5 were found to be significantly enriched in this term.

4.3. Assessment of Platelet Reactivity Utilizing Plasma-derived Extracellular Vesicles

Plasma-derived EVs are released by a variety of cell types including platelets, erythrocytes, and endothelial cells into the circulation [129]. They possess diverse biological functions including modulating platelet reactivity. Both hyperactivity of platelets and platelet-derived EVs play a key role in thrombus formation [130]. The increased tendency of activated platelets to make thrombi has been observed in diabetes patients [131]. Furthermore, acute thrombosis is associated with an increased risk of cardiovascular events [130]. To gain a comprehensive understanding of how plasma-derived EVs from diabetes patients and healthy individuals affect platelet reactivity and the proteome profile of platelets, plasma-derived EVs from diabetes and control groups were enriched. Healthy platelets were then treated with the CD63-positive population of plasma-derived EVs from diabetes patients and healthy individuals.

4.3.1. Plasma-derived Extracellular Vesicles Counting Using Flow Cytometry

The CD63-positive plasma-derived EVs population from both diabetes and healthy individuals were selected in the histogram using flow cytometry. Next, a dot plot was used with forward scattering on the X axis and side scattering on the Y axis to count the CD63-positive plasma-derived EVs subpopulation (0.1-1 micrometer) (Figure 9). The figure shows the gating strategy for a representative sample.

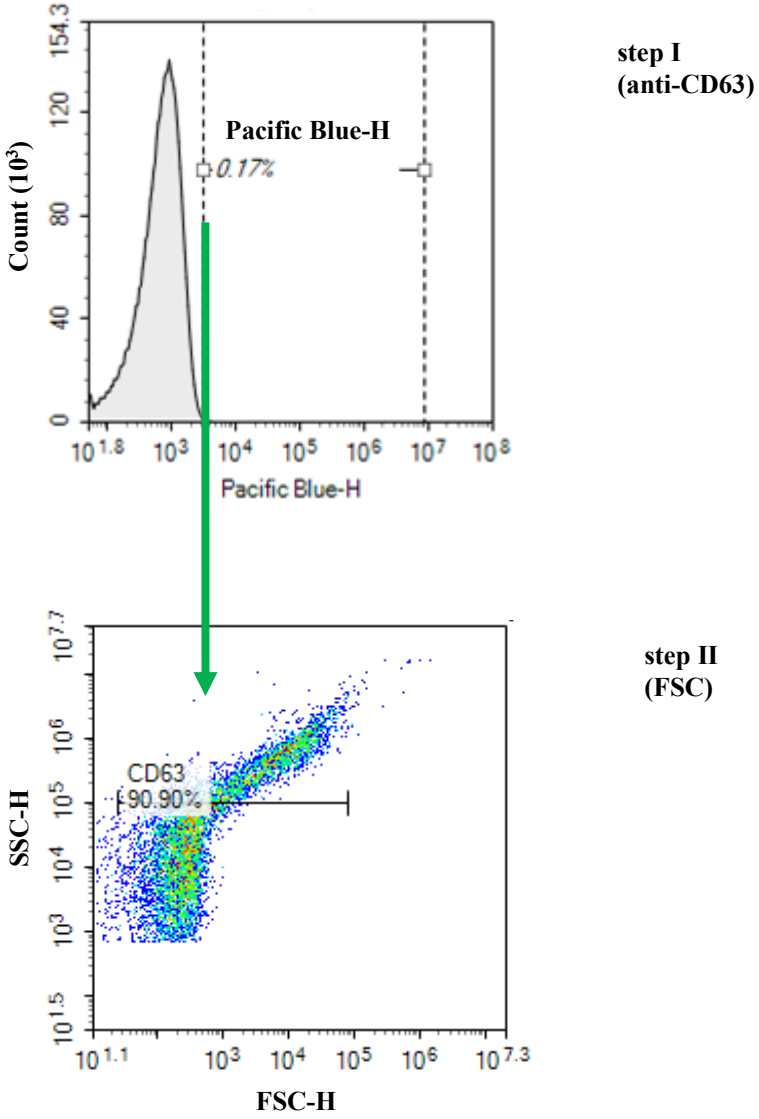

Figure 9: A schematic representation of plasma-derived EVs counting using flow cytometry. First, the histogram was used to select the CD63-BrilliantViolet420 -positive plasma-derived EVs population. Then, using a dot plot, the CD63-positive plasma-derived EVs subpopulation (0.1-1 micrometer, based on previous measurement with size beads) was selected and counted. The NovoCyte Quanteon Flow Cytometer System allows for real number measurements expressed as concentrations.

4.3.2. Platelet Aggregation in Response to Plasma-derived Extracellular Vesicles from Diabetic and Healthy Individuals

Healthy platelets were pre-incubated with plasma-derived EVs either from diabetes patients or control subjects, followed by the addition of 10µg/ml collagen (a platelet agonist), and the resulting platelet aggregation was represented by red and blue curves, respectively (Figure 10A). Similarly, healthy platelets were pre-incubated with plasma-derived EVs either from diabetes patients or control subjects, followed by the addition of 0.05 U/ml thrombin (a platelet agonist), the resulting platelet aggregation was represented by red and blue curves, respectively (Figure 10B). The green curve in both figures indicated the control without EVs treatment. This finding reveals a significant increase in platelet aggregation in response to diabetic EVs in the presence of platelet agonists (thrombin and collagen).

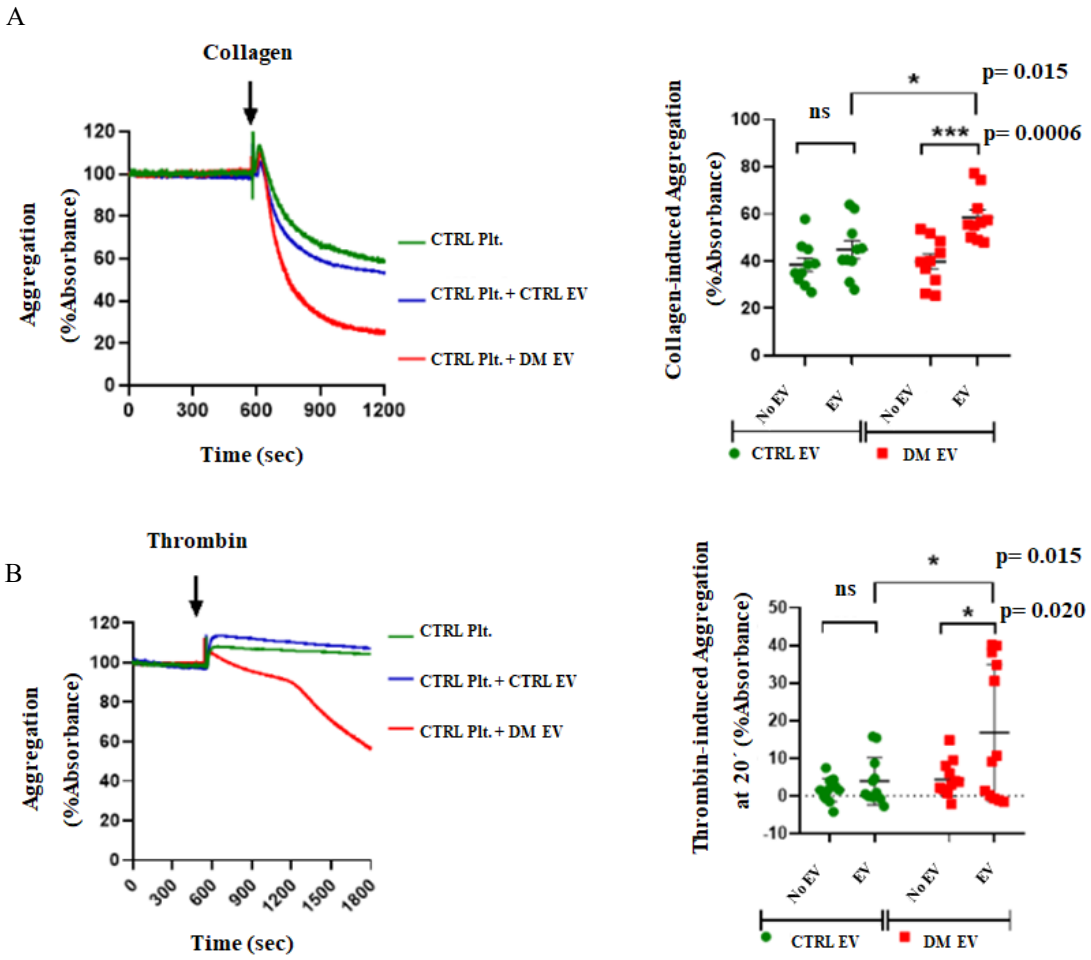

Figure 10: Stimulated aggregation study of healthy platelets in response to plasma-derived EVs from diabetic and healthy individuals, based on the CD63-positive

population of plasma-derived EVs (0.1-1 micrometer). A) Healthy platelets were pre-incubated with EVs extracted from the plasma of diabetes patients (n=10) and control subjects (n=10), followed by the addition of 10μg/ml collagen (the results are shown in red and blue curves, respectively), while the green curve indicates the control without EVs treatment. **B)** Healthy platelets were pre-incubated with EVs extracted from the plasma of diabetes patients (n=10) and control subjects (n=10), followed by the addition of 0.05 U/ml thrombin (the results are shown in red and blue curves, respectively), while the green curve indicates the control without EVs treatment. The figures on the right show the numerical data analyzed by one-way ANOVA. Asterisks represent statistical significance at * $p < 0.05$ and *** $p < 0.001$. The abbreviation 'ns' represents the concept of 'not significant'.

4.3.3. Phosphorylation of Tyrosine Residues in Healthy Platelets Treated with Plasma-Derived Extracellular Vesicles from Diabetic and Healthy Individuals

Phosphorylation of tyrosine residues in platelet proteins belonging to various signaling pathways is associated with platelet activation [132]. The objective is to investigate the phosphorylation of tyrosine residues in platelet proteins of healthy platelets treated with diabetic plasma-derived EVs or control plasma-derived EVs, as platelet aggregation was found to be higher in response to diabetic EVs compared to control EVs in the presence of platelet agonists like collagen and thrombin. To this end, approximately 50 million healthy platelets were treated with either 20,000 diabetes EVs positive for CD63 or 20,000 control EVs positive for CD63. Platelets were then lysed with RIPA buffer, and immunoblotting was performed using anti-p-Tyr antibody. Phosphorylation of tyrosine residues (p-Tyr) in the proteome of platelets treated with diabetic EVs was significantly increased compared to platelets that were not treated with EVs ($p<0.05$) or platelets treated with control EVs (Figure 11).

4. Result

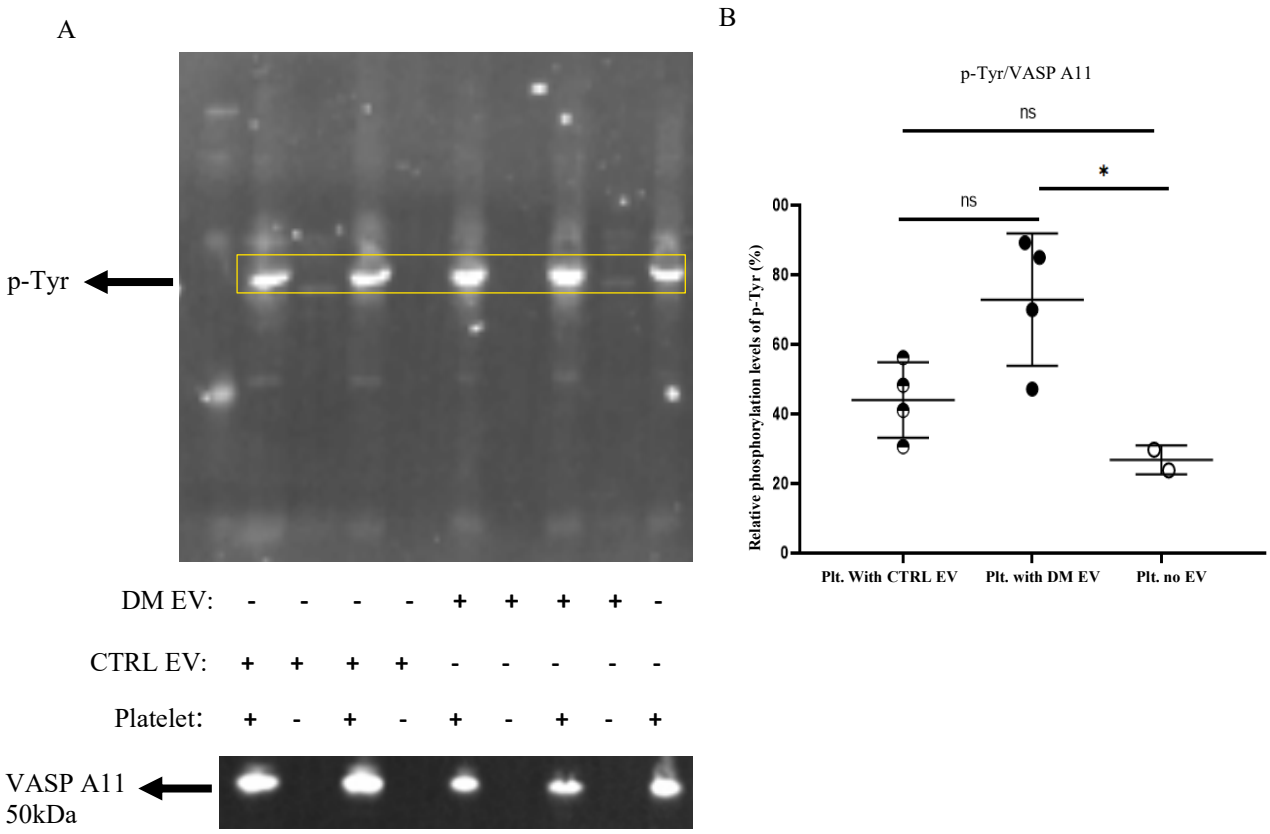

Figure 11: Phosphorylation of tyrosine residues in platelets treated with diabetes and healthy EVs, based on the CD63-positive population of EVs. A) Healthy platelets (approximately 50 million) were treated with either 20,000 diabetes-derived EVs positive for CD63 (n=4) or 20,000 control EVs positive for CD63 (n=4). Lanes with only diabetic EVs or control EVs served as controls. VASP A11 was used as loading control. **B)** The relative phosphorylation of p-Tyr over total VASP was determined using image J, statistical significance was assessed by one-way ANOVA for repeated measures. Asterisk represents statistical significance at * $p < 0.05$. The abbreviation 'ns' represents the concept of 'not significant'.

4.4. Comparison of Plasma-Derived Extracellular Vesicles Proteome Changes between Diabetic and Healthy Individuals Using the RIPA-SP3 Method

Given the observed significant increase in platelet aggregation in response to plasma-derived diabetic EVs in the presence of platelet agonists (thrombin and collagen) compared to those with plasma-derived control EVs, and the identification of increased platelet aggregation partly resulting from increased phosphorylation of tyrosine residues induced by plasma-derived diabetic EVs, the objective was to analyze the protein composition of plasma-derived EVs from both diabetic and healthy individuals.

4.4.1. Selection Criteria for Diabetes Patients and Healthy Controls

To obtain a broad understanding of the proteome of plasma-derived EVs in diabetes and healthy controls, the analysis was centered on plasma-derived EVs from middle-aged diabetes and healthy individuals. This approach could facilitate a comparison between groups that are relatively homogenous in terms of age and health status, while also minimizing the impact of age-related variations in the proteome. Blood samples were collected from a total of 24 individuals, comprising 12 individuals with diabetes and 12 healthy controls, age and gender matched. The volunteers were in the middle age range of 55 to 75 years. Diabetes patients were selected based on HbA1c values > 7.0% (indicative of hyperglycemia), while healthy controls were chosen with HbA1c < 6.0% (indicative of euglycemia). Following that, plasma-derived EVs from both diabetic and control groups were used for the experimental methods (Table 6).

Table 6: Selection criteria for diabetes patients and healthy controls based on the HbA1c values.

Sample number	Diabetes mellitus				Controls			
	Age	Sex	HbA1c	Platelet count	Age	Sex	HbA1c	Platelet count
7	73	F	8.8%	$2.126*10^8$	75	F	5.0%	$2.812*10^8$
8	70	M	7.4%	$1.389*10^8$	74	M	5.9%	$1.27*10^8$
9	75	F	7.1%	$1.814*10^8$	75	F	5.7%	$3.392*10^8$
10	58	M	8.2%	$3.688*10^8$	58	M	4.2%	$1.62*10^8$
11	57	F	7.5%	$2.677*10^8$	57	F	5.4%	$2.216*10^8$
12	61	M	7.2%	$1.114*10^8$	62	M	5.5%	$1.322*10^8$
13	65	M	9.3%	$2.217*10^8$	60	M	5.7%	$1.224*10^8$
14	62	F	11.9%	$1.002*10^8$	58	F	5.6%	$1.923*10^8$
15	69	M	7.4%	$1.634*10^8$	65	M	5.5%	$1.335*10^8$
16	61	F	7.3%	$1.362*10^8$	64	F	5.2%	$2.933*10^8$
17	65	M	7.2%	$2.151*10^8$	62	M	5.7%	$2.538*10^8$
18	70	F	7.7%	$2.828*10^8$	70	F	5.9%	$3.117*10^8$

	Age	Sex	Diabetes	Controls
	Middle	woman	6	6
	Middle	man	6	6
Middle age = 55-75				

4.4.2. Workflow Overview

An overview of the workflow used in the experiment in this study is represented in figure 12 below. To extract plasma-derived EVs, PPP was obtained from the peripheral citrated blood of both diabetes patients (with HbA1c values > 7.0%) and controls (with HbA1c values < 6.0%) through centrifugation. Then, PFP was obtained through additional centrifugation of PPP. The plasma-derived EVs were isolated from PFP using ultracentrifugation and then lysed by ultrasonication in the presence of RIPA buffer. Extracted proteins were proteolyzed by trypsin and identified by LC-MS/MS.

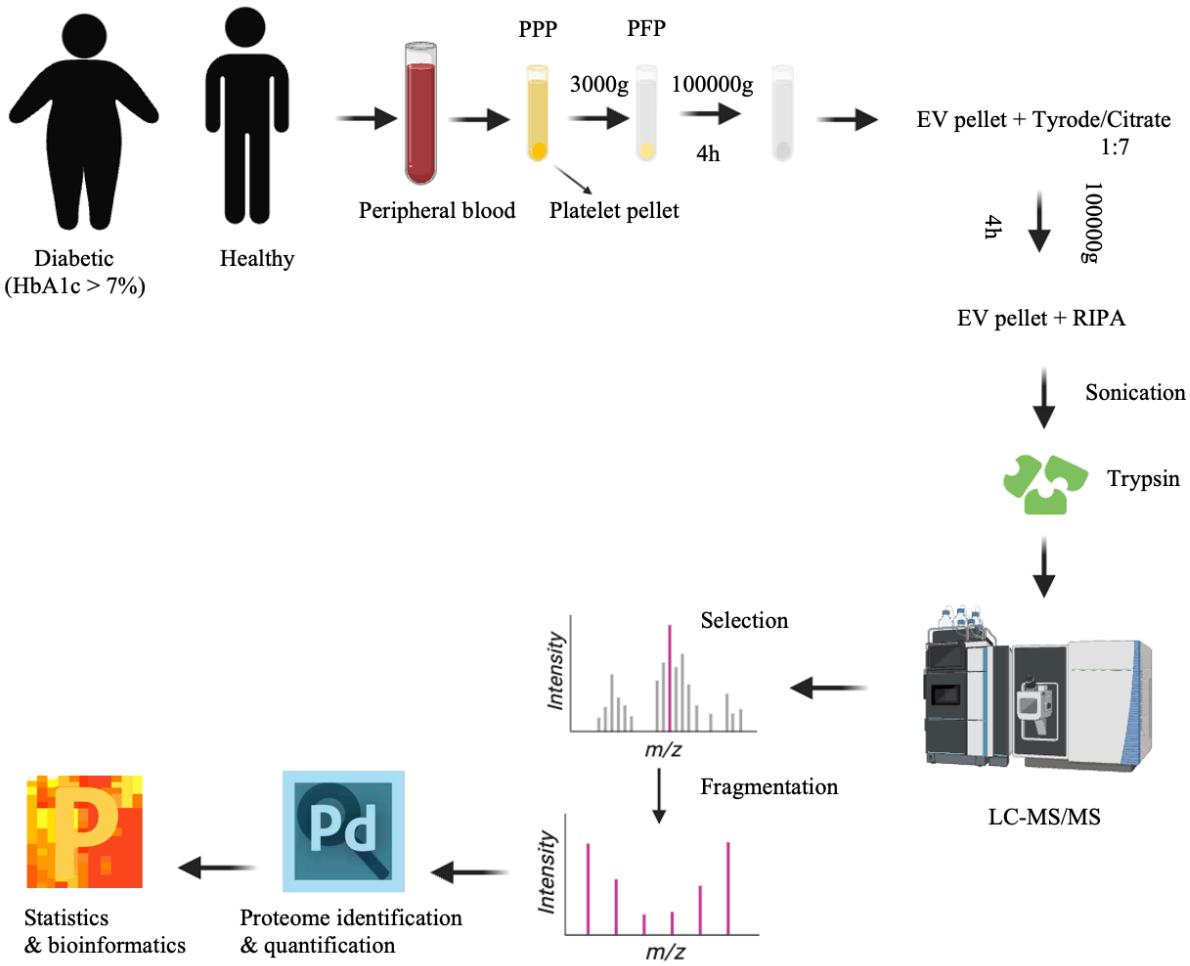

Figure 12: Overall scheme of plasma-derived EVs proteome profiling by using differential quantitative bottom-up proteomics. These include the key steps that were undertaken for protein identification and quantification in plasma-derived EVs from diabetes and healthy individuals.

4.4.3. Plasma-derived Extracellular Vesicles Proteome in Middle-Aged Diabetics versus Healthy Controls

In the plasma-derived EVs proteome of middle-aged individuals, a total of 1652 proteins were identified. Among the plasma-derived EVs proteome of middle-aged individuals, 26 unique proteins were found to be significantly more abundant (at least 1.5-fold) in individuals with diabetes compared to age- and sex-matched healthy controls, meeting the

threshold for statistical significance (p-value < 0.05). Meanwhile, 18 unique proteins were found to be significantly less abundant (at least 1.5-fold) in individuals with diabetes compared to controls. A volcano plot was generated to highlight these differences. Among the significantly differentially downregulated genes, PDIA3, BIN2, GRN, RAC2, RELA, ROCK2, and RELN, and among the significantly differentially upregulated genes, CAPZB, CAT, PPBP, JAK2, VPS45, SNX9, CLTC, and GPD2 may play a role in platelet function (Figure 13A).

66 proteins were identified as significant (p-value < 0.05) and able to clearly separate between middle-aged diabetes and healthy controls. Out of these, 26 proteins were found to be at least 1.5 times more abundant in diabetes, and 18 proteins were found to be at least 1.5 times less abundant in diabetes, both of which were used for further statistical analysis. The supervised cluster analysis clearly separated diabetes patients from healthy controls and revealed a distinct heatmap pattern for upregulated and downregulated proteins (Figure 13B).

To further elaborate on the function of proteins, identified as significantly differentially abundant between middle-aged diabetes and healthy controls, pathway analysis was performed, based on the Bioplanet 2019 database. Proteins, up and down-regulated in diabetes were analyzed separately (Figure 13C, and 13D). Adaptive immune system was identified as the most significantly enriched term that was identified from the significantly downregulated gene set in middle-aged diabetes patients compared to controls. The genes PDIA3, and RELA, which code for "protein disulfide-isomerase A3", and "transcription factor p65", respectively, were found to be significantly enriched in this term. Additionally, ROCK2, RAC2, and RELN, which code for "Rho-associated protein kinase 2", and "Ras-related C3 botulinum toxin substrate 2", and " Reelin", respectively, were found to be significantly enriched in focal adhesion. Of note, RELA was the main contributor to the all significantly enriched gene sets (Figure 13C). In contrast, hemostasis pathway was identified as one of the most significantly enriched term from the significantly upregulated gene set in middle-aged diabetes patients compared to controls. The genes JAK2, CAPZB, VPS45, and PPBP, which code for "tyrosine-protein kinase JAK2", "F-actin-capping protein subunit beta", "vacuolar protein sorting-associated protein 45" and "platelet basic protein", respectively, were found to be significantly enriched in hemostasis pathway (Figure 13D).

4. Result

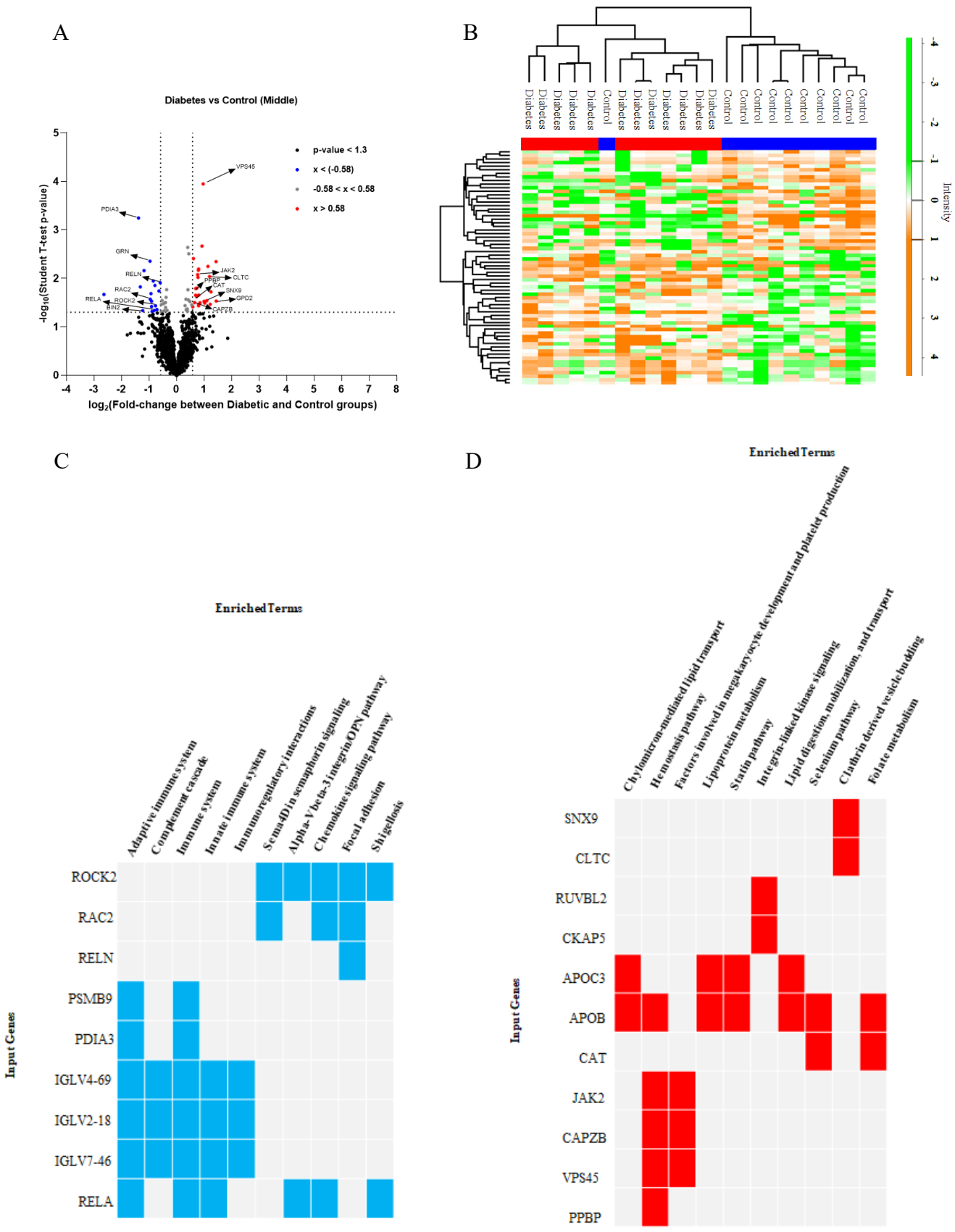
A
Diabetes vs Control (Middle)
p-value < 1.3
x < (-0.58)
-0.58 < x < 0.58
x > 0.58
VPS45
PDIA3
GRN
RELN
RAC2
RELA
ROCK2
BIN2
JAK2
PPBP
CLTC
CAT
SNX9
GPD2
CAPZB
-log10(Student T-test p-value)
log2(Fold-change between Diabetic and Control groups)
B
Diabetes
Control
Intensity
C
Enriched Terms
Adaptive immune system
Complement cascade
Immune system
Innate immune system
Immunoregulatory interactions
Sema4D in semaphorin signaling
Alpha-Vbeta-3 integrin/OPN pathway
Chemokine signaling pathway
Focal adhesion
Shigellosis
ROCK2
RAC2
RELN
PSMB9
PDIA3
IGLV4-69
IGLV2-18
IGLV7-46
RELA
Input Genes
D
Enriched Terms
Chylomicron-mediated lipid transport
Hemostasis pathway
Factors involved in megakaryocyte development and platelet production
Lipoprotein metabolism
Statin pathway
Integrin-linked kinase signaling
Lipid digestion, mobilization, and transport
Selenium pathway
Clathrin derived vesicle budding
Folate metabolism
SNX9
CLTC
RUVBL2
CKAP5
APOC3
APOB
CAT
JAK2
CAPZB
VPS45
PPBP
Input Genes

Figure 13: **Differentially expressed proteins and altered pathways in plasma-derived EVs proteome of middle-aged individuals with diabetes compared to healthy sex- and age-matched controls. A)** The volcano plot shows the two-sided unpaired t-test results for all quantified proteins from the plasma-derived EVs lysate in both diabetic and control groups of the middle-aged group after applying a randomForest-based algorithm for missing data imputation. Each dot indicates a protein. **B)** A heatmap and supervised cluster analysis of proteins extracted from plasma-derived EVs of middle-aged individuals with diabetes, compared to healthy sex- and age-matched controls, after applying a randomForest-based imputation strategy. The color intensity in the heatmap represents the relative abundance of proteins detected in each sample. In the heatmap, each column represents a sample, each row represents a protein, and each rectangle indicates the Pearson's correlation coefficient between a pair of data for the relative abundance of a protein in a sample. The value for the correlation coefficient is represented by the intensity of the orange or green color, as indicated on the color scale. **C**) and **D)** To elucidate the biological functions and pathways associated with the significantly differentially expressed proteins between plasma-derived diabetes EVs and control EVs, gene set enrichment analysis of the downregulated and upregulated genes in diabetes compared to controls from the plasma-derived EVs lysate in the middle-aged group was performed, based on the Bioplanet 2019 database, using EnrichR. Adaptive immune system was identified as the most significantly enriched term that was identified from the significantly downregulated gene set in middle-aged diabetes patients compared to controls. The genes PDIA3, and RELA were found to be significantly enriched in this term (Figure 13C). In contrast, hemostasis pathway was identified as one of the most significantly enriched term from the significantly upregulated gene set in middle-aged diabetes patients compared to controls. The genes JAK2, CAPZB, VPS45, and PPBP, were found to be significantly enriched in hemostasis pathway (Figure 13D).

4.5. Comparison of Proteome Changes in Platelet Soluble Fraction, along with Loosely Associated Membrane Proteins between Diabetic and Healthy Individuals

EVs can affect the target cell through different mechanisms: 1) by combining with the target cell and transferring their contents 2) by endocytosis and release of their contents; and 3) by binding to the target cell and transmitting signals [133].

It is known that Jak2 can increase the phosphorylation of tyrosine residues in the platelet proteome and affect platelet reactivity [134]. Another possible explanation for the increased phosphorylation of tyrosine residues in the proteome of platelets treated with diabetic EVs, compared to those with control EVs (Figure 11), could be the transfer of Jak2 from the EVs' contents into the platelets. Additional information on the platelet proteome that might be influenced by EVs was sought by focusing on the soluble fraction, along with loosely associated membrane proteins of the platelet proteome in both diabetes patients and healthy controls.

4.5.1. Selection Criteria for Diabetes Patients and Healthy Controls

Peripheral blood samples were collected from five diabetes patients and five healthy controls. Due to the requirement for a larger blood volume to enrich loosely associated membrane proteins and the limited number of volunteers willing to donate a large volume of blood, the focus was placed on diabetes patients with HbA1c values ≥ 6.5%, regardless of sex or age-matched controls. Diabetes patients were selected based on HbA1c values ≥ 6.5% (indicative of hyperglycemia), while healthy controls were chosen with HbA1c < 6.0% (indicative of euglycemia) (Table 7).

Table 7: Selection criteria for diabetes patients and healthy controls based on the HbA1c values.

Sample number	Controls			
	Age	Sex	HbA1c	Platelet count
1	43	W	5.5%	$2.638*10^8$
2	61	W	5.7%	$1.988*10^8$
3	85	M	5.2%	$3.127*10^8$
4	40	W	5.3%	$2.21*10^8$
5	53	M	5.4%	$1.89*10^8$
Sample number	**Diabetes**			
	Age	**Sex**	**HbA1c**	**Platelet count**
6	42	W	7.5%	$2.74*10^8$
7	69	M	8.4%	$3.515*10^8$
8	62	M	8.1%	$2.25*10^8$
9	48	W	6.5%	$3.68*10^8$
10	39	M	8.1%	$2.36*10^8$

	Age	Sex	Diabetes	Controls
	39-85	woman	**2**	**3**
	39-85	man	**3**	**2**

4.5.2. Workflow Overview

An overview of the workflow used in the experiment in this study is represented in figure 14 below. Washed platelets from the peripheral blood of diabetes (HbA1c values ≥ 6.5%) and controls (HbA1c values < 6.0%) were isolated by centrifugation and lysed by ultrasonication in the presence of a citrate wash buffer (hypotonic solution). The soluble fraction, along with loosely associated membrane proteins (S2), was proteolyzed by trypsin and identified by LC-MS/MS.

4. Result

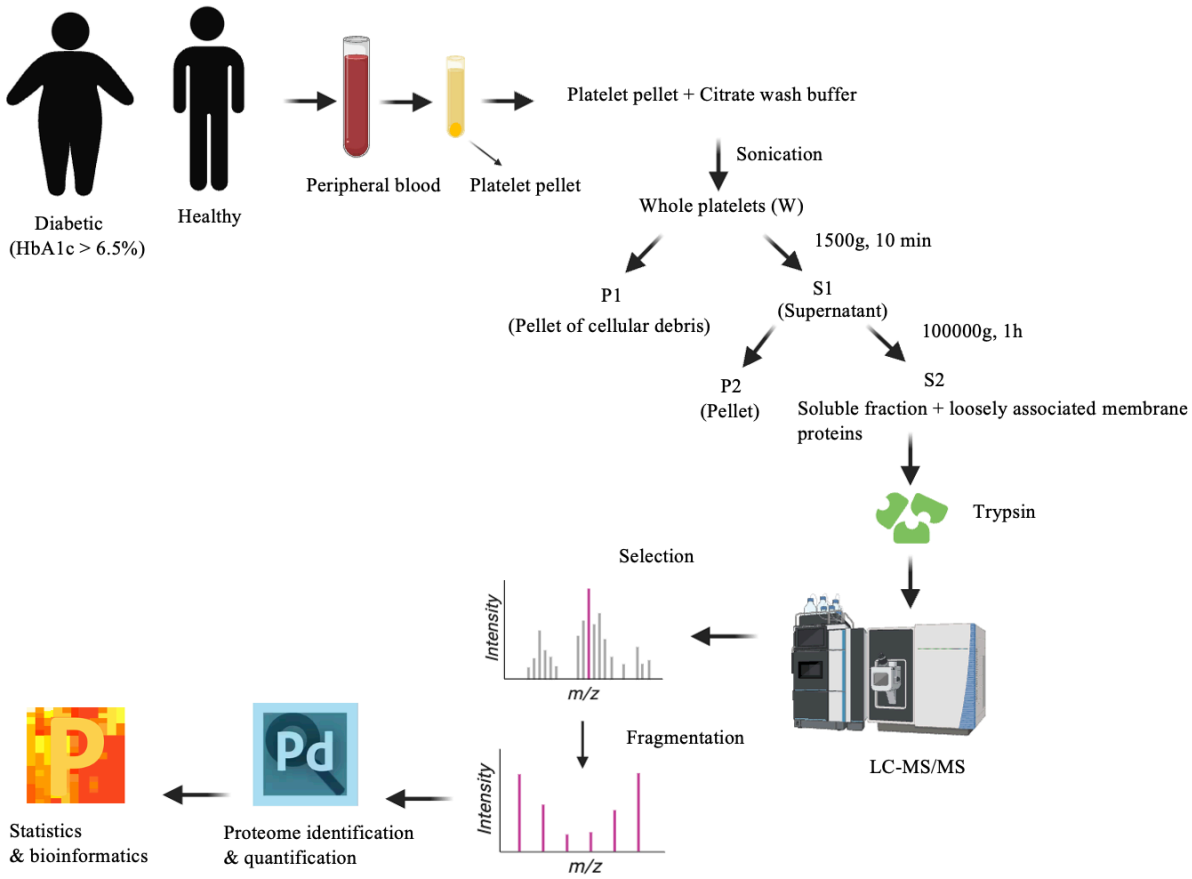

Figure 14: **Overall scheme of platelet proteome profiling from different fractions of platelets between diabetic and healthy individuals by using differential quantitative bottom-up proteomics.** These include the key steps that were undertaken for protein identification and quantification in soluble fraction, along with loosely associated membrane proteins.

4.5.3. Proteome Changes in Platelet Soluble Fraction, along with Loosely Associated Membrane Proteins, in Diabetics versus Healthy Controls

Among all identified proteins in S2 (1969), 32 unique proteins were found to be significantly more abundant (at least 1.5-fold) in individuals with diabetes compared to healthy controls, meeting the threshold for statistical significance (p-value < 0.05). Meanwhile, 35 unique proteins were found to be significantly less abundant (at least 1.5-fold) in individuals with diabetes compared to controls. A volcano plot was generated to highlight these differences. Among the significantly differentially downregulated genes, GP1BB, and GP9, and among the significantly differentially upregulated genes, NCK1 may play a role in platelet function (Figure 15A).

139 proteins were identified as significant (p-value < 0.05) and able to clearly separate between diabetes patients and healthy controls. Out of these, 32 proteins were found to be at least 1.5 times more abundant in diabetes, and 35 proteins were found to be at least 1.5 times less abundant in diabetes, both of which were used for further statistical analysis. The supervised cluster analysis clearly separated diabetes patients from healthy controls and revealed a distinct heatmap pattern for upregulated and downregulated proteins (Figure 15B).

To further elaborate on the function of proteins, identified as significantly differential abundant between individuals with diabetes and healthy controls, pathway analysis was performed, based on the Bioplanet 2019 database. Proteins, up and down-regulated in diabetes were analyzed separately (Figure 15C, and 15D). Platelet adhesion to exposed collagen was the most significant enriched term that was identified from the significantly downregulated gene set in diabetes patients compared to controls. The genes GP9, GP1BB and ITGB1, which code for "Platelet glycoprotein IX", "Platelet glycoprotein Ib beta chain" and "Integrin beta-1", respectively, were found to be significantly enriched in this term (Figure 15C). In contrast, Y branching of actin filaments was identified as one of the most significantly enriched term from the significantly upregulated gene set in diabetes patients compared to controls. The gene NCK1, which code for "Cytoplasmic protein NCK1", was found to be significantly enriched in this term (Figure 15D).

4. Result

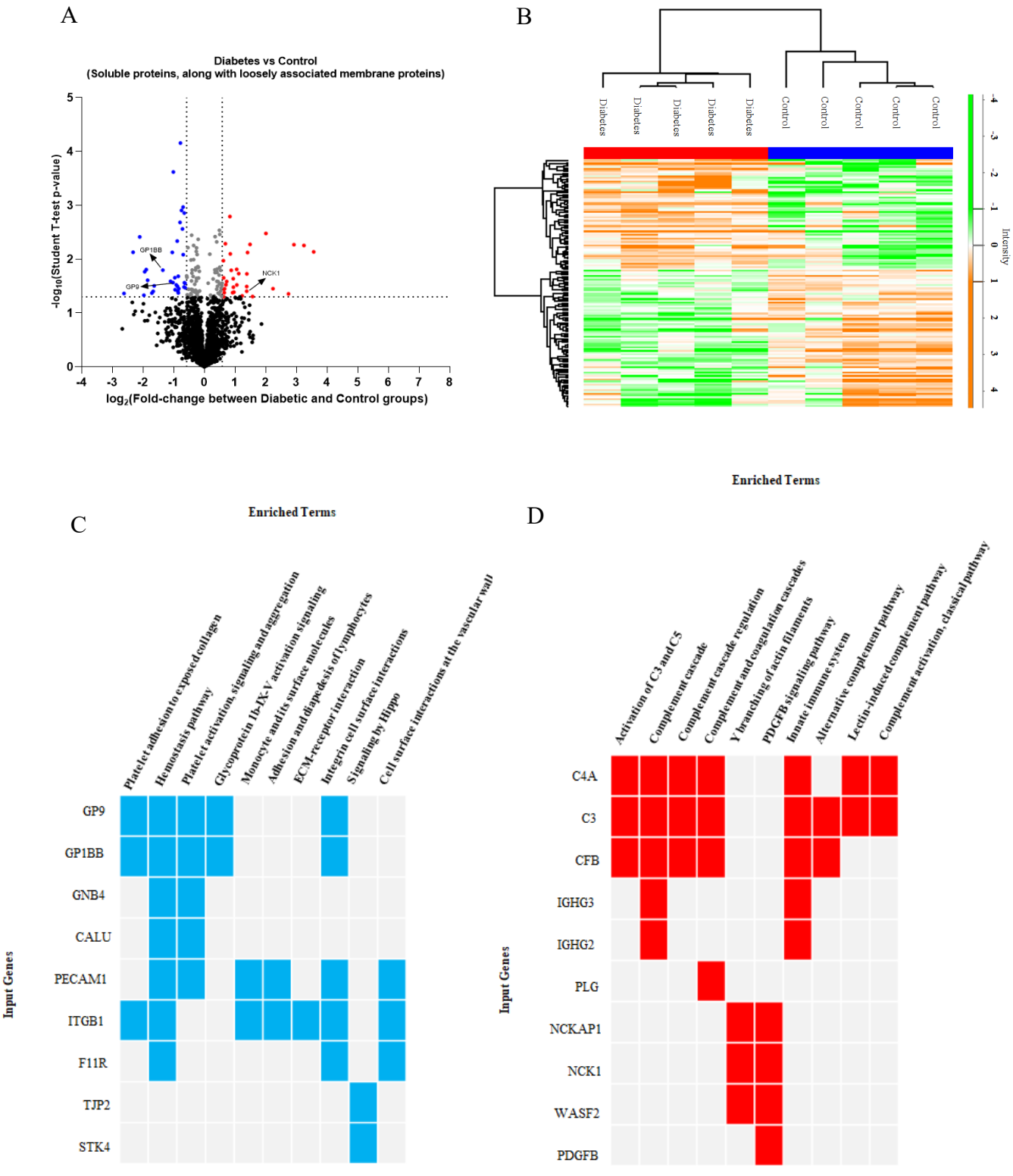

Figure 15: Differentially expressed proteins and altered pathways in the platelet soluble fraction, along with loosely associated membrane proteins from diabetes platelets compared to healthy controls. A) The volcano plot shows the two-sided unpaired t-test results for all quantified proteins from the S2 fraction of both diabetes and

control platelets after applying a randomForest-based algorithm for missing data imputation. Each dot indicates a protein. **B)** A heatmap and supervised cluster analysis of proteins from S2 fraction extracted from platelets of diabetes, compared to healthy controls, after applying a randomForest-based imputation strategy. The color intensity in the heatmap represents the relative abundance of proteins detected in each sample. In the heatmap, each column represents a sample, each row represents a protein, and each rectangle indicates the Pearson's correlation coefficient between a pair of data for the relative abundance of a protein in a sample. The value for the correlation coefficient is represented by the intensity of the orange or green color, as indicated on the color scale. **C)** and **D)** To elucidate the biological functions and pathways associated with the significantly differentially expressed proteins between diabetes and control groups, gene set enrichment analysis of the downregulated and upregulated genes in diabetes compared to controls from S2 was performed, based on the Bioplanet 2019 database, using EnrichR. Platelet adhesion to exposed collagen was the most significant enriched term that was identified from the significantly downregulated gene set in diabetes patients compared to controls. The genes GP9, GP1BB and ITGB1 were found to be significantly enriched in this term (Figure 15C). In contrast, Y branching of actin filaments was identified as one of the most significantly enriched term from the significantly upregulated gene set in diabetes patients compared to controls. The gene NCK1 was found to be significantly enriched in this term (Figure 15D).

5. Discussion

Abnormal platelet function in individuals with DM can be attributed to oxidative stress, dyslipidemia, and a combination of insulin resistance/hyperglycemia [80]. The manner in which platelets are activated determines the size, content, and quantity of released platelet-EVs, which can lead to different effects and varying degrees of involvement in the development of diseases related to platelet activation [135]. In diabetes, platelet-derived EVs may contribute to diabetic complications such as DR, diabetic nephropathy (DN), and atherosclerosis [136], [137], [138]. However, the role of plasma-derived EVs in diabetes is still not fully understood.

Platelets play a crucial role in blood clotting, and their hyperactivity in diabetes can contribute to thrombus formation, a hallmark of many CVDs. Additionally, platelet hyperactivity can cause endothelial dysfunction, which is a significant contributor to the development of several complications associated with diabetes. However, the molecular mechanisms underlying the abnormal activity of platelets in diabetes are not yet fully understood. Studying the platelet proteome, plasma-derived EVs, and platelet fractions from both diabetic and healthy individuals can provide a more comprehensive understanding of the molecular mechanisms involved in platelet hyperactivity, thrombose formation, increased risk of CVDs, and impaired hemostasis in diabetes compared to healthy controls and help to identify potential biomarkers for the hyperactivity of platelet in diabetes.

5.1. Platelet Protein Extraction Using Detergent-Based Methods

Choosing the most appropriate protein extraction method is a critical step in proteomics research. To extract proteins successfully, it is crucial to consider both the nature of the sample and the biological question being pursued [139]. Information about protein yield and data reproducibility is important in choosing an appropriate protein extraction method [140]. Different detergents, such as SDS and SDC, can be used to extract proteins from cells [141], [142]. However, since detergents may suppress both MS signal and protease activity, they have to be removed before protein digestion and MS analysis. FASP and

5. Discussion

SP3 are common methods used to remove detergents [143]. The results of the prior investigation suggest that substituting 1% SDC for 4% SDS (based on FASP protocol) in the protein extraction process from THP1 cell lysate can increase the protein yield. Thus, it is possible to use 1% SDC as a detergent for THP1 cell lysis instead of 4% SDS [144]. Another study indicated that the use of the SP3-based method resulted in the identification of a higher number of total and unique proteins compared to the FASP-based method from the cell lysate of *Symbiodinium tridacnidorum* (cell lysis was performed using a sonicator) [145]. Mikulášek et al. suggested that the SP3 method using carboxylated magnetic beads was superior to the FASP method in terms of protein yield, data reproducibility, cost per assay, and reduced handling time for removing SDS and other impurities from *Arabidopsis thaliana* lysate [143].

Various lysis buffers have been utilized to extract platelet proteins for mass spectrometry analysis. In a recent study, ammonium bicarbonate (NH4HCO3) was used as a lysis buffer to extract platelet proteins from COVID-19 patients and healthy controls [146]. A prior study utilized a lysis buffer with 8 M urea (pH 8.0) to extract platelet proteins from both healthy individuals and patients with Alzheimer's disease [147]. Additionally, the platelet proteome of mice with mild hyperlipidemia and control mice was extracted using SDS lysis buffer [148]. While the FASP method is widely used to remove detergents and impurities from platelet lysates [149], [148], it has been determined that there is no single sample preparation method that can be used universally for all types of samples [150]. Therefore, in the current study, three different experimental methods, namely SDC-SP3, SDS-SP3, and SDS-FASP, were utilized to determine the appropriate protein extraction method for extracting platelet proteins [119], [120], [151]. The SDS-FASP (2092) method had the highest protein yield, followed by SDC-SP3 (1833) and then SDS-SP3 (1772). Although the SDS-FASP method provided a higher protein yield than SDC-SP3 and SDS-SP3, there were no substantial differences in the number of identified proteins among the three groups (Figure 2 and figure 3). Regarding data reproducibility, both SDS-SP3 and SDS-FASP exhibited higher data reproducibility (R^2= 0.9) than SDC-SP3 (R^2= 0.8) (Figure 4), suggesting that the SDS-SP3 and SDS-FASP methods generate more reliable and accurate outcomes than SDC-SP3. Despite the high data reproducibility observed in both SDS-SP3 and SDS-FASP, the SDS-SP3 protocol was chosen for extracting platelet proteins due to its cost-effectiveness [125], [120].

5.2. Platelet Proteome Changes between Diabetic and Healthy Individuals

The risk of developing cardiovascular disease increases with age, partly due to the higher prevalence of comorbid conditions (such as diabetes, obesity, hypertension, hyperlipidemia, etc.) that are commonly observed in older individuals. Since platelets play a crucial role in the progression of thrombotic vascular disease in diabetes patients and are affected by age-related changes in function [152], [127], the platelet proteome was examined in individuals with diabetes and healthy controls across three different age categories (young, middle-aged, and old). The purpose of this analysis was to identify which proteins from diabetes patients in different age groups can impact platelet reactivity and increase the risk of vascular disease. In young-aged, middle-aged, and old-aged diabetes patients, significant downregulation and upregulation of specific platelet proteins were observed (Figures 6A, 7A, and 8A). These changes were associated with increased platelet hyperactivity, increased thrombus formation, and an elevated risk of CVDs in diabetes. Furthermore, certain proteins exhibited a compensatory mechanism, resulting in decreased platelet activation.

5.2.1. Platelet proteome changes between young-aged diabetic and healthy individuals

E3 ubiquitin-protein ligase KCMF1

The different types of ubiquitin ligases, including E1, E2, and E3 ubiquitin ligases, play a crucial role in regulating platelet biology. For example, the E3 ligase RNF181 binds to the platelet integrin αIIbβ3. Another study has indicated that mice lacking the ubiquitin ligase c-Cbl show hyperactivation of platelets when stimulated with GPVI agonists, which corresponds to the loss of Syk ubiquitylation [153]. In the obtained data, E3 ubiquitin-protein ligase KCMF1 was significantly downregulated (Figure 6A), which might be a reason for platelet hyperactivity in young-aged diabetes.

5. Discussion

Mitochondrial contact site and cristae organizing system complex subunit MIC27

The abnormal mitochondrial inner membrane structure is associated with several diseases, including diabetes. The mitochondrial contact site and cristae organizing system (MICOS) complex is involved in controlling the shape and formation of the mitochondrial cristae [154]. In the obtained data, the MICOS complex subunit MIC27 was significantly downregulated (Figure 6A), which may contribute to mitochondrial dysfunction and platelet hyperactivity in young individuals with diabetes.

Pyruvate dehydrogenase E1 component subunit alpha, somatic form, mitochondrial

Platelets from diabetes patients display increased pyruvate dehydrogenase E2 activity and higher levels of acetyl-CoA, resulting in a more significant accumulation of ATP/ADP than platelets from healthy control. Therefore, thrombin caused higher ATP/ADP release in diabetic platelets, leading to excessive production of ROS and stronger platelet aggregation compared to platelets from healthy controls. The function of PDHA1, which code for pyruvate dehydrogenase E1 component subunit alpha, somatic form, mitochondrial is not known in diabetes platelets [155]. In the obtained data, PDHA1 protein was significantly downregulated in platelet of young-aged diabetes compared to control (Figure 6A). This may be a compensatory mechanism to reduce platelet aggregation in diabetes platelet.

Peroxiredoxin-2

Peroxiredoxin-2 negatively regulates platelet activation through the collagen-GPVI engagement pathway. Deficiency of peroxiredoxin-2 increased GPVI-mediated platelet activation and resulted in elevated levels of tyrosine phosphorylation of Syk, Btk, and phospholipase Cγ2. In mice, peroxiredoxin-2 deficiency led to increased thrombus formation in injured carotid arteries when compared to control mice [156]. Furthermore, peroxiredoxins maintain the balance of ROS levels against excessive ROS production that can contribute to the pathogenesis of CVDs [157]. In the obtained data, peroxiredoxin-2 was significantly downregulated (Figure 6A), which may increase platelet activation, ROS generation, and the risk of CVDs in young diabetic individuals.

5. Discussion

Guanylate cyclase soluble subunit alpha-3

Guanylate cyclase soluble subunit alpha-3 (GUCY1A3), which encodes the α_1-subunit of the soluble guanylyl cyclase (sGC), is highly expressed in both platelets and vascular smooth muscle cells [158], [159]. The sGC complex serves as the receptor for NO and catalyzes the production of cyclic guanosine monophosphate (cGMP), which has various cellular functions, such as the inhibition of platelet aggregation and smooth muscle cell relaxation [160]. In this study, the downregulation of GUCY1A3 in platelets of young patients with diabetes (Figure 6A) is likely due to several factors. The exact mechanism by which GUCY1A3 is downregulated in diabetes platelets is unknown. However, it is proposed that hyperglycemia, oxidative stress, and inflammation, all of which are known to occur in diabetes, can contribute to the downregulation of GUCY1A3 expression. Additionally, the reduction in cGMP synthesis due to the downregulation of GUCY1A3 might be linked to platelet hyperactivity and increased risk of thrombotic events in diabetes. Therefore, strategies to increase GUCY1A3 expression or enhance cGMP production may have potential therapeutic benefits in diabetes.

Guanine nucleotide-binding protein G(s) subunit alpha isoforms XLas

Guanine nucleotide-binding protein G(s) subunit alpha isoforms XLas (GNAS) can encode a large variant of Gsα called extra-large α-subunit (XLαs), and changes in XLαs abundance or activity have been linked to several human disorders [161]. The Gsα protein, which includes the XLαs isoform, is expressed in platelets [162]. The majority of platelet physiological activators such as thrombin, thromboxane A2, and ADP act through G-protein-coupled receptors (GPCRs), which implies that Gsα protein plays a role in this process [163]. At the biochemical level, XLαs acts comparably to Gαs and increases the production of cyclic adenosine monophosphate (cAMP) through activation of GPCRs when its abundance is raised [164], [165]. In the obtained data, the downregulation of GNAS in platelets of young-aged diabetes patients (Figure 6A) can lead to decreased cAMP production and increased platelet activation and aggregation. This can result in an increased risk of thrombosis in diabetes patients.

As discussed before GUCY1A3 and GNAS play a role in platelet activation and aggregation, as well as in regulating intracellular signaling pathways that modulate

platelet function. Therefore, the downregulation of GUCY1A3 and GNAS expression in diabetes platelets may contribute to platelet hyperactivity and increased release of vasoconstrictive and pro-inflammatory factors, ultimately leading to impaired ion channel function in vascular endothelial cells and the development of cardiovascular complications (Figure 6C).

Macrophage migration inhibitory factor

Macrophage migration inhibitory factor (MIF) is released from activated platelets and is involved in various biological processes, including inflammation, glucose metabolism, insulin resistance, diabetes, and cardiovascular disease [166], [167], [168]. The interaction between MIF and CXCR7 modulates the survival of platelets and leads to a reduction in thrombus formation, as observed in both *in vitro* and *in vivo* conditions [169]. The upregulation of MIF in the platelet proteome in young-aged diabetes patients (Figure 6A) may act as a compensatory mechanism to reduce the risk of thrombotic events and CVDs.

C6, C8G, and complement factor H

Complement activation may lead to CVDs in T2DM patients [170]. The presence of C3, C5, C6, C7, C8, and C9 of human complement enhances thrombin-mediated platelet aggregation and release. The arachidonic acid transformation pathway is likely responsible for the enhancement of platelet function induced by complement [171]. In C6-deficient rats, platelet aggregation induced by adenosine diphosphate was significantly decreased. Furthermore, the rats exhibited prolonged tail bleeding times, which were ameliorated by administering purified rat C6 protein [172]. Schmiedt et al. proposed that deficiency of C6 complement in rabbits provides protection against the development of atherosclerotic plaques induced by a cholesterol-rich diet [173]. In the obtained data, significant upregulation of C6 and C8G in young-aged diabetes patients was observed (Figure 6A). These proteins were found to be enriched in various pathways, such as the terminal pathway of complement, alternative complement pathway, complement and coagulation cascade, lectin-induced complement pathway, and the complement cascade (Figure 6D). Although it has been shown that inhibitors of cyclo-

oxygenase, such as aspirin and indomethacin, can reduce thrombin-induced release of platelet serotonin in the presence of C3, C5, C6, C7, C8, and C9 [171], it remains unclear whether the complement proteins interact directly with platelets or indirectly through other factors. Furthermore, since the previous study used a mixture of complement proteins, it is difficult to determine which specific complement components were responsible for the observed effect. However, given the upregulation of C6 and C8G in young-age diabetes patients, it is possible that these complement proteins may be involved in the enhanced platelet aggregation seen in diabetic patients. Further research is needed to fully understand the relationship between complement activation and platelet function in diabetes and to identify potential targets for drug development. In contrast, complement factor H (CFH) significantly upregulated in the obtained data (Figure 6A) and enriched in complement and coagulation cascade, and complement cascade (Figure 6D). CFH is the major inhibitor of the alternative pathway of the complement system and prevents the activation of the complement system by inhibiting the formation of the C3 convertase enzyme complex. CFH can be secreted by different cells including platelet. Additionally, CFH can bind to the platelet αIIbβ3 integrin, which could possibly decrease the ability of platelets to bind to adhesive ligands during thrombus formation [174]. The involvement of CFH in cardiovascular diseases has been observed elsewhere [175], [176], [177]. The upregulation of CFH in the young-aged diabetes patients can be considered as a compensatory mechanism to counterbalance the increased complement activation and chronic inflammation associated with diabetes. It is notable that, except for CFH, there is no recorded proof of platelets secreting C6 and C8G. Interestingly, the fact that these complements are absent in the obtained EVs proteome data suggests that they are unlikely to come from EVs that coated platelets. Instead, their presence in the platelet proteome might result from interactions involving binding or scavenging. The higher levels of C6 and C8G in the platelet proteome of diabetes patients compared to those with healthy platelets could be due to the complex interplay between platelets and the immune system, possibly linked to inflammatory processes.

Sirtuin-2

Sirtuins are implicated in various physiological processes and are associated with diabetes, cardiovascular disease, oxidative stress, insulin resistance, endothelial

dysfunction, and other conditions [178], [179], [180]. According to a previous finding, the expression of NAD-dependent protein deacetylase sirtuin-2 (SIRT2) was found to be reduced in various parts of the vasculature of aged mice, including the aorta, aortic valve, and cardiac endothelial cells. This decrease in SIRT2 expression was accompanied by an increase in both global cellular senescence and endothelial dysfunction [179]. Another study indicated that SIRT2 can reduce oxidative stress and mitochondrial dysfunction, ultimately improving insulin sensitivity in hepatocytes [178]. It was revealed that Sirt1, Sirt2, and Sirt3 are expressed in platelets and increased platelet survival *via* deacetylation and ubiquitination of P53. Therefore, sirtuins may be considered a potential therapeutic target to reduce the severity of thrombosis and thrombocytosis [181]. In the obtained data, the upregulation of SIRT2 in young-age diabetes patients (Figure 6A) may increase platelet survival and the risk of thrombosis.

cGMP-inhibited 3',5'-cyclic phosphodiesterase A

cGMP-inhibited 3',5'-cyclic phosphodiesterase A (PDE3A) is an enzyme that is crucial in controlling cAMP-related signaling within cardiac myocytes and platelets [182]. Thrombin stimulation of platelets can increase the activity of PDE3A *via* the phosphorylation of Ser^{312}, Ser^{428}, Ser^{438}, Ser^{465}, and Ser^{492} in a PKC-dependent manner [183]. PDE3A can cause platelet activation by hydrolyzing intracellular cAMP [182]. A previous finding indicated that cilostazol, a PDE3A inhibitor, was effective in preventing graft occlusion in an experimental model of thrombosis in rabbits [184]. Moreover, *in vivo* study suggested that cilostazol results in reduced platelet accumulation and decreases the initial rate of platelet accrual by increasing intracellular cAMP levels. The intracellular cAMP level controls the rate at which platelets attach and detach from sites of arteriolar injury [185]. The upregulation of PDE3A has been observed in diabetic cardiomyopathy [186]. PDE3A was significantly upregulated in young-aged diabetes patients (Figure 6A). Using a known PDE3A inhibitor such as cilostazol or developing inhibitors for different phosphorylation sites of PDE3A may be a possible approach to reduce PDE3A activity in young patients with diabetes.

5. Discussion

The adapter protein disabled-2

The adapter protein disabled-2 (DAB2) is highly expressed in platelets and is distributed in platelet alpha-granules. Upon platelet activation, DAB2 can be released from these granules [187]. The phosphotyrosine-binding domain (PTB) of Dab2 exhibits involvement in various cellular functions, such as signal transduction, membrane trafficking, and cytoskeleton assembly [188]. Notably, this domain does not show a preference for phosphorylation in tyrosine residues or nonphosphorylated NPX(Y/F)-containing proteins, despite its initial characterization [189]. Dab2, through its PTB domain, hinders platelet aggregation by competing with fibrinogen for binding to the αIIbβ3 integrin receptor [187]. According to a recent finding, Dab2-serine 723 phosphorylation (Dab2-pSer723) is predominantly found in the cytosol of activated platelets and is involved in integrin inside-out signaling. On the other hand, Dab2-serine 24 phosphorylation (Dab2-pSer24) is primarily located in the membrane fraction of activated platelets and is associated with integrin outside-in signaling [190]. However, it is worth noting that Dab2 is necessary for normal hemostasis, as $Dab2^{-/-}$ mice exhibited prolonged bleeding time and impaired thrombus formation [191]. In addition to its crucial role in regulating platelet-platelet aggregation, Dab2 also modulates platelet-leukocyte interactions [192]. Dab2 is implicated in CVDs, and elevated expression of Dab2 has been observed in cases of acute myocardial infarction [193]. While increased levels of Dab2 are associated with CVDs, the upregulation of Dab2 in young-age diabetes patients (Figure 6A) may serve as a compensatory mechanism to impede platelet aggregation.

Phosphatidylinositol 3,4,5-trisphosphate 5-phosphatase

SHIP1, a phosphatidylinositol 3,4,5-trisphosphate 5-phosphatase, plays a crucial role in regulating phosphoinositide levels in platelets. It downregulates PtdIns(3,4,5)P3-dependent events and initiates PtdIns(3,4)P2-mediated mechanisms. SHIP1 knock-out mice demonstrate an accumulation of PtdIns(3,4,5)P3, a decrease in PtdIns(3,4)P2, impaired arterial thrombus formation, and a prolonged tail bleeding time. Additionally, SHIP1 serves a dual function in platelets, negatively regulating adhesion and spreading on fibrinogen-coated surfaces, while positively influencing platelet-platelet interactions and facilitating thrombus growth in suspension [194], [195]. Upregulation of SHIP1 in young-

aged diabetes patients (Figure 6A) may enhance platelet aggregation and elevate the risk of thrombus formation.

Pigment epithelium-derived factor

Pigment epithelium-derived factor (PEDF) is a type of glycoprotein that can prevent the overexpression of platelet CD40L in individuals with diabetes by blocking the impact of AGEs on platelets. Consequently, this mechanism could potentially have a protective effect against CVDs in diabetes patients [196]. *In vitro*, PEDF significantly decreased the production of ROS in collagen-induced platelets, which subsequently led to the inhibition of platelet activation and aggregation. *In vivo*, PEDF administration can prevent the formation of thrombi by inhibiting platelet activation and aggregation, which is attributed to its anti-oxidative properties [197], [198], and reduced tail bleeding time in diabetic rats [199]. PEDF reduces platelet aggregation not only through its anti-oxidative properties but also by suppressing the activity of plasminogen activator inhibitor-1 (PAI-1), a key inhibitor of fibrinolysis [200]. PEDF plays a protective role against CVDs and increased levels of PEDF have been observed in individuals with T2DM [201]. Increased levels of PEDF have been seen in DR and DN patients [202], [203]. The upregulation of PEDF in young-aged diabetes patients (Figure 6A) may act as a compensatory mechanism to reduce platelet activation and aggregation. It may also reduce the risk of CVDs.

5.2.2. Platelet proteome changes between middle-aged diabetic and healthy individuals

Glycogen synthase kinase 3 alpha

Glycogen synthase kinase 3 (GSK3) alpha, and GSK3β are phosphorylated on Ser^{21} and Ser^{9}, respectively, *via* phosphoinositide 3-kinase (PI3K) activity in human platelets stimulated with collagen, convulxin, and thrombin [204]. Phosphorylation of a serine at the N-terminal region (Ser^{21} in GSK3α and Ser^{9} in GSK3β) reduces their kinase activity towards substrates. Differential roles of GSK3α and GSK3β phosphorylation in regulating platelet function were revealed through GSK3 single knock-in mouse models. Enhanced

5. Discussion

GPVI-mediated platelet activation was observed upon expression of phosphorylation-resistant GSK3α, whereas a decrease in PAR-mediated platelet activation and impairment *in vitro* thrombus formation under flow was observed upon expression of phosphorylation-resistant GSK3β [205]. There are multiple pathways involved in phosphorylating GSK3α/β in platelets. Another study indicated that both the PI3K-independent pathway, which involves protein Kinase C α (PKCα), and the PI3Kβ/Akt pathway play a role in mediating the phosphorylation of GSK3α/β in platelets. Herein, early thrombin-mediated GSK3 phosphorylation is predominantly associated with PKCα, while late thrombin-mediated GSK3 phosphorylation is dependent on the PI3K/Akt pathway [206]. The role of GSK3 has been reported in retinal neuron apoptosis in early diabetic retinopathy. It has been observed that the administration of lithium chloride, an inhibitor of GSK3, can effectively reduce retinal neuron apoptosis [207]. Additionally, in streptozotocin-induced diabetic rat liver, the stability of glycogen synthase kinase-3 alpha mRNA is modified by insulin, leading to a decrease in its levels [208]. Downregulation of GSK3α in middle-aged diabetes patients (Figure 7A) may have different reasons: In diabetes, impaired insulin signaling is often observed. Insulin typically activates the PI3K/protein kinase B (Akt) pathway, which in turn inhibits GSK3 [209], [210], [211], [205]. The downregulation of GSK3α in the platelet proteome of middle-aged diabetes (Figure 7A) may result in increased GPVI-mediated platelet activation due to a decrease in the phosphorylation of GSK3α. Additionally, pro-inflammatory cytokines, such as interleukin-6 (IL-6), tumor necrosis factor-alpha (TNF-α), and interleukin-1 beta (IL-1β), can inhibit GSK3 activity [212]. Therefore, the downregulation of GSK3α isoform in platelets of middle-aged diabetes may be a result of the chronic inflammatory state.

Annexin A1

Annexin A1 (ANXA1) regulates platelet function, and its deletion upregulates the expression of its receptor, Fpr2/3, which is the orthologue of the human FPR2/ALX. Furthermore, ANXA1 plays a role in enhancing the phagocytosis of activated human platelets by neutrophils, initiating the resolution of thromboinflammation. Platelets derived-Anxa1$^{-/-}$ mice show reduced levels of GPIbα. Additionally, in the presence of CRP-XL and ADP, the reactivity of Anxa1$^{-/-}$ platelets was significantly reduced in a dose-dependent manner compared to those in the control group [213]. In a recent study,

the addition of full-length ANXA1 to platelets effectively prevented thrombosis *in vivo* by inhibiting their activation and diminishing their aggregating capability [214]. Annexin A1 has anti-inflammatory properties and can contribute to reducing inflammation in cardiovascular tissues [215]. Several studies demonstrated that expression of ANXA1 is reduced in diabetes. This protein has been proposed as a novel therapeutic target for addressing diabetes and managing microvascular diseases [216]. However, the expression of ANXA1 in platelets of individuals with diabetes has not been investigated so far. The reduced level of ANXA1 in platelets of middle-aged diabetes (Figure 7A) may increase platelet activation and aggregation.

Exocyst complex component 3-like protein 4

Exocyst complex component 3 (EXOC3) knockout (KO) platelets exhibited significant deficiencies in platelet aggregation, integrin activation, and the secretion of various granules, including α-granules, dense granules, and lysosomal granules, following treatment with collagen-related peptide (CRP). However, when the KO platelets were stimulated through protease-activated receptor 4 (PAR4) activation, either *via* PAR4-activating peptide or thrombin, a paradoxical effect was observed. Dense granule secretion, integrin activation, and surface expression of CD41 were notably increased, although calcium responses remained unaffected. The increased integrin activation responses were effectively suppressed by a P2Y12 receptor antagonist, indicating that enhanced secretion of adenosine 5'-diphosphate from dense granules played a crucial role in these responses. Moreover, the knockout mice exhibited accelerated arterial thrombosis and reduced tail bleeding times [217]. It is probable that EXOC3-like protein 4 (EXOC3L4) is a component of the exocyst complex. The presence of variability in the splicing regulatory element (SRE) sites within EXOC3L4 could potentially affect the transport of vesicles, leading to the emergence of phenotypes associated with Alzheimer's disease [218]. EXOC3-like 2 (EXOC3L2), is likely a component of the exocyst complex, which plays a role in normal cardiovascular development in mice [219]. The function of EXOC3L4 in platelets and its association with CVDs in diabetes patients remains unclear. As EXOC3L4 is a member of the EXOC3 family, the diminished expression of EXOC3L4 (Figure 7A) may potentially increase or decrease the risk of thrombus

formation in middle-aged diabetes patients, depending on the type of platelet agonist involved.

Vimentin

Platelet vimentin, which is part of the platelet cytoskeleton, has the potential to modulate fibrinolysis in both plasma and thrombi. This regulation occurs through its interaction with platelet-derived vitronectin (Vn)·type 1 plasminogen activator inhibitor (PAI)-complexes, thereby influencing the fibrinolytic process [220]. Vimentin plays a role in diminishing the adherence of human leukocytes to platelets and the endothelium through its binding to P-selectin, which is present on leukocytes and endothelial cells. As leukocyte adhesion to vascular endothelium and platelets is an early step in the acute inflammatory response, the use of recombinant vimentin may attenuate inflammation [221]. The co-expression of insulin and vimentin within the cytoplasm of pancreatic islet cells, as well as the coexpression of vimentin and glucagon, has been detected in T2DM [222]. Additionaly, vimentin plays a role in atherosclerosis [223]. The function of vimentin in diabetes platelets is not clear. The decreased expression of vimentin in the platelet proteome of middle-aged diabetes patients (Figure 7A) may enhance the formation of platelet-leukocyte aggregates, thereby potentially increasing thrombus formation.

Ephrin-B1

EphA4 and EphB1, two types of Eph kinases, as well as their ligand ephrinB1, can be found on the surface of human platelets. By itself, EphB1 is insufficient to cause the binding of soluble fibrinogen to αIIbβ3 and subsequent platelet aggregation. However, it can potentiate platelet aggregation in the presence of platelet agonists (SFLLRN, U46619, and ionomycin) [224]. EFNB1 mutation has been observed in a girl and her mother, both of whom have craniofrontonasal syndrome along with T1DM and Autoimmune Thyroiditis [225]. Overexpression of EphB2 in atherosclerotic tissue has been mentioned elsewhere [226]. Downregulation of EphB1 in middle-aged diabetes patients (Figure 7A) may act as a compensatory mechanism to reduce the risk of thrombus formation in this group.

5. Discussion

G protein-coupled receptor kinase 5

G protein-coupled receptor kinase 5 (GRK5) plays a regulatory role in the platelet response to thrombin *via* the PAR-1 pathway. When platelets were exposed to thrombin, an increased response was observed in Grk5$^{-/-}$ platelets. The activation of human platelets by thrombin leads to the binding of GRK5 to PAR-1, and the deletion of the mouse equivalent Grk5 enhances the sensitivity of platelets to thrombin-induced activation, resulting in increased platelet accumulation at the site of vascular injury. Additionally, the presence of the G allele of rs10886430 (rs10886430-G) in humans is associated with lower GRK5 transcript levels in platelets, increased platelet sensitivity to PAR-1 activation, and an elevated risk for cardiovascular disease [227], [228]. GRK5 serves as a positive regulator for insulin sensitivity and may associate with the pathogenesis of T2DM [229]. A variant of GRK5 (rs10886471) has been observed in T2DM patients [230]. Low levels of GRK5 in the platelet proteome of middle-aged diabetes patients (Figure 7A) may increase thrombin-induced platelet activation and the risk of CVDs in T2DM patients.

Platelet factor 4

Platelet factor 4 (PF4) is a protein that is produced in the maturing megakaryocytes. It is then packaged into the platelet α-granules and released upon platelet activation [231]. The greatest concentration of PF4 is released in the vicinity of growing fibrin clots, and even tiny quantities of PF4 at subnanomolar levels boost the polymerization of fibrin fibers. This process occurs during blood clot formation as part of the coagulation cascade [232]. Despite its primary role in promoting blood coagulation, PF4 also plays a significant role in the immune response. Specifically, when platelets become activated in response to infections, PF4 participates in both innate and adaptive immunity processes [233]. PF4 can bind to vWF at the site of vascular injury, resulting in the formation of a complex known as PF4/vWF. This complex might play a crucial role in platelet activation and inflammation, which can contribute to the development and exacerbation of immune-associated thrombosis [234]. Elevated levels of plasma PF4 have been noted in diabetes patients and also in individuals with CAD [235], [236]. The increased expression of PF4 in the platelet proteome of middle-aged diabetes patients (Figure 7A) may increase platelet activation and CVDs in this group.

5. Discussion

Coagulation factor XII

Factor XII in the coagulation cascade serves as the trigger for the contact phase of coagulation, which is important in facilitating blood clot formation on negatively charged surfaces. While FXII plays a role in intravascular thrombus formation, it is not essential for hemostasis in both humans and mice [237], [238]. Although activated coagulation factor XII (α-FXIIa) is involved in clot formation, it may have indirect effects on fibrinolysis through its effect on clot stability and plasminogen activation [239]. FXII deficiency is associated with an increased risk of arterial thrombosis and myocardial infarction. Despite the role of FXII in thrombin generation, the deficiency of FXII does not significantly impact the profiles of thrombin generation [240]. FXII levels were higher in T2DM than in T1DM [241]. The increased expression of factor XII in the platelet proteome of middle-aged diabetes patients (Figure 7A) may increase the risk of thrombus formation and CVDs in this group.

Alpha-2-macroglobulin

Alpha-2-macroglobulin (A2M) has been seen in platelets and blood plasma [242], [243]. A2M serves a dual role in hemostasis, acting as both an inhibitor of fibrinolysis by targeting plasmin and kallikrein and as an inhibitor of coagulation by targeting thrombin [244]. Although A2M can inhibit thrombin, which is known to be involved in platelet activation, the impact of A2M on platelet activation and aggregation has not been extensively studied [245]. Increased plasma concentration of A2M has been observed in diabetes patients [243]. The increased expression of A2M in the platelet proteome of middle-aged diabetes patients (Figure 7A) may act as a compensatory mechanism to reduce platelet activation in this group.

Complement component C7

As discussed previously, the presence of C3, C5, C6, C7, C8, and C9 of the human complement enhances thrombin-mediated platelet aggregation and release [171]. The regulation of complements can be affected by the aging process, which is considered a prominent risk factor for the occurrence of diseases such as diabetes and cardiovascular

disorders [246], [247], [248]. Upregulation of C7 in middle-aged diabetes patients (Figure 7A) may increase the risk of platelet aggregation and CVDs in this group.

PF4, F12, and A2M are significantly involved in fibrin clot formation. Additionally, F12, A2M, and C7 are enriched in the complement and coagulation cascades (Figure 7C).

Serine/threonine-protein kinase D2

Serine/threonine-protein kinase D (PKD) is a subfamily of kinases that specifically phosphorylate serine and threonine residues. There are three isoforms of PKD, namely PKD1, PKD2, and PKD3, which are alternatively referred to as PKCμ, PKD2, and PKCv in humans. PKD2 is the major isoform of PKD found in both human and mouse platelets. In platelets, PKD2 is a frequently targeted signaling molecule activated by various agonist receptors. PKD2 can be activated in a Gq-dependent manner downstream of PAR4, as well as by calcium and specific isoforms of novel PKC, notably PKCδ. Therefore, PKD2 may mediate dense granule secretion [249]. In a mouse model with mutations (Ser707Ala/Ser711Ala) in two crucial phosphorylation sites of PKD2, dense granule secretion in platelets was significantly reduced upon agonist stimulation. Consequently, this led to decreased platelet aggregation and a significant decrease in thrombus formation [250]. A recent finding indicated that obesity and its associated diabetes can be alleviated by inhibiting PKD2 [251]. The role of platelet-derived PKD2 in diabetes has not been investigated. In the obtained data, PKD2 is significantly upregulated in middle-aged diabetes patients (Figure 7A) compared to controls. The upregulation of PKD2 may potentially contribute to increased platelet aggregation and thrombus formation in this group.

5.2.3. Platelet proteome changes between old-aged diabetic and healthy individuals

GDP-mannose pyrophosphorylase A and dolichyl-phosphate beta-glucosyltransferase

GDP-mannose pyrophosphorylase is an enzyme involved in glycosylation processes. It facilitates the synthesis of GDP-mannose by catalyzing a reaction between mannose-1-phosphate and guanosine triphosphate (GTP) [252], [31]. GMPP-alpha plays a role in the initial steps of protein glycosylation [253]. Alterations in glycosylation patterns can have important implications for platelet function and hemostasis [254]. Congenital disorders of glycosylation (CDG), is associated with hypoglycosylation. Patients with CDG exhibit abnormalities in clotting and anticlotting factors, leading to an increased risk of both thrombosis and bleeding [255]. Abnormal glycosylation can contribute to the development of different diseases, including diabetes [256]. Another enzyme involved in protein glycosylation is dolichyl-phosphate beta-glucosyltransferase, which is located in the endoplasmic reticulum (ER). It facilitates the transfer of glucose from UDP-glucose to dolichyl phosphate through its catalytic activity, resulting in the formation of dolichyl phosphate glucose. This reaction is an essential step in N-linked protein glycosylation in the ER [257]. In pathway analysis related to N-glycan precursor substrate biosynthesis and the biosynthesis of the N-glycan precursor and transfer to a nascent protein, GMPP-alpha and dolichyl-phosphate beta-glucosyltransferase have been found to be enriched in individuals with old-aged diabetes (Figure 8C). However, the specific function of GMPP-alpha and dolichyl-phosphate beta-glucosyltransferase in platelets remains unknown. The downregulation of these enzymes in old-aged diabetes (Figure 8A) could potentially have significant implications in the initial stages of N-glycosylation. This downregulation may affect the synthesis and modification of complex N-glycan structures attached to proteins, potentially leading to an increased tendency for thrombus formation.

SH2-containing inositol phosphatase 2

SHIP2, also referred to as SH2-containing inositol phosphatase 2, is an essential regulator of phosphoinositide levels in platelets. Similar to SHIP1, SHIP2 plays a significant role in

regulating phosphoinositide levels in platelets. It downregulates PtdIns(3,4,5)P3-dependent events and initiates PtdIns(3,4)P2-mediated mechanisms. Additionally, it participates in the control of membrane ruffling through its interaction with filamin [258], [259], [260]. Herein, SHIP2 interacts with actin, filamin, and the GPIb-IX-V complex, which serves as the receptor for the vWF glycoprotein. This complex may contribute to the localized breakdown of PtdIns(3,4,5)P3, thereby influencing the arrangement and function of actin structures in the cortical and submembraneous regions of platelets [259]. It is known that the actin cytoskeleton undergoes remodeling upon platelet activation [261]. A previous study has indicated an association between SHIP2 and diabetes [262]. However, the precise mechanism by which SHIP2 influences platelet function through actin rearrangement remains unclear. The downregulation of SHIP2 in old-aged diabetes (Figure 8A) may work as a compensatory mechanism to reduce platelet activation in this group.

Glycogenin-1

Elevated levels of glycogenin-1 (GYG1), a glycogenin glucosyltransferase, have been observed in platelets following prolonged storage. The authors of the study suggested that the increased GYG1 levels in aged platelets (after 13 days of storage) could be attributed to either the ingestion of this protein by platelets or its binding to platelets during storage. However, the authors did not mention the possibility that the elevated protein levels may be a result of mRNA translation in platelets, which could be influenced by various factors including aging (platelet storage effect) [263]. Interestingly, the level of GYG1 in platelets from individuals with old-age diabetes was significantly lower compared to those in healthy individuals (Figure 8A). The downregulation of GYG1 in old-aged diabetes (Figure 8A) may work as a compensatory mechanism to reduce platelet activation in this group.

Glycogen synthase kinase-3 alpha

Glycogen synthase kinase-3 (GSK3), a widely expressed cytoplasmic serine/threonine protein kinase, includes the GSK3α and GSK3β isoforms found in human platelets. Platelet stimulation *via* collagen, convulxin, and thrombin in a time- and concentration-

dependent manner induces GSK3α phosphorylation mediated by PI3K activity [204]. Phosphorylation of GSK3α at Ser^{21} is essential for inhibiting GPVI-induced platelet activation [205]. Elevated expression and activity of GSK3 have been observed in diabetic rodents and humans [264]. However, it is still unclear whether both isoforms of GSK3 or only one of them are increased in diabetes. Furthermore, the role of the GSK3α isoform in platelet from diabetes has not been investigated. In the obtained data, a significant upregulation of GSK3α in the platelet proteome of old-aged diabetes compared to healthy controls was observed (Figure 8A). The correlation between increased GSK3α expression and phosphorylation at Ser^{21} of GSK3α needs to be investigated. If there is a positive correlation between increased GSK3α expression and phosphorylation of GSK3α at Ser^{21}, it is possible that the upregulation of GSK3α in this group may serve as a compensatory mechanism to reduce platelet activation by inhibiting GPVI-induced platelet activation.

Ferritin heavy chain

Ferritin is a widely distributed protein involved in storing iron within cells in various organisms, including animals, plants, molds, and bacteria. Its primary role is to protect these cells from the harmful effects of excessive intracellular iron levels. Ferritin stores iron within a hollow protein shell composed of two types of subunits, H and L [265]. The identification of extracellular ferritin and its presence in exosomes suggests that ferritin may also be implicated in the regulation of tissue and body iron homeostasis [266]. Previous studies indicated that serum ferritin serves as a significant marker for both inflammatory diseases and oxidative stress [267], [268]. Animal studies indicated that female livers and kidneys exhibit higher levels of ferritin expression and greater iron accumulation compared to males. The expression of both FtL and FtH, the subunits of ferritin, is influenced by factors such as sex, sex hormones, and age [269]. Besides, elevated serum ferritin is associated with diabetes [270], [271]. T1DM patients with microvascular complications demonstrated higher serum ferritin concentrations compared to those without microvascular complications [272]. A recent finding suggested that increased level of plasma ferritin leads to platelet hyperactivity [273]. The increased expression of ferritin heavy chain in the platelet proteome of old-aged diabetes compared to controls (Figure 8A) can be attributed to several reasons. Firstly, it remains unclear

whether ferritin directly influences platelet reactivity or acts indirectly through mechanisms involving oxidative stress and inflammation. Secondly, the expression of ferritin in platelets has not been thoroughly investigated. Although platelets lack a nucleus, it is plausible that the presence of ferritin heavy chain in platelets from old individuals may be due to remnants of mRNA that persist in platelets and retain the capacity to synthesize certain proteins. Thirdly, considering that ferritin has been identified in exosomes, it is possible that platelet-derived EVs from old-aged diabetes exhibit higher levels of ferritin heavy chain compared to those in control subjects. Consequently, these EVs may transfer their cargo, including ferritin heavy chain, to platelets, offering another potential explanation for the elevated ferritin levels observed in platelets from old-aged diabetes.

Endophilin A2

Endophilin A2 and B2, members of the endophilin protein family, have the potential to influence cargo uptake and receptor trafficking in platelets. Endophilin A2 has a higher copy number compared to endophilin B2. Both endophilin A2 and B2 participate in the uptake of cargo through clathrin-mediated endocytosis. In platelets, endocytosis plays a crucial role in loading specific cargo, including fibrinogen, into α-granules. Moreover, the process of endocytosis can have implications for thrombosis by affecting proteins such as αIIbβ3 [274]. The increased expression of endophilin A2 in platelets from old-aged diabetes compared to controls has not been investigated. However, if endophilin A2 levels are elevated in these platelets (Figure 8A), it could potentially impact the content of alpha granules, including fibrinogen. Consequently, platelet activation in diabetes may trigger the release of stored fibrinogen, enabling its involvement in the formation of a fibrin clot at the site of vascular injury. This, in turn, can contribute to platelet aggregation and thrombus formation.

ATPase secretory pathway Ca^{2+} transporting 1

ATPase secretory pathway Ca^{2+} transporting 1 (ATP2C1) is a protein found on the Golgi apparatus that plays a role in Ca^{2+}/Mn^{2+} transport [275], as well as in membrane trafficking. A previous study demonstrated that a deficiency of ATP2C1 disrupts the

secretory pathways. Platelets contain both ATP2C1 RNA and protein. While platelets are known to release ATP2C1, it has been observed that this release is diminished when platelets interact with E. coli strains K12 and O18:K1. In the presence of bacteria, the diminished levels of ATP2C1 RNA within platelets, as well as the decreased ATP2C1 protein levels in the supernatant, suggest that there might be an active translation of ATP2C1 protein and its subsequent retention within the platelets [276]. Except for its role as a defense mechanism against E. coli, the role of platelet-derived ATP2C1 protein remains poorly investigated. Increased expression of ATP2C1 has been observed in platelets from old-aged diabetes compared to controls (Figure 8A). Chronic low-grade inflammation and oxidative stress associated with diabetes may influence the expression of ATP2C1 in platelets, suggesting that ATP2C1 may serve as a defense mechanism in this group. Additionally, ATP2C1 is involved in the transport of Ca^{2+} and Mn^{2+}, which may potentially impact cytosolic Ca^{2+} levels in platelets. Further investigation is necessary to clarify the precise role of this protein in platelets from old-aged diabetes.

5.3. Plasma-derived Extracellular Vesicles

Plasma-derived EVs are released into the circulation by various cell types, such as platelets, erythrocytes, and endothelial cells [277], and play a crucial role in various physiological and pathophysiological processes, including T1DM [278], and T2DM [279]. Plasma-derived EVs are particularly important in mediating thrombotic events, inflammation, endothelial dysfunction [280], and vascular complications associated with diabetes. Additionally, during both healthy and diseased conditions, EVs play a crucial role in facilitating cell communication. Specifically, the release of the majority of EVs occurs when platelets are activated or during the process of aging [281].

Based on the obtained data, there was a significant increase in platelet aggregation when exposed to plasma-derived diabetic EVs in the presence of platelet agonists (thrombin and collagen), compared to plasma-derived control EVs (Figure 10). Increased platelet aggregation can be attributed, at least in part, to the increased phosphorylation of tyrosine residues caused by diabetic EVs (Figure 11). Considering that phosphorylation of tyrosine residues in platelet proteins can activate various signaling pathways involved in platelet aggregation [236], it is possible that the EVs proteome in diabetes directly affects platelet

activation and aggregation through factors like phosphatases and kinases, or indirectly influences the phosphorylation of tyrosine residues. By analyzing the protein composition of plasma-derived EVs obtained from both diabetic and healthy individuals, we can gain a better understanding of the proteins involved in platelet activation and aggregation, thrombus formation, and the pathophysiology of diabetes-associated complications, such as CVDs. Furthermore, this study can contribute to the advancement of targeted therapeutic strategies that aim to modulate platelet activation in diabetes patients.

5.3.1. Plasma-derived Extracellular Vesicles Proteome in Middle-Aged Diabetics versus Healthy Controls

Protein disulfide-isomerase A3

Protein disulfide isomerase (PDI) consists of four main domains (a, b, b', and a') along with an acidic C-terminal extension and an x-linker sequence. The substrate binding b' domain of PDI is crucial for its interaction with αIIbβ3 on platelets, while a, and a' domains contribute to efficient binding. Within a' domain, the C-terminal CGHC active site motif plays a role in activating the platelet αIIbβ3 integrin, which is necessary for platelet aggregation and accumulation *in vivo* [282]. Protein disulfide-isomerase A3 (PDIA3) is a member of the PDI family [283]. PDIA3, primarily found in ER [284], and plays a role in a wide range of physiological and pathological processes. It is expressed in various cell types, such as neuronal cells, immune cells, and certain cancer cells [285], [286], [287]. Furthermore, it can be released from platelets and translocate to the cell surface after activation. It is known that platelet-derived PDIA3 exhibits a direct interaction with the αIIbβ3 receptor during its activation, playing a crucial role in facilitating the incorporation of platelets into a developing thrombus. Additionally, platelet-derived microparticle fractions contain PDIA3, indicating its potential role in regulating coagulation and platelet function [288], [289]. Activation of platelet GPVI can enhance the release of PDIA3 from platelets [290]. Furthermore, the administration of catalytically inactive PDIA3 in mice increased tail bleeding time, indicating the potential involvement of circulating or intravascular PDIA3 in the process of hemostasis [291]. Previous study indicated that the secretion of PDIA3 from vascular cells is essential for complete thrombus formation *in vivo* [292]. PDIA3 is an essential component of the

peptide loading complex, which is necessary for presenting antigens through MHC Class I molecules [293]. Consequently, PDIA3 plays a role in adaptive immunity [294]. In the obtained data, the proteome of plasma-derived EVs from middle-aged individuals with diabetes showed significant downregulation of PDIA3 compared to healthy controls (Figure 13A). Additionally, PDIA3 is found to be significantly enriched in the immune system and adaptive immune system (Figure 13C). The decreased expression of PDIA3 in the plasma-derived EVs proteome of middle-aged individuals with diabetes, compared to healthy controls, may serve as a compensatory mechanism and reduce the risk of thrombus formation in this group. It is important to further investigate the role of PDIA3 in platelet activation as it can be released from diverse cell types.

Bridging integrator 2

The BIN (bridging integrator) family has been associated with diverse cellular functions, such as membrane dynamics, actin cytoskeleton organization, cell cycle regulation, and tumor suppression. Bridging integrator 2 (BIN2) is one of the isoforms within the BIN family [295]. Bin2 expression has been observed in both myeloid and lymphoid lineages, indicating its potential involvement across all types of leukocytes. It influences key aspects of leukocyte function, including podosome formation, cellular motility, and phagocytosis [296]. In platelets, BIN2 is primarily localized in the cytoplasm and regulates Ca^{2+} signaling through direct or indirect interactions with both STIM1 and IP3R. Deletion of BIN2 in platelets led to the diminished release of Ca^{2+} from intracellular stores and reduced Ca^{2+} influx in response to various platelet agonists. These included GPCR agonists such as ADP, thrombin, and the stable TxA2 analog U46619, as well as (hem)ITAM-dependent agonists that act on GPVI, such as CRP and convulxin (CVX), and on CLEC-2, such as rhodocytin (RC). Notably, platelets lacking BIN2 exhibited significantly diminished aggregation responses compared to wild-type (WT) platelets when stimulated with (hem)ITAM-dependent agonists targeting GPVI (CVX) and CLEC-2 (RC). However, there were no discernible differences in platelet aggregation between the two groups when stimulated with GPCR agonists such as thrombin, ADP, and U46619, or the combination of ADP/U46619. Additionally, deficiency of BIN2 in platelets leads to impaired formation of thrombi under flow and provides significant protection against arterial thrombosis [295]. BIN2 has not been reported in extracellular

vesicles and also in diabetes patients. The low level of BIN2 in plasma-derived diabetes EVs compared to plasma-derived control EVs (Figure 13A) may have several reasons: 1) Low expression of BIN2 from their origin cells 2) Differential packaging of BIN2 from their origin cells into EVs 3) Cellular stress and inflammation. Given that individuals with diabetes face an increased risk of oxidative stress and inflammation, these conditions can affect protein stability and their release from cells. The low level of BIN2 in plasma-derived diabetes EVs compared to plasma-derived control EVs may work as a compensatory mechanism to reduce thrombosis in this group.

Progranulin

Progranulin (PGRN) is extensively present in a range of cell types, including hematopoietic cells, T cells, dendritic cells, and chondrocytes. It serves various functions including the regulation of neuropathology, promotion of cancer cell proliferation, involvement in immune responses against infections, and facilitation of the wound healing process [297], [298], and antiplatelet and anticoagulant properties. The antiplatelet and anticoagulant properties of progranulin may play a significant physiological role in providing protection against thrombotic disorders linked to obesity and atherosclerosis [299]. Elevated levels of plasma progranulin have been observed in individuals with T2DM and obesity [300]. Moreover, serum levels of PGRN were significantly higher in T2DM patients with microvascular complication [301]. In streptozotocin-induced diabetic mice, a decrease in PGRN levels has been observed in kidney samples compared to healthy controls. Additionally, PGRN deficiency increased mitochondrial dysfunction in podocytes from diabetic mice. *In vitro*, the addition of recombinant human PGRN (rPGRN) was found to reduce high glucose-induced mitochondrial dysfunction in podocytes. These findings suggest that progranulin plays a role in regulating mitochondrial homeostasis, and this could have therapeutic potential for the treatment of DN [302]. Another study indicated that PGRN is primarily released in its N-glycosylated form, in association with exosomes. However, in the case of the progranulin gene (GRN) mut human fibroblasts, there is a significant decrease in the amount of exosomal progranulin released [303]. A previous finding indicated that $Grn^{-/-}$ mice exhibited higher levels of brain EVs and distinct protein compositions within these EVs in an age-dependent manner compared to wild-type mice [304]. Taking into

consideration that T2DM patients exhibit elevated levels of larger circulating EVs, the diminished presence of PGRN in plasma-derived diabetes EVs (Figure 13A) may increase the risk of thrombus formation, and may attribute to a decreased expression of this protein in the originating cells. Consequently, this may influence the size of EVs released from various cell types in diabetes patients, providing a possible explanation for the larger EVs observed in this group.

Ras-related C3 botulinum toxin substrate 2

Ras-related C3 botulinum toxin substrate 1 (Rac1) GTPase and Ras-related C3 botulinum toxin substrate 2 (Rac2) GTPase play distinct and crucial roles in intracellular signaling pathways downstream of H4 receptor-PI3K in histamine-induced chemotaxis of mast cells. Herein, the downregulation of Rac1 resulted in a reduced response in calcium mobilization, whereas the downregulation of Rac2 led to a diminished response in ERK activation [305]. Another research study provided evidence that Rac2 is a crucial regulator responsible for the activation of neutrophil NADPH oxidase, acting downstream of chemoattractant and Fcgamma receptors [306]. The involvement of RAC2 in extracellular vesicles has been reported. Liu et al. proposed that RAC2 levels are upregulated in exosomes derived from mesenchymal stem cells obtained from both umbilical cord and adipose tissue [307]. The involvement of Rac2 in vascular oxidative stress and inflammation in diabetes patients is suggested. Treating diabetic mice with atorvastatin reduces the activation of Rac1/2 and Nox, leading to a decline in vascular oxidative stress and inflammation [308]. The Rac2 GTPase, which represents the active form of Rac2, contributes to cathepsin H-mediated protection against cytokine-induced apoptosis in insulin-secreting cells. This protective effect was abolished when Rac2 was knocked down. These findings suggest that Rac2 could be a potential candidate gene associated with the development of T1DM [309]. RAC2 plays a crucial role in regulating the dynamic organization of focal adhesions and is associated with cancer cell migration [310]. In the obtained data, Rac2 shows significant downregulation in plasma-derived diabetes EVs compared to plasma-derived control EVs (Figure 13A). Additionally, it plays a role in the chemokine signaling pathway and focal adhesion (Figure 13C). While Rac2 expression is limited to hematopoietic cells [311], it has not been detected in platelets. The decreased levels of RAC2 in plasma-derived diabetes EVs may serve as a

compensatory mechanism to reduce vascular oxidative stress and inflammation in diabetes patients. However, it remains to be investigated whether RAC2 present in plasma-derived EVs can impact platelet reactivity. For example, RAC2 may influence NADPH activation in platelets through cargo transfer or binding to platelet receptors.

Rho-associated protein kinase 2

ROCK2, a specific isoform of Rho-associated coiled-coil containing kinase (ROCK), has a crucial role in platelet activation and thrombus formation. The lack of ROCK2 in platelets results in decreased binding of αIIbβ3 integrin to fibrinogen and reduced expression of P-selectin. As a result, platelets lacking ROCK2 form significantly fewer aggregates with both leukocytes and other platelets, compared to WT platelets. In the ferric chloride-induced carotid artery injury model, it was observed that the selective absence of ROCK2 in platelets resulted in decreased thrombus formation at the site of injury [312]. The involvement of ROCK2 in mediating lysophosphatidic acid-induced monocyte migration and monocyte adhesion to endothelial cells underscores its critical function as a regulator of endothelial inflammation. Therefore, targeting endothelial ROCK2 can be a promising candidate for attenuating atherosclerosis [313]. The involvement of ROCK2 in the shedding of microparticles from endothelial cells has been reported elsewhere [314]. Patients with poorly controlled diabetes exhibit elevated ROCK activity in their platelets [315]. Another study indicated an increased ROCK activity in T2DM [316]. ROCK2 is significantly downregulated in plasma-derived diabetes EVs compared to plasma-derived control EVs (Figure 13A). Additionally, ROCK2 is enriched in focal adhesion and chemokine signaling pathways (Figure 13C). Although various studies have indicated increased ROCK activity in diabetes patients, there is currently no evidence suggesting the presence of ROCK expression in EVs associated with diabetes. The low expression of ROCK2 in plasma-derived diabetes EVs could potentially attributed to the reduced expression of these proteins in their origin cells. Since ROCK2 plays a role in EV shedding from endothelial cells, the reduced levels of ROCK2 in plasma-derived diabetes EVs might be due to impaired ROCK2 function in endothelial cells or even platelets. The impact of ROCK2 in plasma-derived EVs on platelet function remains to be elucidated. It is possible that the decreased levels of ROCK2 in diabetes

5. Discussion

EVs act as a compensatory mechanism to reduce the risk of thrombus formation in this group.

Reelin

Reelin is a glycoprotein that is predominantly located in the extracellular matrix. It is produced by Cajal-Retzius cells during brain development and plays a vital role in controlling neural migration and the maturation of dendritic spines. Additionally, Reelin can be detected in other tissues, including blood [317], [318]. Reelin can be found in various cell types such as platelets. The interaction between extracellular Reelin and platelets occurs through a receptor belonging to the low-density lipoprotein receptor gene family. This interaction facilitates platelet spreading on fibrinogen, leading to an increase in lamellipodia formation and bundling of F-actin. However, Reelin does not impact the activation of integrin αIIbβ3 or platelet aggregation induced by agonists [319]. A few years later, Tseng et al. proposed that the receptors known to interact with Reelin, namely ApoE receptor 2 (ApoER2), very low-density lipoprotein receptor (VLDLR), integrin β1, and platelet integrin β3, are not involved in the interaction between Reelin and platelets. Instead, Reelin can bind to various other molecules present on platelets, including phosphatidylserine (PS), phosphatidic acid (PA), cardiolipin, and to a lesser extent, 3-sulfogalactosylceramide. Additionally, Reelin can interact with coagulation factors such as thrombin and FXa. Reelin-deficient mice exhibited a significant increase in both the duration of bleeding and the rate of rebleeding [320]. Moreover, Reelin protects mice against arterial thrombosis. Interestingly, Reelin can be secreted upon platelet activation and subsequently regulates platelet activation through the interaction between amyloid precursor protein (APP) and GPIb. This underscores Reelin's role in GPIb signaling [321]. Besides, Reelin interacts with GPVI, leading to the GPVI-dependent phosphorylation of tyrosine residues. This interaction enhances platelet binding to collagen, triggers RAC1 activation, facilitates PLC gamma 2 phosphorylation, and ultimately promotes platelet activation and aggregation [322]. A significant rise in Reelin expression was observed in the retinas of a mouse model with DR induced by streptozotocin [323]. Circulating Reelin exacerbates atherosclerosis by promoting vascular inflammation, whereas depletion of Reelin protects against atherosclerosis by reducing the adhesion of leukocytes to the blood vessels [324], [325]. It has been

observed that Reelin is enriched in focal adhesions (Figure 13C). Reelin shows significant downregulation in plasma-derived diabetes EVs compared to plasma-derived control EVs (Figure 13A). Furthermore, it is enriched in innate immune system. Regarding innate immunity, neutrophils release human neutrophil peptides (HNPs) into the extracellular milieu upon activation. HNPs have been implicated in endothelial dysfunction, platelet activation, and aggregation, and these effects were mediated by the interaction between the ApoER2 and its ligand, Reelin [325]. It is known that diabetes patients often exhibit dysregulated immune responses and increased inflammation, which can further exacerbate the negative consequences of HNPs on endothelial function, platelet activation, and aggregation. Low levels of Reelin in plasma-derived diabetes EVs may act as a compensatory mechanism to reduce the risk of thrombus formation in this group.

Transcription factor p65

The most prominent biological function of NF-κB is its involvement in the development and function of the immune system, where it regulates both innate and adaptive immune responses [326]. In innate immune cells, the NF-κB pathway plays a crucial role in the transcriptional induction of pro-inflammatory cytokines, chemokines, and other inflammatory mediators [327]. In adaptive immune cells, NF-κB plays a role in regulating lymphopoiesis, which is the process of producing lymphocytes, including B cells and T cells. Additionally, NF-κB is involved in the regulation of anti-apoptotic factors that are necessary for the survival of early lymphoid cells when faced with pro-apoptotic stimuli [326]. The NFκB family comprises five transcription factors: p50, p52, p65, RelB, and c-Rel. Normally, NFκB complexes are inactive and reside in the cytoplasm, bound to inhibitory proteins called IκBs. NF-κB has non-genomic functions in platelets. Platelet activation by thrombin triggers the activation of IKK, which phosphorylates IκB, leading to its degradation. Consequently, Transcription factor p65 (NF-κB p65) is released from the IκB complex. Within the cytoplasm of platelets, NF-κB p65 can interact with other signaling molecules and participate in various cellular processes, such as the expression of p-selectin and the binding of fibrinogen to integrin αIIbβ3 [328], [329]. Not only thrombin but also collagen can induce NF-κB p65 phosphorylation. Auraptene reduces the phosphorylation of both NF-κB p65 and IκBα, thereby reversing the degradation of IκBα in collagen-activated platelets. This suggests that auraptene reduces the risk of

arterial thrombus formation by modulating the NF-κB pathway [330]. Another non-genomic function of NF-κB p65 is the regulation of platelet responses induced by Toll-like receptor 2 and 4 ligands. This suggested that targeting NF-κB p65 could be a promising approach to prevent platelet activation in inflammatory or infectious diseases [331]. Another study indicated that the pathway mediated by NF-κB p65 is implicated in the release of small EVs from senescent and proinflammatory mesenchymal stem cells (MSCs) [332]. In a recent study the involvement of NF-κB p65 in DN has been reported [333]. In the obtained data, RELA (gene name of Transcription factor p65) is significantly downregulated in plasma-derived diabetes EVs compared to plasma-derived control EVs (Figure 13A). It is enriched in different pathways, including the innate and adaptive immune systems, as well as the chemokine signaling pathway (Figure 13C). The exact mechanism by which NF-κB p65 in diabetes EVs can influence platelet reactivity remains unclear. However, it is possible that the lower levels of NF-κB p65 in diabetes EVs are a result of reduced NF-κB p65 levels in their origin cells, such as platelets. This could provide an additional explanation for the larger size of EVs observed in diabetes patients compared to healthy controls.

Glycerol-3-phosphate dehydrogenase, mitochondrial

Glycerol-3-phosphate dehydrogenase, mitochondrial (mGPDH), plays a significant role in regulating glucose-induced insulin secretion and has been suggested as a potential contributor to the pathogenesis of T2DM [334], [335]. Decreased activity of this enzyme has been reported in T2DM [335]. The downregulation of podocyte-dominated mGPDH has been indicated in the glomeruli of both patients and mice suffering from DKD and adriamycin nephropathy [336]. A previous study indicated that mice lacking mGPDH exhibited increased ER stress, hepatic steatosis, accumulation of lipid droplets, and increased liver weight-to-body weight ratio (LW/BW) and triglyceride (TG) content when compared to control mice following tunicamycin treatment [337]. Given that ER stress can contribute to the development of diabetes, the upregulation of mGPDH in plasma-derived diabetes EVs compared to plasma-derived control EVs (Figure 13A) may serve as a compensatory response to mitigate the effects of ER stress in this group.

5. Discussion

Clathrin heavy chain 1 and Sorting nexin-9

Clathrin is a key protein present on the inner surface of certain cellular compartments known as coated vesicles and coated pits. These specialized compartments play essential roles in the intracellular trafficking of receptors and the process of endocytosis, which involves the uptake of various macromolecules within the cell [338]. Ma et al. suggested that the mRNA of clathrin heavy chain 1 (CLTC) is downregulated in peripheral blood mononuclear cells of patients with T2DM [339]. According to a previous study, it was proposed that clathrin heavy chain 1 (CHC1) has a significant function in the brain for the recycling of vesicles and the release of neurotransmitters at the nerve terminals of pre-synaptic neurons [340]. Interestingly, the internalization of exosomes through clathrin-mediated endocytosis has been reported in non-senescent bone marrow stem cells [341]. CLTC (the gene name of CHC1) is significantly upregulated in plasma-derived diabetes EVs compared to plasma-derived control EVs (Figure 13A), and it is enriched in clathrin-derived vesicle budding (Figure 13D). The upregulation of CHC1 in diabetes EVs may have several reasons. First, CHC1 is likely involved in the formation of clathrin-coated vesicles during endocytosis in platelets or other cells. This process potentially enables platelets to uptake various substances, including growth factors and adhesion molecules, which play essential roles in platelet activation and function. Second, as mentioned earlier, clathrin-mediated endocytosis has been implicated in the biogenesis of specific EV types, such as exosomes. This could provide an additional explanation for the larger size of EVs in diabetes blood compared to those in healthy individuals, potentially due to the uptake of exosomes from platelets or other cells. Further research is required to determine the CHC1 function in platelet reactivity.

Sorting nexin-9 is another protein, which is significantly upregulated in plasma-derived diabetes EVs compared to plasma-derived control EVs (Figure 13A), and it is enriched in clathrin-derived vesicle budding (Figure 13D). SNX9 consists of an amino terminus that includes a Src homology 3 (SH3) domain and a region with predicted low complexity. It also has a carboxyl-terminal part containing the phox domain. The low complexity region in SNX9 exhibits cooperative binding with the alpha and beta2-appendages of the adaptor protein complex 2 (AP-2), a crucial protein involved in the formation of clathrin-coated vesicles at the plasma membrane. On the other hand, dynamin-2 binds to the SH3 domain of SNX9 [342]. Knockdown of SNX9 using small-interfering RNA (siRNA) resulted in a decrease in synaptic vesicle endocytosis. It is proposed that the impact of SNX9 on

endocytosis is largely attributed to its interaction with dynamin 1 [343]. SNX9 facilitates the recruitment of dynamin to the plasma membrane and enhances its GTPase activity. Furthermore, SNX9 plays a crucial role in the late stages of clathrin-mediated endocytosis in non-neuronal cells, where it synergizes with dynamin to facilitate the formation and scission of the vesicle neck, which is essential for efficient membrane internalization [344], [345]. Another study indicated that suppression of bulge formation in adrenaline-stimulated endothelial cells was observed when sorting nexin-9, involved in clathrin-mediated endocytosis, was knocked down using siRNA [346]. Considering the involvement of SNX9 in the late stages of clathrin-mediated endocytosis in non-neuronal cells, it could serve as an additional reason for the larger EVs observed in diabetes compared to healthy individuals.

Catalase

Catalase, an enzymatic antioxidant, maintains redox balance in platelets. Platelet activation leads to the generation of ROS, which, in turn, increase platelet activation. Antioxidants mitigate ROS effects, regulate redox signaling, and exert anti-thrombotic effects by converting ROS into stable molecules and increasing NO production [347]. The activation of platelets during collagen-induced aggregation is accompanied by a rapid generation of hydrogen peroxide (H_2O_2), an oxidative compound that plays a crucial role in platelet activation. The production of H_2O_2 during collagen-induced platelet aggregation was found to be effectively neutralized by the presence of catalase [348]. The increased expression of catalase in diabetes EVs compared to control EVs (Figure 13A) may result from the increased oxidative stress observed in individuals with diabetes compared to healthy controls. This elevated catalase expression likely serves as a compensatory mechanism aimed at reducing ROS levels, thereby decreasing platelet activation, and reducing the risk of thrombus formation.

Tyrosine-protein kinase JAK2, Platelet basic protein, F-actin-capping protein subunit beta, and vacuolar protein sorting-associated protein 45

Tyrosine-protein kinase JAK2 is a protein involved in the activation of platelets. The JAK2-STAT3 pathway participates in collagen-induced platelet activation by activating

the JAK2-JNK/PKC-STAT3 signaling. Inhibiting JAK2 effectively reduces collagen-induced platelet aggregation and calcium mobilization. Furthermore, it inhibits the phosphorylation of PLCγ2, PKC, Akt, and JNK in collagen-induced platelet aggregation [349]. As observed in the current study, the presence of diabetes EVs, followed by the addition of collagen or thrombin, significantly enhanced the aggregation of healthy platelets (Figure 10). Additionally, healthy platelets treated with diabetes EVs exhibited higher levels of tyrosine phosphorylation compared to the control group (Figure 11B). Based on the proteomics data, tyrosine-protein kinase JAK2 may play a role in the tyrosine phosphorylation of the platelet proteome when treated with diabetes EVs in the presence of collagen. To further validate this, the tyrosine phosphorylation of PLCγ2, PKC, Akt, and JNK can be investigated. The JAK/STAT pathway is proposed to contribute to the development and progression of DKD by influencing autophagy in podocytes [350]. Furthermore, the involvement of JAK2/STAT3/SOCS1 pathway has been reported in DKD rats [351]. Mice lacking JAK2 exhibited hemostatic defects and impaired thrombus formation [134].

Platelet basic protein (PBP) is a chemokine produced by megakaryocytes and stored in the alpha-granules of platelets [352], [353]. PBP is released upon platelet activation and acts as a chemoattractant for neutrophils and monocytes, promoting their recruitment to inflammation sites [354]. It is suggested that the expression of PBP and its derivatives is not limited to the lineage of megakaryocytic cells [355]. The function of PBP in diabetes patients is not clear. PBP may contribute to the inflammatory response associated with the disease. Furthermore, the elevated levels of PBP in plasma-derived EVs from diabetes patients (Figure 13A) may indicate increased platelet activation within the diabetes group compared to healthy individuals.

The function of F-actin-capping protein subunit beta (CapZ beta) in platelets is poorly understood, but the available information suggests that it may play a role in platelet function. This is demonstrated by its identification in a study analyzing the sulfenylome of pathogen-inactivated platelets. During platelet activation, various changes occur, including protein modification through post-translational modifications. Sulfenic acid modifications are one type of modification that can occur during platelet activation. Sulphenylated CapZ beta, which refers to cysteine residues of the protein oxidized to sulfenic acid, may be involved in the function of this protein in platelet cytoskeleton regulation [356]. Increased levels of CapZ beta in plasma-derived diabetes EVs compared

to control (Figure 13A) and its effect on platelet function may have several reasons: Firstly, CapZ beta might affect platelet reactivity by transferring its RNA and impacting cytoskeleton regulation. Secondly, the elevated level of CapZ beta in diabetes EVs could result from the increased CapZ beta levels in their origin cells, such as platelets, which may lead to platelet shape change. Thirdly, CapZ beta may undergo post-translational modifications, such as the oxidation of cysteine residues, which could serve as a marker of increased oxidative stress in diabetes compared to controls.

Although the precise function of vacuolar protein sorting-associated protein 45 remains unknown, its prominent expression in peripheral blood mononuclear cells indicates its involvement in protein trafficking, including the transportation of inflammatory mediators [357]. The mutation in the VPS45 gene, which was reported in primary infantile myelofibrosis, causes platelet dysfunction [358].

Vacuolar protein sorting-associated protein 45, tyrosine-protein kinase JAK2, platelet basic protein, and F-actin-capping protein subunit beta are significantly enriched in the hemostasis pathway (Figure 13D).

5.4. Platelet Soluble Fraction, along with Loosely Associated Membrane Proteins

The findings of the platelet aggregation study revealed that treating healthy platelets with diabetes EVs resulted in increased tyrosine phosphorylation compared to control EVs (Figure 11B). This increase in tyrosine phosphorylation could be attributed to the presence of the protein kinase JAK2, which was found to be elevated in diabetes EVs compared to control EVs. In order to enhance the understanding of platelet proteins and their potential interaction with EVs in diabetes patients, the objective was to analyze the soluble fraction along with loosely associated membrane proteins in platelets obtained from both diabetes patients and healthy controls. The findings may contribute to the reduction of the risk of blood clot formation and bleeding complications in diabetes patients, including the investigation of proteins undergoing phosphorylation and proteins associated with phosphotyrosine residues.

5.4.1. Proteome Changes in the Soluble Fraction of Platelets, along with Loosely Associated Membrane Proteins, in Diabetics versus Healthy Controls

Platelet glycoprotein Ibβ and platelet glycoprotein IX

Platelet glycoprotein Ibβ (GPIbβ), which is a subunit of GPIb, and platelet glycoprotein IX (GP9) are important components of the GPIb-IX-V complex. GPIb-IX-V acts as a receptor for vWF. This complex is found on the surface of platelets and alpha granule membranes [359], [360], [361]. The binding of GPIb-IX to vWF allows platelets to adhere to exposed vWF on the subendothelium at sites of vascular injury, initiating the hemostatic process [362]. L. Springer et al. revealed that GPIbβ is significantly downregulated in the platelet proteome of diabetes patients compared to controls. On the other hand, platelet GP9 did not show significant differences in the platelet proteome between diabetes and controls in this study. However, after five days of platelet storage, both GPIbβ and GP9 were significantly upregulated in the plasma membrane of platelets from individuals with diabetes compared to healthy controls [363]. This upregulation could be attributed to platelet activation and the release of alpha granules, which may increase the level of platelet GP9 and GPIbβ on the surface of platelets. Another possibility is that the age of platelets during storage may affect the mRNA expression of GP9 and GPIbβ.

Interestingly, the frequency of GPIbβ is two times higher than that of GP9 in the platelet GPIb-IX receptor complex [364]. This disparity might be one of the reasons why GP9 did not emerge as a significant protein in the results of L. Springer et al. prior to the impact of platelet storage. In the obtained data, GPIbβ, similar to the previous findings, was significantly downregulated in diabetes patients compared to controls. Surprisingly, we were able to identify GP9 as a significant protein between these two groups without the influence of platelet storage. The significant downregulation of GPIBB and GP9 in the platelet fraction of diabetes compared to controls (Figure 15A), which is enriched in platelet adhesion to exposed collagen and the hemostasis pathway (Figure 15C), may provide a potential explanation for bleeding complications in diabetes patients.

5. Discussion

Cytoplasmic protein NCK1

Nck is an adapter protein widely expressed in cells, composed of one SH2 domain and three SH3 domains [365]. The SH2 domain of Nck binds to phosphotyrosine residues on proteins and is involved in protein-protein interactions and signaling pathways [366]. The SH3 domains of Nck facilitate the formation of a local signaling scaffold by interacting with proteins that have proline-rich regions. This interaction brings together proteins responsible for cytoskeletal remodeling [367]. The role of the cytoplasmic protein NCK1 in diabetes patients is still not fully understood. However, it is known that NCK is connected to misshapen/Nck-interacting kinase (NIK)–related kinase 1 (MINK1), which plays a role in platelet function, hemostasis, and thrombus formation [368]. The specific mechanisms by which NCK1 affects MINK1 in platelets require further investigation. It is worth noting that the increased expression of NCK1 in the platelet proteome of diabetes patients (Figure 15A) may potentially contribute to an elevated risk of thrombus formation through the involvement of MINK1. Furthermore, NCK1 exhibits a notable enrichment in the Y-branching of actin filaments (Figure 15D). Considering the essential role of the platelet cytoskeleton in maintaining the proper hemostatic function [369], the increased expression of NCK1 in platelet of diabetes patients may be implicated in the occurrence of bleeding complications in this group.

6. Conclusion and Outlook

This study provided valuable insights into age-related platelet activation, thrombus formation, and CVDs in diabetes patients. This was partially achieved by analyzing platelet proteins in young, middle-aged, and old individuals with diabetes and comparing them to healthy matched controls using bottom-up proteomics. Additionally, the study aimed to gain better insight into the role of plasma-derived EVs on platelet activation in diabetes patients by analyzing EV proteins from middle-aged diabetes patients compared to healthy matched controls using bottom-up proteomics. The findings of the platelet aggregation study revealed that treating healthy platelets with diabetes EVs resulted in increased tyrosine phosphorylation compared to control EVs. This increase in tyrosine phosphorylation could be attributed to the presence of protein kinase JAK2, which was found to be elevated in diabetes EVs compared to control EVs. However, other EVs proteins that may increase platelet activation and aggregation and thereby increase tyrosine phosphorylation need to be investigated. Moreover, the larger size of diabetes EVs may be attributed to the downregulation of progranulin, downregulation of transcription factor p65, upregulation of sortin nexin-9, and upregulation of clatherin heavy chain 1. This may highlight the importance of EV size in understanding their functional implications since large platelet-derived EVs have been associated with inflammation and thrombosis [370]. However, the role of large plasma-derived EVs in these processes remains unknown and requires further investigation. Additionally, proteome analysis of the soluble fraction along with loosely associated membrane proteins in platelets between two groups indicated an increased expression of cytoplasmic protein NCK1 in diabetes group, which may increase the risk of thrombus formation through the involvement of MINK1. It may also bind to phosphotyrosine residues on proteins and thereby play a role in platelet signaling pathway. One limitation of this study is that the sample size was relatively small. To confirm the findings, further studies with larger and more diverse populations are needed. The study also did not investigate the underlying mechanisms through which specific proteins in diabetes platelets and diabetes EVs could potentially increase platelet activation. Functional studies are necessary to validate the role of the identified proteins in platelet activation, aggregation, and thrombus formation in diabetes group. Additionally, exploring the impact of other factors, such as lifestyle factors and comorbidities, on platelet activation would be beneficial.

6. Conclusion and Outlook

Moreover, investigating the potential clinical implications of the identified proteins and pathways as targets for preventative and therapeutic strategies in managing diabetes-associated CVDs and thrombosis would be of interest.

7. References

[1] N. H. Cho *et al.*, “IDF Diabetes Atlas: Global estimates of diabetes prevalence for 2017 and projections for 2045,” *Diabetes Res Clin Pract*, vol. 138, pp. 271–281, Apr. 2018, doi: 10.1016/j.diabres.2018.02.023.

[2] N. J. Pagidipati *et al.*, “Secondary Prevention of Cardiovascular Disease in Patients With Type 2 Diabetes Mellitus: International Insights From the TECOS Trial (Trial Evaluating Cardiovascular Outcomes With Sitagliptin).,” *Circulation*, vol. 136, no. 13, pp. 1193–1203, Sep. 2017, doi: 10.1161/CIRCULATIONAHA.117.027252.

[3] D. Dabelea *et al.*, “Trends in the prevalence of ketoacidosis at diabetes diagnosis: the SEARCH for diabetes in youth study.,” *Pediatrics*, vol. 133, no. 4, pp. e938-45, Apr. 2014, doi: 10.1542/peds.2013-2795.

[4] C. A. Newton and P. Raskin, “Diabetic ketoacidosis in type 1 and type 2 diabetes mellitus: clinical and biochemical differences.,” *Arch Intern Med*, vol. 164, no. 17, pp. 1925–31, Sep. 2004, doi: 10.1001/archinte.164.17.1925.

[5] W. S. Borgnakke, “‘Non-modifiable’ Risk Factors for Periodontitis and Diabetes,” *Curr Oral Health Rep*, vol. 3, no. 3, pp. 270–281, Sep. 2016, doi: 10.1007/s40496-016-0098-7.

[6] J. Yang *et al.*, “Modifiable risk factors and long term risk of type 2 diabetes among individuals with a history of gestational diabetes mellitus: prospective cohort study,” *BMJ*, p. e070312, Sep. 2022, doi: 10.1136/bmj-2022-070312.

[7] A. Dizdarevic-Bostandzic, E. Begovic, A. Burekovic, Z. Velija-Asimi, A. Godinjak, and V. Karlovic, “Cardiovascular Risk Factors in Patients with Poorly Controlled Diabetes Mellitus.,” *Med Arch*, vol. 72, no. 1, pp. 13–16, Feb. 2018, doi: 10.5455/medarh.2018.72.13-16.

[8] P. J. Hantzidiamantis and S. L. Lappin, *Physiology, Glucose*. 2023.

[9] E. Rajaei, M. T. Jalali, S. Shahrabi, A. A. Asnafi, and S. M. S. Pezeshki, “HLAs in Autoimmune Diseases: Dependable Diagnostic Biomarkers?,” *Curr Rheumatol Rev*, vol. 15, no. 4, pp. 269–276, 2019, doi: 10.2174/1573397115666190115143226.

[10] American Diabetes Association, “2. Classification and Diagnosis of Diabetes: Standards of Medical Care in Diabetes-2018.,” *Diabetes Care*, vol. 41, no. Suppl 1, pp. S13–S27, Jan. 2018, doi: 10.2337/dc18-S002.

[11] B. E. Klein, R. Klein, S. E. Moss, and K. J. Cruickshanks, “Parental history of diabetes in a population-based study.,” *Diabetes Care*, vol. 19, no. 8, pp. 827–30, Aug. 1996, doi: 10.2337/diacare.19.8.827.

7. References

[12] L. U. and N. I. of B. R. Diabetes Genetics Initiative of Broad Institute of Harvard and MIT *et al.*, "Genome-wide association analysis identifies loci for type 2 diabetes and triglyceride levels.," *Science*, vol. 316, no. 5829, pp. 1331–6, Jun. 2007, doi: 10.1126/science.1142358.

[13] R. Sladek *et al.*, "A genome-wide association study identifies novel risk loci for type 2 diabetes.," *Nature*, vol. 445, no. 7130, pp. 881–5, Feb. 2007, doi: 10.1038/nature05616.

[14] A. Mahajan *et al.*, "Fine-mapping type 2 diabetes loci to single-variant resolution using high-density imputation and islet-specific epigenome maps.," *Nat Genet*, vol. 50, no. 11, pp. 1505–1513, Nov. 2018, doi: 10.1038/s41588-018-0241-6.

[15] S. E. Kahn, "The relative contributions of insulin resistance and beta-cell dysfunction to the pathophysiology of Type 2 diabetes.," *Diabetologia*, vol. 46, no. 1, pp. 3–19, Jan. 2003, doi: 10.1007/s00125-002-1009-0.

[16] J. E. Gerich, "Is reduced first-phase insulin release the earliest detectable abnormality in individuals destined to develop type 2 diabetes?," *Diabetes*, vol. 51 Suppl 1, pp. S117-21, Feb. 2002, doi: 10.2337/diabetes.51.2007.s117.

[17] S. E. Kahn *et al.*, "Quantification of the relationship between insulin sensitivity and beta-cell function in human subjects. Evidence for a hyperbolic function.," *Diabetes*, vol. 42, no. 11, pp. 1663–72, Nov. 1993, doi: 10.2337/diab.42.11.1663.

[18] U. P. Gujral, K. M. V. Narayan, S. E. Kahn, and A. M. Kanaya, "The relative associations of β-cell function and insulin sensitivity with glycemic status and incident glycemic progression in migrant Asian Indians in the United States: the MASALA study.," *J Diabetes Complications*, vol. 28, no. 1, pp. 45–50, 2014, doi: 10.1016/j.jdiacomp.2013.10.002.

[19] L. Qian *et al.*, "Early insulin secretion failure leads to diabetes in Chinese subjects with impaired glucose regulation.," *Diabetes Metab Res Rev*, vol. 25, no. 2, pp. 144–9, Feb. 2009, doi: 10.1002/dmrr.922.

[20] L. Qian *et al.*, "Metabolic characteristics of subjects with normal glucose tolerance and 1-h hyperglycaemia.," *Clin Endocrinol (Oxf)*, vol. 69, no. 4, pp. 575–9, Oct. 2008, doi: 10.1111/j.1365-2265.2008.03209.x.

[21] M. A. Atkinson, "The pathogenesis and natural history of type 1 diabetes.," *Cold Spring Harb Perspect Med*, vol. 2, no. 11, Nov. 2012, doi: 10.1101/cshperspect.a007641.

[22] R. Mallone and D. L. Eizirik, "Presumption of innocence for beta cells: why are they vulnerable autoimmune targets in type 1 diabetes?," *Diabetologia*, vol. 63, no. 10, pp. 1999–2006, Oct. 2020, doi: 10.1007/s00125-020-05176-7.

7. References

[23] American Diabetes Association, “Diagnosis and classification of diabetes mellitus.,” *Diabetes Care*, vol. 33 Suppl 1, no. Suppl 1, pp. S62-9, Jan. 2010, doi: 10.2337/dc10-S062.

[24] American Diabetes Association, “Standards of medical care in diabetes--2012.,” *Diabetes Care*, vol. 35 Suppl 1, no. Suppl 1, pp. S11-63, Jan. 2012, doi: 10.2337/dc12-s011.

[25] S. Park, H.-J. Kang, J.-H. Jeon, M.-J. Kim, and I.-K. Lee, “Recent advances in the pathogenesis of microvascular complications in diabetes.,” *Arch Pharm Res*, vol. 42, no. 3, pp. 252–262, Mar. 2019, doi: 10.1007/s12272-019-01130-3.

[26] A. Perrone, A. Giovino, J. Benny, and F. Martinelli, “Advanced Glycation End Products (AGEs): Biochemistry, Signaling, Analytical Methods, and Epigenetic Effects.,” *Oxid Med Cell Longev*, vol. 2020, p. 3818196, 2020, doi: 10.1155/2020/3818196.

[27] V. P. Reddy, P. Aryal, and E. K. Darkwah, “Advanced Glycation End Products in Health and Disease.,” *Microorganisms*, vol. 10, no. 9, Sep. 2022, doi: 10.3390/microorganisms10091848.

[28] M. E. Garay-Sevilla, A. Rojas, M. Portero-Otin, and J. Uribarri, “Dietary AGEs as Exogenous Boosters of Inflammation.,” *Nutrients*, vol. 13, no. 8, Aug. 2021, doi: 10.3390/nu13082802.

[29] J. Koska *et al.*, “Advanced Glycation End Products, Oxidation Products, and Incident Cardiovascular Events in Patients With Type 2 Diabetes.,” *Diabetes Care*, vol. 41, no. 3, pp. 570–576, Mar. 2018, doi: 10.2337/dc17-1740.

[30] S. Zoungas *et al.*, “Effects of intensive glucose control on microvascular outcomes in patients with type 2 diabetes: a meta-analysis of individual participant data from randomised controlled trials.,” *Lancet Diabetes Endocrinol*, vol. 5, no. 6, pp. 431–437, Jun. 2017, doi: 10.1016/S2213-8587(17)30104-3.

[31] I. Pearce, R. Simó, M. Lövestam-Adrian, D. T. Wong, and M. Evans, “Association between diabetic eye disease and other complications of diabetes: Implications for care. A systematic review.,” *Diabetes Obes Metab*, vol. 21, no. 3, pp. 467–478, Mar. 2019, doi: 10.1111/dom.13550.

[32] M. Brownlee, “Biochemistry and molecular cell biology of diabetic complications.,” *Nature*, vol. 414, no. 6865, pp. 813–20, Dec. 2001, doi: 10.1038/414813a.

[33] T. R. Einarson, A. Acs, C. Ludwig, and U. H. Panton, “Economic Burden of Cardiovascular Disease in Type 2 Diabetes: A Systematic Review.,” *Value Health*, vol. 21, no. 7, pp. 881–890, Jul. 2018, doi: 10.1016/j.jval.2017.12.019.

[34] M. Brownlee, “The pathobiology of diabetic complications: a unifying mechanism.,” *Diabetes*, vol. 54, no. 6, pp. 1615–25, Jun. 2005, doi: 10.2337/diabetes.54.6.1615.

7. References

[35] H. Fu, S. Liu, S. I. Bastacky, X. Wang, X.-J. Tian, and D. Zhou, "Diabetic kidney diseases revisited: A new perspective for a new era.," *Mol Metab*, vol. 30, pp. 250–263, Dec. 2019, doi: 10.1016/j.molmet.2019.10.005.

[36] K. Earle, J. Walker, C. Hill, and G. Viberti, "Familial clustering of cardiovascular disease in patients with insulin-dependent diabetes and nephropathy.," *N Engl J Med*, vol. 326, no. 10, pp. 673–7, Mar. 1992, doi: 10.1056/NEJM199203053261005.

[37] P. L. Drury *et al.*, "Estimated glomerular filtration rate and albuminuria are independent predictors of cardiovascular events and death in type 2 diabetes mellitus: the Fenofibrate Intervention and Event Lowering in Diabetes (FIELD) study.," *Diabetologia*, vol. 54, no. 1, pp. 32–43, Jan. 2011, doi: 10.1007/s00125-010-1854-1.

[38] G. A. Nichols, A. Déruaz-Luyet, S. J. Hauske, and K. G. Brodovicz, "The association between estimated glomerular filtration rate, albuminuria, and risk of cardiovascular hospitalizations and all-cause mortality among patients with type 2 diabetes.," *J Diabetes Complications*, vol. 32, no. 3, pp. 291–297, Mar. 2018, doi: 10.1016/j.jdiacomp.2017.12.003.

[39] P. K. Rani, R. Raman, A. Gupta, S. S. Pal, V. Kulothungan, and T. Sharma, "Albuminuria and Diabetic Retinopathy in Type 2 Diabetes Mellitus Sankara Nethralaya Diabetic Retinopathy Epidemiology And Molecular Genetic Study (SN-DREAMS, report 12).," *Diabetol Metab Syndr*, vol. 3, no. 1, p. 9, May 2011, doi: 10.1186/1758-5996-3-9.

[40] J. R. W. Brownrigg *et al.*, "Microvascular disease and risk of cardiovascular events among individuals with type 2 diabetes: a population-level cohort study.," *Lancet Diabetes Endocrinol*, vol. 4, no. 7, pp. 588–97, Jul. 2016, doi: 10.1016/S2213-8587(16)30057-2.

[41] S. V Arnold *et al.*, "Impact of micro- and macrovascular complications of type 2 diabetes on quality of life: Insights from the DISCOVER prospective cohort study.," *Endocrinol Diabetes Metab*, vol. 5, no. 2, p. e00321, Mar. 2022, doi: 10.1002/edm2.321.

[42] A. O. Yakimenko, F. Y. Verholomova, Y. N. Kotova, F. I. Ataullakhanov, and M. A. Panteleev, "Identification of different proaggregatory abilities of activated platelet subpopulations.," *Biophys J*, vol. 102, no. 10, pp. 2261–9, May 2012, doi: 10.1016/j.bpj.2012.04.004.

[43] S. EBBE and F. STOHLMAN, "MEGAKARYOCYTOPOIESIS IN THE RAT.," *Blood*, vol. 26, pp. 20–35, Jul. 1965.

[44] T. T. Odell and C. W. Jackson, "Polyploidy and maturation of rat megakaryocytes.," *Blood*, vol. 32, no. 1, pp. 102–10, Jul. 1968.

7. References

[45] T. T. Odell, C. W. Jackson, and T. J. Friday, "Megakaryocytopoiesis in rats with special reference to polyploidy.," *Blood*, vol. 35, no. 6, pp. 775–82, Jun. 1970.

[46] A. L. Sørensen *et al.*, "Role of sialic acid for platelet life span: exposure of beta-galactose results in the rapid clearance of platelets from the circulation by asialoglycoprotein receptor-expressing liver macrophages and hepatocytes.," *Blood*, vol. 114, no. 8, pp. 1645–54, Aug. 2009, doi: 10.1182/blood-2009-01-199414.

[47] J. W. Semple and J. Freedman, "Platelets and innate immunity.," *Cell Mol Life Sci*, vol. 67, no. 4, pp. 499–511, Feb. 2010, doi: 10.1007/s00018-009-0205-1.

[48] M. Holinstat, "Normal platelet function.," *Cancer Metastasis Rev*, vol. 36, no. 2, pp. 195–198, Jun. 2017, doi: 10.1007/s10555-017-9677-x.

[49] B. Savage, E. Saldívar, and Z. M. Ruggeri, "Initiation of platelet adhesion by arrest onto fibrinogen or translocation on von Willebrand factor.," *Cell*, vol. 84, no. 2, pp. 289–97, Jan. 1996, doi: 10.1016/s0092-8674(00)80983-6.

[50] D. Varga-Szabo, I. Pleines, and B. Nieswandt, "Cell adhesion mechanisms in platelets.," *Arterioscler Thromb Vasc Biol*, vol. 28, no. 3, pp. 403–12, Mar. 2008, doi: 10.1161/ATVBAHA.107.150474.

[51] J. Chung *et al.*, "Super-resolution imaging of platelet-activation process and its quantitative analysis.," *Sci Rep*, vol. 11, no. 1, p. 10511, May 2021, doi: 10.1038/s41598-021-89799-9.

[52] S. Ciferri, C. Emiliani, G. Guglielmini, A. Orlacchio, G. G. Nenci, and P. Gresele, "Platelets release their lysosomal content in vivo in humans upon activation.," *Thromb Haemost*, vol. 83, no. 1, pp. 157–64, Jan. 2000.

[53] J. Etulain *et al.*, "Control of angiogenesis by galectins involves the release of platelet-derived proangiogenic factors.," *PLoS One*, vol. 9, no. 4, p. e96402, 2014, doi: 10.1371/journal.pone.0096402.

[54] G. Vanderstocken *et al.*, "P2Y2 receptor regulates VCAM-1 membrane and soluble forms and eosinophil accumulation during lung inflammation.," *J Immunol*, vol. 185, no. 6, pp. 3702–7, Sep. 2010, doi: 10.4049/jimmunol.0903908.

[55] J. N. Thon *et al.*, "T granules in human platelets function in TLR9 organization and signaling.," *J Cell Biol*, vol. 198, no. 4, pp. 561–74, Aug. 2012, doi: 10.1083/jcb.201111136.

[56] T. A. Blair, A. D. Michelson, and A. L. Frelinger, "Mass Cytometry Reveals Distinct Platelet Subtypes in Healthy Subjects and Novel Alterations in Surface Glycoproteins in Glanzmann Thrombasthenia.," *Sci Rep*, vol. 8, no. 1, p. 10300, Jul. 2018, doi: 10.1038/s41598-018-28211-5.

7. References

[57] T. Tochigi *et al.*, “Aromatase is a novel neosubstrate of cereblon responsible for immunomodulatory drug-induced thrombocytopenia.,” *Blood*, vol. 135, no. 24, pp. 2146–2158, Jun. 2020, doi: 10.1182/blood.2019003749.

[58] V. K. A. K. A. J. C. A. Authors: Richard N Mitchell, *Pocket Companion to Robbins & Cotran Pathologic Basis of Disease*. 2011.

[59] P. Prandoni *et al.*, “An association between atherosclerosis and venous thrombosis.,” *N Engl J Med*, vol. 348, no. 15, pp. 1435–41, Apr. 2003, doi: 10.1056/NEJMoa022157.

[60] P. von Hundelshausen and C. Weber, “Platelets as immune cells: bridging inflammation and cardiovascular disease.,” *Circ Res*, vol. 100, no. 1, pp. 27–40, Jan. 2007, doi: 10.1161/01.RES.0000252802.25497.b7.

[61] E. A. Middleton, A. S. Weyrich, and G. A. Zimmerman, “Platelets in Pulmonary Immune Responses and Inflammatory Lung Diseases.,” *Physiol Rev*, vol. 96, no. 4, pp. 1211–59, Oct. 2016, doi: 10.1152/physrev.00038.2015.

[62] L. Guo and M. T. Rondina, “The Era of Thromboinflammation: Platelets Are Dynamic Sensors and Effector Cells During Infectious Diseases.,” *Front Immunol*, vol. 10, p. 2204, 2019, doi: 10.3389/fimmu.2019.02204.

[63] M. E. Powers, R. E. N. Becker, A. Sailer, J. R. Turner, and J. Bubeck Wardenburg, “Synergistic Action of Staphylococcus aureus α-Toxin on Platelets and Myeloid Lineage Cells Contributes to Lethal Sepsis.,” *Cell Host Microbe*, vol. 17, no. 6, pp. 775–87, Jun. 2015, doi: 10.1016/j.chom.2015.05.011.

[64] P. J. Lefèbvre and A. J. Scheen, “Glucose metabolism and the postprandial state.,” *Eur J Clin Invest*, vol. 29 Suppl 2, pp. 1–6, Jun. 1999, doi: 10.1046/j.1365-2362.1999.00003.x.

[65] M. Tominaga, H. Eguchi, H. Manaka, K. Igarashi, T. Kato, and A. Sekikawa, “Impaired glucose tolerance is a risk factor for cardiovascular disease, but not impaired fasting glucose. The Funagata Diabetes Study.,” *Diabetes Care*, vol. 22, no. 6, pp. 920–4, Jun. 1999, doi: 10.2337/diacare.22.6.920.

[66] F. Cavalot *et al.*, “Postprandial blood glucose is a stronger predictor of cardiovascular events than fasting blood glucose in type 2 diabetes mellitus, particularly in women: lessons from the San Luigi Gonzaga Diabetes Study.,” *J Clin Endocrinol Metab*, vol. 91, no. 3, pp. 813–9, Mar. 2006, doi: 10.1210/jc.2005-1005.

[67] P. Ferroni, S. Basili, A. Falco, and G. Davì, “Platelet activation in type 2 diabetes mellitus.,” *J Thromb Haemost*, vol. 2, no. 8, pp. 1282–91, Aug. 2004, doi: 10.1111/j.1538-7836.2004.00836.x.

[68] L. Monnier *et al.*, “Activation of oxidative stress by acute glucose fluctuations compared with sustained chronic hyperglycemia in patients with type 2 diabetes.,” *JAMA*, vol. 295, no. 14, pp. 1681–7, Apr. 2006, doi: 10.1001/jama.295.14.1681.

7. References

[69] F. Santilli *et al.*, "Postprandial hyperglycemia is a determinant of platelet activation in early type 2 diabetes mellitus.," *J Thromb Haemost*, vol. 8, no. 4, pp. 828–37, Apr. 2010, doi: 10.1111/j.1538-7836.2010.03742.x.

[70] P. Gresele *et al.*, "Acute, short-term hyperglycemia enhances shear stress-induced platelet activation in patients with type II diabetes mellitus.," *J Am Coll Cardiol*, vol. 41, no. 6, pp. 1013–20, Mar. 2003, doi: 10.1016/s0735-1097(02)02972-8.

[71] T. Przygodzki *et al.*, "Diabetes and Hyperglycemia Affect Platelet GPIIIa Expression. Effects on Adhesion Potential of Blood Platelets from Diabetic Patients under In Vitro Flow Conditions.," *Int J Mol Sci*, vol. 21, no. 9, May 2020, doi: 10.3390/ijms21093222.

[72] R. C. R. Meex, E. E. Blaak, and L. J. C. van Loon, "Lipotoxicity plays a key role in the development of both insulin resistance and muscle atrophy in patients with type 2 diabetes.," *Obes Rev*, vol. 20, no. 9, pp. 1205–1217, Sep. 2019, doi: 10.1111/obr.12862.

[73] P. Sangwung, K. F. Petersen, G. I. Shulman, and J. W. Knowles, "Mitochondrial Dysfunction, Insulin Resistance, and Potential Genetic Implications.," *Endocrinology*, vol. 161, no. 4, Apr. 2020, doi: 10.1210/endocr/bqaa017.

[74] C. Falcon, G. Pfliegler, H. Deckmyn, and J. Vermylen, "The platelet insulin receptor: detection, partial characterization, and search for a function.," *Biochem Biophys Res Commun*, vol. 157, no. 3, pp. 1190–6, Dec. 1988, doi: 10.1016/s0006-291x(88)81000-3.

[75] M. Udvardy, G. Pfliegler, and K. Rak, "Platelet insulin receptor determination in non-insulin dependent diabetes mellitus.," *Experientia*, vol. 41, no. 3, pp. 422–3, Mar. 1985, doi: 10.1007/BF02004539.

[76] S. M. Bode-Böger, R. H. Böger, A. Galland, and J. C. Frölich, "Differential inhibition of human platelet aggregation and thromboxane A2 formation by L-arginine in vivo and in vitro," *Naunyn Schmiedebergs Arch Pharmacol*, vol. 357, no. 2, pp. 143–150, Jan. 1998, doi: 10.1007/PL00005148.

[77] M. Trovati, G. Anfossi, F. Cavalot, P. Massucco, E. Mularoni, and G. Emanuelli, "Insulin directly reduces platelet sensitivity to aggregating agents. Studies in vitro and in vivo.," *Diabetes*, vol. 37, no. 6, pp. 780–6, Jun. 1988, doi: 10.2337/diab.37.6.780.

[78] O. N. Ogurkova, T. Ye. Suslova, A. V. Sitoshevsky, and O. A. Koshelskaya, "Research of cGMP- and cAMP-dependent intracellular signaling systems in the insulin-mediated regulation of platelets aggregation activity in patients with heart failure and metabolic disturbances," *Bulletin of Siberian Medicine*, vol. 11, no. 6, pp. 76–81, Dec. 2012, doi: 10.20538/1682-0363-2012-6-76-81.

7. References

[79] A. Taniguchi *et al.*, "Platelet count is independently associated with insulin resistance in non-obese Japanese type 2 diabetic patients.," *Metabolism*, vol. 52, no. 10, pp. 1246–9, Oct. 2003, doi: 10.1016/s0026-0495(03)00099-4.

[80] D. J. Schneider, "Factors contributing to increased platelet reactivity in people with diabetes.," *Diabetes Care*, vol. 32, no. 4, pp. 525–7, Apr. 2009, doi: 10.2337/dc08-1865.

[81] R. Kaur, M. Kaur, and J. Singh, "Endothelial dysfunction and platelet hyperactivity in type 2 diabetes mellitus: molecular insights and therapeutic strategies.," *Cardiovasc Diabetol*, vol. 17, no. 1, p. 121, Aug. 2018, doi: 10.1186/s12933-018-0763-3.

[82] A. M. Schmidt, S. D. Yan, J. L. Wautier, and D. Stern, "Activation of receptor for advanced glycation end products: a mechanism for chronic vascular dysfunction in diabetic vasculopathy and atherosclerosis.," *Circ Res*, vol. 84, no. 5, pp. 489–97, Mar. 1999, doi: 10.1161/01.res.84.5.489.

[83] S. H. Lee *et al.*, "Inducing mitophagy in diabetic platelets protects against severe oxidative stress.," *EMBO Mol Med*, vol. 8, no. 7, pp. 779–95, Jul. 2016, doi: 10.15252/emmm.201506046.

[84] D. Vara, E. Cifuentes-Pagano, P. J. Pagano, and G. Pula, "A novel combinatorial technique for simultaneous quantification of oxygen radicals and aggregation reveals unexpected redox patterns in the activation of platelets by different physiopathological stimuli.," *Haematologica*, vol. 104, no. 9, pp. 1879–1891, Sep. 2019, doi: 10.3324/haematol.2018.208819.

[85] R. Cangemi *et al.*, "Platelet isoprostane overproduction in diabetic patients treated with aspirin.," *Diabetes*, vol. 61, no. 6, pp. 1626–32, Jun. 2012, doi: 10.2337/db11-1243.

[86] R. Carnevale *et al.*, "Different degrees of NADPH oxidase 2 regulation and in vivo platelet activation: lesson from chronic granulomatous disease.," *J Am Heart Assoc*, vol. 3, no. 3, p. e000920, Jun. 2014, doi: 10.1161/JAHA.114.000920.

[87] A. Gaiz, S. Mosawy, N. Colson, and I. Singh, "Thrombotic and cardiovascular risks in type two diabetes; Role of platelet hyperactivity.," *Biomed Pharmacother*, vol. 94, pp. 679–686, Oct. 2017, doi: 10.1016/j.biopha.2017.07.121.

[88] J. L. Ferreiro, J. A. Gómez-Hospital, and D. J. Angiolillo, "Platelet abnormalities in diabetes mellitus.," *Diab Vasc Dis Res*, vol. 7, no. 4, pp. 251–9, Oct. 2010, doi: 10.1177/1479164110383994.

[89] A. C. Calkin *et al.*, "Reconstituted high-density lipoprotein attenuates platelet function in individuals with type 2 diabetes mellitus by promoting cholesterol efflux.," *Circulation*, vol. 120, no. 21, pp. 2095–104, Nov. 2009, doi: 10.1161/CIRCULATIONAHA.109.870709.

7. References

[90] M.-R. Taskinen and J. Borén, "New insights into the pathophysiology of dyslipidemia in type 2 diabetes.," *Atherosclerosis*, vol. 239, no. 2, pp. 483–95, Apr. 2015, doi: 10.1016/j.atherosclerosis.2015.01.039.

[91] M. M. Boulet *et al.*, "Large triglyceride-rich lipoproteins from fasting patients with type 2 diabetes activate platelets.," *Diabetes Metab*, vol. 46, no. 1, pp. 54–60, Feb. 2020, doi: 10.1016/j.diabet.2019.03.002.

[92] M. Mathieu, L. Martin-Jaular, G. Lavieu, and C. Théry, "Specificities of secretion and uptake of exosomes and other extracellular vesicles for cell-to-cell communication.," *Nat Cell Biol*, vol. 21, no. 1, pp. 9–17, Jan. 2019, doi: 10.1038/s41556-018-0250-9.

[93] M. P. Zaborowski, L. Balaj, X. O. Breakefield, and C. P. Lai, "Extracellular Vesicles: Composition, Biological Relevance, and Methods of Study.," *Bioscience*, vol. 65, no. 8, pp. 783–797, Aug. 2015, doi: 10.1093/biosci/biv084.

[94] S. Gurung, D. Perocheau, L. Touramanidou, and J. Baruteau, "The exosome journey: from biogenesis to uptake and intracellular signalling.," *Cell Commun Signal*, vol. 19, no. 1, p. 47, Apr. 2021, doi: 10.1186/s12964-021-00730-1.

[95] M. Battistelli and E. Falcieri, "Apoptotic Bodies: Particular Extracellular Vesicles Involved in Intercellular Communication.," *Biology (Basel)*, vol. 9, no. 1, Jan. 2020, doi: 10.3390/biology9010021.

[96] G. Turturici, R. Tinnirello, G. Sconzo, and F. Geraci, "Extracellular membrane vesicles as a mechanism of cell-to-cell communication: advantages and disadvantages.," *Am J Physiol Cell Physiol*, vol. 306, no. 7, pp. C621-33, Apr. 2014, doi: 10.1152/ajpcell.00228.2013.

[97] A. S. Eustes and S. Dayal, "The Role of Platelet-Derived Extracellular Vesicles in Immune-Mediated Thrombosis.," *Int J Mol Sci*, vol. 23, no. 14, Jul. 2022, doi: 10.3390/ijms23147837.

[98] J. Wu, Y. Piao, Q. Liu, and X. Yang, "Platelet-rich plasma-derived extracellular vesicles: A superior alternative in regenerative medicine?," *Cell Prolif*, vol. 54, no. 12, p. e13123, Dec. 2021, doi: 10.1111/cpr.13123.

[99] M. Vismara *et al.*, "Proteomic and functional profiling of platelet-derived extracellular vesicles released under physiological or tumor-associated conditions.," *Cell Death Discov*, vol. 8, no. 1, p. 467, Nov. 2022, doi: 10.1038/s41420-022-01263-3.

[100] F. Puhm, E. Boilard, and K. R. Machlus, "Platelet Extracellular Vesicles: Beyond the Blood.," *Arterioscler Thromb Vasc Biol*, vol. 41, no. 1, pp. 87–96, Jan. 2021, doi: 10.1161/ATVBAHA.120.314644.

[101] P. M. Ferreira *et al.*, "Mode of induction of platelet-derived extracellular vesicles is a critical determinant of their phenotype and function.," *Sci Rep*, vol. 10, no. 1, p. 18061, Oct. 2020, doi: 10.1038/s41598-020-73005-3.

7. References

[102] K. Wei, H. Huang, M. Liu, D. Shi, and X. Ma, "Platelet-Derived Exosomes and Atherothrombosis.," *Front Cardiovasc Med*, vol. 9, p. 886132, 2022, doi: 10.3389/fcvm.2022.886132.

[103] J. Liu, Y. Zhang, Y. Tian, W. Huang, N. Tong, and X. Fu, "Integrative biology of extracellular vesicles in diabetes mellitus and diabetic complications.," *Theranostics*, vol. 12, no. 3, pp. 1342–1372, 2022, doi: 10.7150/thno.65778.

[104] S. F. Wu, N. Noren Hooten, D. W. Freeman, N. A. Mode, A. B. Zonderman, and M. K. Evans, "Extracellular vesicles in diabetes mellitus induce alterations in endothelial cell morphology and migration.," *J Transl Med*, vol. 18, no. 1, p. 230, Jun. 2020, doi: 10.1186/s12967-020-02398-6.

[105] K. Zifkos, C. Dubois, and K. Schäfer, "Extracellular Vesicles and Thrombosis: Update on the Clinical and Experimental Evidence.," *Int J Mol Sci*, vol. 22, no. 17, Aug. 2021, doi: 10.3390/ijms22179317.

[106] M. R. Wilkins *et al.*, "Progress with proteome projects: why all proteins expressed by a genome should be identified and how to do it.," *Biotechnol Genet Eng Rev*, vol. 13, pp. 19–50, 1996, doi: 10.1080/02648725.1996.10647923.

[107] T. E. Angel *et al.*, "Mass spectrometry-based proteomics: existing capabilities and future directions.," *Chem Soc Rev*, vol. 41, no. 10, pp. 3912–28, May 2012, doi: 10.1039/c2cs15331a.

[108] M. A. Olshina and M. Sharon, "Mass Spectrometry: A Technique of Many Faces.," *Q Rev Biophys*, vol. 49, Jan. 2016, doi: 10.1017/S0033583516000160.

[109] F. T. FW McLafferty, *Interpretation of mass spectra*. 1993.

[110] A. Steckel and G. Schlosser, "An Organic Chemist's Guide to Electrospray Mass Spectrometric Structure Elucidation.," *Molecules*, vol. 24, no. 3, Feb. 2019, doi: 10.3390/molecules24030611.

[111] R. B. M. E. G. L. L. L. Y. N. KK Murray, "Definitions of terms relating to mass spectrometry (IUPAC Recommendations 2013)," 2013.

[112] A. P. Bruins, "Mechanistic aspects of electrospray ionization," *J Chromatogr A*, vol. 794, no. 1–2, pp. 345–357, Jan. 1998, doi: 10.1016/S0021-9673(97)01110-2.

[113] C. S. Ho *et al.*, "Electrospray ionisation mass spectrometry: principles and clinical applications.," *Clin Biochem Rev*, vol. 24, no. 1, pp. 3–12, 2003.

[114] S. Eliuk and A. Makarov, "Evolution of Orbitrap Mass Spectrometry Instrumentation," *Annual Review of Analytical Chemistry*, vol. 8, no. 1, pp. 61–80, Jul. 2015, doi: 10.1146/annurev-anchem-071114-040325.

7. References

[115] J. Wandy *et al.*, "Simulated-to-real benchmarking of acquisition methods in untargeted metabolomics.," *Front Mol Biosci*, vol. 10, p. 1130781, 2023, doi: 10.3389/fmolb.2023.1130781.

[116] K.-C. Cho *et al.*, "Deep Proteomics Using Two Dimensional Data Independent Acquisition Mass Spectrometry.," *Anal Chem*, vol. 92, no. 6, pp. 4217–4225, Mar. 2020, doi: 10.1021/acs.analchem.9b04418.

[117] U. H. Toprak, L. C. Gillet, A. Maiolica, P. Navarro, A. Leitner, and R. Aebersold, "Conserved peptide fragmentation as a benchmarking tool for mass spectrometers and a discriminating feature for targeted proteomics.," *Mol Cell Proteomics*, vol. 13, no. 8, pp. 2056–71, Aug. 2014, doi: 10.1074/mcp.O113.036475.

[118] L. E. Donovan *et al.*, "Exploring the potential of the platelet membrane proteome as a source of peripheral biomarkers for Alzheimer's disease.," *Alzheimers Res Ther*, vol. 5, no. 3, p. 32, 2013, doi: 10.1186/alzrt186.

[119] M. Sielaff *et al.*, "Evaluation of FASP, SP3, and iST Protocols for Proteomic Sample Preparation in the Low Microgram Range," *J Proteome Res*, vol. 16, no. 11, pp. 4060–4072, Nov. 2017, doi: 10.1021/acs.jproteome.7b00433.

[120] C. S. Hughes, S. Moggridge, T. Müller, P. H. Sorensen, G. B. Morin, and J. Krijgsveld, "Single-pot, solid-phase-enhanced sample preparation for proteomics experiments," *Nat Protoc*, vol. 14, no. 1, pp. 68–85, Jan. 2019, doi: 10.1038/s41596-018-0082-x.

[121] J. R. Wiśniewski, "Filter-Aided Sample Preparation for Proteome Analysis," 2018, pp. 3–10. doi: 10.1007/978-1-4939-8695-8_1.

[122] G. von Amsberg *et al.*, "Salvage Chemotherapy with Cisplatin, Ifosfamide, and Paclitaxel in Aggressive Variant of Metastatic Castration-Resistant Prostate Cancer.," *Int J Mol Sci*, vol. 23, no. 23, Nov. 2022, doi: 10.3390/ijms232314948.

[123] S. P. Holly, X. Chen, and L. V. Parise, "Abundance- and Activity-Based Proteomics in Platelet Biology," *Curr Proteomics*, vol. 8, no. 3, pp. 216–228, Oct. 2011, doi: 10.2174/157016411797247512.

[124] J. Li *et al.*, "Comprehensive proteomics and functional annotation of mouse brown adipose tissue," *PLoS One*, vol. 15, no. 5, p. e0232084, May 2020, doi: 10.1371/journal.pone.0232084.

[125] M. A. Gonzalez-Lozano, F. Koopmans, I. Paliukhovich, A. B. Smit, and K. W. Li, "A Fast and Economical Sample Preparation Protocol for Interaction Proteomics Analysis," *Proteomics*, vol. 19, no. 9, p. 1900027, May 2019, doi: 10.1002/pmic.201900027.

[126] D. L. Springer *et al.*, "Platelet Proteome Changes Associated with Diabetes and during Platelet Storage for Transfusion," *J Proteome Res*, vol. 8, no. 5, pp. 2261–2272, May 2009, doi: 10.1021/pr800885j.

7. References

[127] A. Nusca *et al.*, "Platelet Effects of Anti-diabetic Therapies: New Perspectives in the Management of Patients with Diabetes and Cardiovascular Disease," *Front Pharmacol*, vol. 12, May 2021, doi: 10.3389/fphar.2021.670155.

[128] J. E. Aslan, "Platelet Proteomes, Pathways, and Phenotypes as Informants of Vascular Wellness and Disease," *Arterioscler Thromb Vasc Biol*, vol. 41, no. 3, pp. 999–1011, Mar. 2021, doi: 10.1161/ATVBAHA.120.314647.

[129] E. Eitan *et al.*, "Age-Related Changes in Plasma Extracellular Vesicle Characteristics and Internalization by Leukocytes," *Sci Rep*, vol. 7, no. 1, p. 1342, May 2017, doi: 10.1038/s41598-017-01386-z.

[130] Y. He and Q. Wu, "The Effect of Extracellular Vesicles on Thrombosis," *J Cardiovasc Transl Res*, vol. 16, no. 3, pp. 682–697, Jun. 2023, doi: 10.1007/s12265-022-10342-w.

[131] A. R. Vaidya, N. Wolska, D. Vara, R. K. Mailer, K. Schröder, and G. Pula, "Diabetes and Thrombosis: A Central Role for Vascular Oxidative Stress," *Antioxidants*, vol. 10, no. 5, p. 706, Apr. 2021, doi: 10.3390/antiox10050706.

[132] N. Y. Maeda, S. P. Bydlowski, and A. A. Lopes, "Increased tyrosine phosphorylation of platelet proteins including pp125(FAK) suggests endogenous activation and aggregation in pulmonary hypertension.," *Clin Appl Thromb Hemost*, vol. 11, no. 4, pp. 411–5, Oct. 2005, doi: 10.1177/107602960501100407.

[133] G. Turturici, R. Tinnirello, G. Sconzo, and F. Geraci, "Extracellular membrane vesicles as a mechanism of cell-to-cell communication: advantages and disadvantages," *American Journal of Physiology-Cell Physiology*, vol. 306, no. 7, pp. C621–C633, Apr. 2014, doi: 10.1152/ajpcell.00228.2013.

[134] N. Eaton *et al.*, "Bleeding diathesis in mice lacking JAK2 in platelets.," *Blood Adv*, vol. 5, no. 15, pp. 2969–2981, Aug. 2021, doi: 10.1182/bloodadvances.2020003032.

[135] M. T. K. Zaldivia, J. D. McFadyen, B. Lim, X. Wang, and K. Peter, "Platelet-Derived Microvesicles in Cardiovascular Diseases.," *Front Cardiovasc Med*, vol. 4, p. 74, 2017, doi: 10.3389/fcvm.2017.00074.

[136] W. Zhang, X. Dong, T. Wang, and Y. Kong, "Exosomes derived from platelet-rich plasma mediate hyperglycemia-induced retinal endothelial injury via targeting the TLR4 signaling pathway.," *Exp Eye Res*, vol. 189, p. 107813, Dec. 2019, doi: 10.1016/j.exer.2019.107813.

[137] G.-H. Wang *et al.*, "Platelet microparticles contribute to aortic vascular endothelial injury in diabetes via the mTORC1 pathway.," *Acta Pharmacol Sin*, vol. 40, no. 4, pp. 468–476, Apr. 2019, doi: 10.1038/s41401-018-0186-4.

[138] Y. Zhang *et al.*, "Platelet Microparticles Mediate Glomerular Endothelial Injury in Early Diabetic Nephropathy.," *J Am Soc Nephrol*, vol. 29, no. 11, pp. 2671–2695, Nov. 2018, doi: 10.1681/ASN.2018040368.

7. References

[139] X. Wu, F. Gong, and W. Wang, "Protein extraction from plant tissues for 2DE and its application in proteomic analysis.," *Proteomics*, vol. 14, no. 6, pp. 645–58, Mar. 2014, doi: 10.1002/pmic.201300239.

[140] M. Cilia, T. Fish, X. Yang, M. McLaughlin, T. W. Thannhauser, and S. Gray, "A comparison of protein extraction methods suitable for gel-based proteomic studies of aphid proteins.," *J Biomol Tech*, vol. 20, no. 4, pp. 201–15, Sep. 2009.

[141] S. M. Moore, S. M. Hess, and J. W. Jorgenson, "Extraction, Enrichment, Solubilization, and Digestion Techniques for Membrane Proteomics.," *J Proteome Res*, vol. 15, no. 4, pp. 1243–52, Apr. 2016, doi: 10.1021/acs.jproteome.5b01122.

[142] L. J. White *et al.*, "The impact of detergents on the tissue decellularization process: A ToF-SIMS study.," *Acta Biomater*, vol. 50, pp. 207–219, Mar. 2017, doi: 10.1016/j.actbio.2016.12.033.

[143] K. Mikulášek, H. Konečná, D. Potěšil, R. Holánková, J. Havliš, and Z. Zdráhal, "SP3 Protocol for Proteomic Plant Sample Preparation Prior LC-MS/MS.," *Front Plant Sci*, vol. 12, p. 635550, 2021, doi: 10.3389/fpls.2021.635550.

[144] E. Scheerlinck *et al.*, "Minimizing technical variation during sample preparation prior to label-free quantitative mass spectrometry.," *Anal Biochem*, vol. 490, pp. 14–9, Dec. 2015, doi: 10.1016/j.ab.2015.08.018.

[145] K. M. Supasri *et al.*, "Evaluation of Filter, Paramagnetic, and STAGETips Aided Workflows for Proteome Profiling of Symbiodiniaceae Dinoflagellate," *Processes*, vol. 9, no. 6, p. 983, Jun. 2021, doi: 10.3390/pr9060983.

[146] M. R. O. Trugilho *et al.*, "Platelet proteome reveals features of cell death, antiviral response and viral replication in covid-19.," *Cell Death Discov*, vol. 8, no. 1, p. 324, Jul. 2022, doi: 10.1038/s41420-022-01122-1.

[147] H. Yu *et al.*, "Platelet biomarkers for a descending cognitive function: A proteomic approach.," *Aging Cell*, vol. 20, no. 5, p. e13358, May 2021, doi: 10.1111/acel.13358.

[148] J. P. van Geffen *et al.*, "Mild hyperlipidemia in mice aggravates platelet responsiveness in thrombus formation and exploration of platelet proteome and lipidome.," *Sci Rep*, vol. 10, no. 1, p. 21407, Dec. 2020, doi: 10.1038/s41598-020-78522-9.

[149] A. Bianchetti *et al.*, "A Blood Bank Standardized Production of Human Platelet Lysate for Mesenchymal Stromal Cell Expansion: Proteomic Characterization and Biological Effects.," *Front Cell Dev Biol*, vol. 9, p. 650490, 2021, doi: 10.3389/fcell.2021.650490.

[150] G. Song, P. Y. Hsu, and J. W. Walley, "Assessment and Refinement of Sample Preparation Methods for Deep and Quantitative Plant Proteome Profiling.," *Proteomics*, vol. 18, no. 17, p. e1800220, Sep. 2018, doi: 10.1002/pmic.201800220.

7. References

[151] J. R. Wiśniewski, “Filter-Aided Sample Preparation for Proteome Analysis,” 2018, pp. 3–10. doi: 10.1007/978-1-4939-8695-8_1.

[152] S. X. Gu and S. Dayal, “Redox Mechanisms of Platelet Activation in Aging.,” *Antioxidants (Basel)*, vol. 11, no. 5, May 2022, doi: 10.3390/antiox11050995.

[153] A. J. Unsworth *et al.*, “Human Platelet Protein Ubiquitylation and Changes following GPVI Activation.,” *Thromb Haemost*, vol. 119, no. 1, pp. 104–116, Jan. 2019, doi: 10.1055/s-0038-1676344.

[154] R. Anand, A. S. Reichert, and A. K. Kondadi, “Emerging Roles of the MICOS Complex in Cristae Dynamics and Biogenesis.,” *Biology (Basel)*, vol. 10, no. 7, Jun. 2021, doi: 10.3390/biology10070600.

[155] A. Michno, K. Grużewska, H. Bielarczyk, M. Zyśk, and A. Szutowicz, “Inhibition of pyruvate dehydrogenase complex activity by 3-bromopyruvate affects blood platelets responses in type 2 diabetes.,” *Pharmacol Rep*, vol. 72, no. 1, pp. 225–237, Feb. 2020, doi: 10.1007/s43440-019-00005-0.

[156] J. Y. Jang *et al.*, “Peroxiredoxin II is an antioxidant enzyme that negatively regulates collagen-stimulated platelet function.,” *J Biol Chem*, vol. 290, no. 18, pp. 11432–42, May 2015, doi: 10.1074/jbc.M115.644260.

[157] S.-J. Jeong, J.-G. Park, and G. T. Oh, “Peroxiredoxins as Potential Targets for Cardiovascular Disease.,” *Antioxidants (Basel)*, vol. 10, no. 8, Aug. 2021, doi: 10.3390/antiox10081244.

[158] T. Kessler *et al.*, “Functional Characterization of the GUCY1A3 Coronary Artery Disease Risk Locus.,” *Circulation*, vol. 136, no. 5, pp. 476–489, Aug. 2017, doi: 10.1161/CIRCULATIONAHA.116.024152.

[159] R. Feil and B. Kemp-Harper, “cGMP signalling: from bench to bedside. Conference on cGMP generators, effectors and therapeutic implications.,” *EMBO Rep*, vol. 7, no. 2, pp. 149–53, Feb. 2006, doi: 10.1038/sj.embor.7400627.

[160] J. Wobst, T. Kessler, T. A. Dang, J. Erdmann, and H. Schunkert, “Role of sGC-dependent NO signalling and myocardial infarction risk.,” *J Mol Med (Berl)*, vol. 93, no. 4, pp. 383–94, Apr. 2015, doi: 10.1007/s00109-015-1265-3.

[161] R. H. Kehlenbach, J. Matthey, and W. B. Huttner, “XL alpha s is a new type of G protein.,” *Nature*, vol. 372, no. 6508, pp. 804–9, doi: 10.1038/372804a0.

[162] H. A. Pasolli, M. Klemke, R. H. Kehlenbach, Y. Wang, and W. B. Huttner, “Characterization of the extra-large G protein alpha-subunit XLalphas. I. Tissue distribution and subcellular localization.,” *J Biol Chem*, vol. 275, no. 43, pp. 33622–32, Oct. 2000, doi: 10.1074/jbc.M001335200.

7. References

[163] A. Shenker, P. Goldsmith, C. G. Unson, and A. M. Spiegel, “The G protein coupled to the thromboxane A2 receptor in human platelets is a member of the novel Gq family.,” *J Biol Chem*, vol. 266, no. 14, pp. 9309–13, May 1991.

[164] M. Klemke, H. A. Pasolli, R. H. Kehlenbach, S. Offermanns, G. Schultz, and W. B. Huttner, “Characterization of the extra-large G protein alpha-subunit XLalphas. II. Signal transduction properties.,” *J Biol Chem*, vol. 275, no. 43, pp. 33633–40, Oct. 2000, doi: 10.1074/jbc.M006594200.

[165] M. Bastepe, Y. Gunes, B. Perez-Villamil, J. Hunzelman, L. S. Weinstein, and H. Jüppner, “Receptor-mediated adenylyl cyclase activation through XLalpha(s), the extra-large variant of the stimulatory G protein alpha-subunit.,” *Mol Endocrinol*, vol. 16, no. 8, pp. 1912–9, Aug. 2002, doi: 10.1210/me.2002-0054.

[166] G. Liu *et al.*, “CD44 sensitivity of platelet activation, membrane scrambling and adhesion under high arterial shear rates.,” *Thromb Haemost*, vol. 115, no. 1, pp. 99–108, Jan. 2016, doi: 10.1160/TH14-10-0847.

[167] M. C. Morrison and R. Kleemann, “Role of Macrophage Migration Inhibitory Factor in Obesity, Insulin Resistance, Type 2 Diabetes, and Associated Hepatic Co-Morbidities: A Comprehensive Review of Human and Rodent Studies.,” *Front Immunol*, vol. 6, p. 308, 2015, doi: 10.3389/fimmu.2015.00308.

[168] C. Toso, J. A. Emamaullee, S. Merani, and A. M. J. Shapiro, “The role of macrophage migration inhibitory factor on glucose metabolism and diabetes.,” *Diabetologia*, vol. 51, no. 11, pp. 1937–46, Nov. 2008, doi: 10.1007/s00125-008-1063-3.

[169] M. Chatterjee *et al.*, “Macrophage migration inhibitory factor limits activation-induced apoptosis of platelets via CXCR7-dependent Akt signaling.,” *Circ Res*, vol. 115, no. 11, pp. 939–49, Nov. 2014, doi: 10.1161/CIRCRESAHA.115.305171.

[170] M. M. J. van Greevenbroek, C. G. Schalkwijk, and C. D. A. Stehouwer, “Obesity-associated low-grade inflammation in type 2 diabetes mellitus: causes and consequences.,” *Neth J Med*, vol. 71, no. 4, pp. 174–87, May 2013.

[171] M. J. Polley and R. L. Nachman, “Human complement in thrombin-mediated platelet function: uptake of the C5b-9 complex.,” *J Exp Med*, vol. 150, no. 3, pp. 633–45, Sep. 1979, doi: 10.1084/jem.150.3.633.

[172] D. Bhole and G. L. Stahl, “Molecular basis for complement component 6 (C6) deficiency in rats and mice.,” *Immunobiology*, vol. 209, no. 7, pp. 559–68, 2004, doi: 10.1016/j.imbio.2004.08.001.

[173] W. Schmiedt *et al.*, “Complement C6 deficiency protects against diet-induced atherosclerosis in rabbits.,” *Arterioscler Thromb Vasc Biol*, vol. 18, no. 11, pp. 1790–5, Nov. 1998, doi: 10.1161/01.atv.18.11.1790.

7. References

[174] C. Puy *et al.*, "Cross-Talk between the Complement Pathway and the Contact Activation System of Coagulation: Activated Factor XI Neutralizes Complement Factor H.," *J Immunol*, vol. 206, no. 8, pp. 1784–1792, Apr. 2021, doi: 10.4049/jimmunol.2000398.

[175] E. Valoti *et al.*, "Impact of a Complement Factor H Gene Variant on Renal Dysfunction, Cardiovascular Events, and Response to ACE Inhibitor Therapy in Type 2 Diabetes.," *Front Genet*, vol. 10, p. 681, 2019, doi: 10.3389/fgene.2019.00681.

[176] K. C. M. C. Koeijvoets *et al.*, "Complement factor H Y402H decreases cardiovascular disease risk in patients with familial hypercholesterolaemia.," *Eur Heart J*, vol. 30, no. 5, pp. 618–23, Mar. 2009, doi: 10.1093/eurheartj/ehn568.

[177] W.-T. Liao, W.-L. Chen, Y.-L. Tain, and C.-N. Hsu, "Complement Factor H and Related Proteins as Markers of Cardiovascular Risk in Pediatric Chronic Kidney Disease.," *Biomedicines*, vol. 10, no. 6, Jun. 2022, doi: 10.3390/biomedicines10061396.

[178] V. Lemos *et al.*, "The NAD+-dependent deacetylase SIRT2 attenuates oxidative stress and mitochondrial dysfunction and improves insulin sensitivity in hepatocytes.," *Hum Mol Genet*, vol. 26, no. 21, pp. 4105–4117, Nov. 2017, doi: 10.1093/hmg/ddx298.

[179] A. Taneja, V. Ravi, J. Y. Hong, H. Lin, and N. R. Sundaresan, "Emerging roles of Sirtuin 2 in cardiovascular diseases.," *FASEB J*, vol. 35, no. 10, p. e21841, Oct. 2021, doi: 10.1096/fj.202100490R.

[180] Z. Zhou, T. Ma, Q. Zhu, Y. Xu, and X. Zha, "Recent advances in inhibitors of sirtuin1/2: an update and perspective.," *Future Med Chem*, vol. 10, no. 8, pp. 907–934, Apr. 2018, doi: 10.4155/fmc-2017-0207.

[181] S. Kumari, S. N. Chaurasia, M. K. Nayak, R. L. Mallick, and D. Dash, "Sirtuin Inhibition Induces Apoptosis-like Changes in Platelets and Thrombocytopenia.," *J Biol Chem*, vol. 290, no. 19, pp. 12290–9, May 2015, doi: 10.1074/jbc.M114.615948.

[182] Y. R. Kim *et al.*, "Identification and functional study of genetic polymorphisms in cyclic nucleotide phosphodiesterase 3A (PDE3A).," *Ann Hum Genet*, vol. 85, no. 2, pp. 80–91, Mar. 2021, doi: 10.1111/ahg.12411.

[183] R. W. Hunter, C. Mackintosh, and I. Hers, "Protein kinase C-mediated phosphorylation and activation of PDE3A regulate cAMP levels in human platelets.," *J Biol Chem*, vol. 284, no. 18, pp. 12339–48, May 2009, doi: 10.1074/jbc.M807536200.

[184] R. W. Colman, "Platelet cyclic adenosine monophosphate phosphodiesterases: targets for regulating platelet-related thrombosis.," *Semin Thromb Hemost*, vol. 30, no. 4, pp. 451–60, Aug. 2004, doi: 10.1055/s-2004-833480.

[185] D. S. Sim, G. Merrill-Skoloff, B. C. Furie, B. Furie, and R. Flaumenhaft, "Initial accumulation of platelets during arterial thrombus formation in vivo is inhibited by

elevation of basal cAMP levels.," *Blood*, vol. 103, no. 6, pp. 2127–34, Mar. 2004, doi: 10.1182/blood-2003-04-1133.

[186] R. Hanna *et al.*, "Cardiac Phosphodiesterases Are Differentially Increased in Diabetic Cardiomyopathy.," *Life Sci*, vol. 283, p. 119857, Oct. 2021, doi: 10.1016/j.lfs.2021.119857.

[187] C.-L. Huang, J.-C. Cheng, A. Stern, J.-T. Hsieh, C.-H. Liao, and C.-P. Tseng, "Disabled-2 is a novel alphaIIb-integrin-binding protein that negatively regulates platelet-fibrinogen interactions and platelet aggregation.," *J Cell Sci*, vol. 119, no. Pt 21, pp. 4420–30, Nov. 2006, doi: 10.1242/jcs.03195.

[188] J. P. DiNitto and D. G. Lambright, "Membrane and juxtamembrane targeting by PH and PTB domains.," *Biochim Biophys Acta*, vol. 1761, no. 8, pp. 850–67, Aug. 2006, doi: 10.1016/j.bbalip.2006.04.008.

[189] M. T. Uhlik, B. Temple, S. Bencharit, A. J. Kimple, D. P. Siderovski, and G. L. Johnson, "Structural and evolutionary division of phosphotyrosine binding (PTB) domains.," *J Mol Biol*, vol. 345, no. 1, pp. 1–20, Jan. 2005, doi: 10.1016/j.jmb.2004.10.038.

[190] H.-J. Tsai *et al.*, "Integrin αIIbβ3 outside-in signaling activates human platelets through serine 24 phosphorylation of Disabled-2.," *Cell Biosci*, vol. 11, no. 1, p. 32, Feb. 2021, doi: 10.1186/s13578-021-00532-5.

[191] H.-J. Tsai *et al.*, "Disabled-2 is required for efficient hemostasis and platelet activation by thrombin in mice.," *Arterioscler Thromb Vasc Biol*, vol. 34, no. 11, pp. 2404–12, Nov. 2014, doi: 10.1161/ATVBAHA.114.302602.

[192] J. D. Welsh *et al.*, "Disabled-2 modulates homotypic and heterotypic platelet interactions by binding to sulfatides.," *Br J Haematol*, vol. 154, no. 1, pp. 122–33, Jul. 2011, doi: 10.1111/j.1365-2141.2011.08705.x.

[193] S. C. Ogbu, P. R. Musich, J. Zhang, Z. Q. Yao, P. H. Howe, and Y. Jiang, "The role of disabled-2 (Dab2) in diseases.," *Gene*, vol. 769, p. 145202, Feb. 2021, doi: 10.1016/j.gene.2020.145202.

[194] S. Séverin *et al.*, "Deficiency of Src homology 2 domain-containing inositol 5-phosphatase 1 affects platelet responses and thrombus growth.," *J Clin Invest*, vol. 117, no. 4, pp. 944–52, Apr. 2007, doi: 10.1172/JCI29967.

[195] M.-P. Gratacap, S. Séverin, G. Chicanne, M. Plantavid, and B. Payrastre, "Different roles of SHIP1 according to the cell context: the example of blood platelets.," *Adv Enzyme Regul*, vol. 48, pp. 240–52, 2008, doi: 10.1016/j.advenzreg.2007.11.004.

[196] S. Yamagishi, T. Matsui, S. Ueda, and M. Takeuchi, "Pigment epithelium-derived factor (PEDF) inhibits diabetes- or advanced glycation end product (AGE)-induced

platelet CD40 ligand overexpression in rats.," *Int J Cardiol*, vol. 144, no. 2, pp. 283–5, Oct. 2010, doi: 10.1016/j.ijcard.2009.01.071.

[197] K. Takenaka *et al.*, "Pigment epithelium-derived factor (PEDF) administration inhibits occlusive thrombus formation in rats: a possible participation of reduced intraplatelet PEDF in thrombosis of acute coronary syndromes.," *Atherosclerosis*, vol. 197, no. 1, pp. 25–33, Mar. 2008, doi: 10.1016/j.atherosclerosis.2007.07.041.

[198] S. Yamagishi, T. Matsui, K. Nakamura, and K. Takenaka, "Pigment epithelium-derived factor (PEDF) inhibits collagen-induced platelet activation by reducing intraplatelet nitrotyrosine levels.," *Int J Cardiol*, vol. 140, no. 1, pp. 121–2, Apr. 2010, doi: 10.1016/j.ijcard.2008.11.015.

[199] S.-I. Yamagishi, T. Matsui, K. Takenaka, K. Nakamura, M. Takeuchi, and H. Inoue, "Pigment epithelium-derived factor (PEDF) prevents platelet activation and aggregation in diabetic rats by blocking deleterious effects of advanced glycation end products (AGEs).," *Diabetes Metab Res Rev*, vol. 25, no. 3, pp. 266–71, Mar. 2009, doi: 10.1002/dmrr.906.

[200] S. Yamagishi, T. Matsui, K. Nakamura, and K. Takenaka, "Administration of pigment epithelium-derived factor prolongs bleeding time by suppressing plasminogen activator inhibitor-1 activity and platelet aggregation in rats.," *Clin Exp Med*, vol. 9, no. 1, pp. 73–6, Mar. 2009, doi: 10.1007/s10238-008-0010-4.

[201] D. Karasek *et al.*, "Association of pigment epithelium derived factor with von Willebrand factor and plasminogen activator inhibitor 1 in patients with type 2 diabetes.," *Physiol Res*, vol. 68, no. 3, pp. 409–418, Jun. 2019, doi: 10.33549/physiolres.934013.

[202] P. J. Unung, I. E. Bassey, M. H. Etukudo, A. E. Udoh, M. B. Alhassan, and U. O. Akpan, "Effect of glycemic control and dyslipidemia on plasma vascular endothelial growth factor and pigment epithelium-derived factor in diabetic retinopathy patients in Northern Nigeria.," *Int J Health Sci (Qassim)*, vol. 14, no. 6, pp. 4–12, 2020.

[203] A. Fayed *et al.*, "Urinary pigment epithelium-derived factor as a marker of diabetic nephropathy in Egyptian patients with type 2 diabetes mellitus.," *Saudi J Kidney Dis Transpl*, vol. 32, no. 5, pp. 1340–1347, 2021, doi: 10.4103/1319-2442.344753.

[204] F. A. Barry, G. J. Graham, M. J. Fry, and J. M. Gibbins, "Regulation of glycogen synthase kinase 3 in human platelets: a possible role in platelet function?," *FEBS Lett*, vol. 553, no. 1–2, pp. 173–8, Oct. 2003, doi: 10.1016/s0014-5793(03)01015-9.

[205] S. F. Moore *et al.*, "Opposing Roles of GSK3α and GSK3β Phosphorylation in Platelet Function and Thrombosis.," *Int J Mol Sci*, vol. 22, no. 19, Sep. 2021, doi: 10.3390/ijms221910656.

7. References

[206] S. F. Moore, M. T. J. van den Bosch, R. W. Hunter, K. Sakamoto, A. W. Poole, and I. Hers, "Dual regulation of glycogen synthase kinase 3 (GSK3)α/β by protein kinase C (PKC)α and Akt promotes thrombin-mediated integrin αIIbβ3 activation and granule secretion in platelets.," *J Biol Chem*, vol. 288, no. 6, pp. 3918–28, Feb. 2013, doi: 10.1074/jbc.M112.429936.

[207] Z. Li *et al.*, "Glycogen synthase kinase-3: a key kinase in retinal neuron apoptosis in early diabetic retinopathy.," *Chin Med J (Engl)*, vol. 127, no. 19, pp. 3464–70, 2014.

[208] P. V Rao, S. Pugazhenthi, and R. L. Khandelwal, "Insulin decreases the glycogen synthase kinase-3 alpha mRNA levels by altering its stability in streptozotocin-induced diabetic rat liver.," *Biochem Biophys Res Commun*, vol. 217, no. 1, pp. 250–6, Dec. 1995, doi: 10.1006/bbrc.1995.2771.

[209] P. De Meyts, *The Insulin Receptor and Its Signal Transduction Network*. 2000.

[210] A. L. Kearney *et al.*, "Akt phosphorylates insulin receptor substrate to limit PI3K-mediated PIP3 synthesis.," *Elife*, vol. 10, Jul. 2021, doi: 10.7554/eLife.66942.

[211] L. Nigi *et al.*, "MicroRNAs as Regulators of Insulin Signaling: Research Updates and Potential Therapeutic Perspectives in Type 2 Diabetes.," *Int J Mol Sci*, vol. 19, no. 12, Nov. 2018, doi: 10.3390/ijms19123705.

[212] R. T. McCallum and M. L. Perreault, "Glycogen Synthase Kinase-3: A Focal Point for Advancing Pathogenic Inflammation in Depression.," *Cells*, vol. 10, no. 9, Sep. 2021, doi: 10.3390/cells10092270.

[213] O. Zharkova *et al.*, "Deletion of Annexin A1 in Mice Upregulates the Expression of Its Receptor, Fpr2/3, and Reactivity to the AnxA1 Mimetic Peptide in Platelets.," *Int J Mol Sci*, vol. 24, no. 4, Feb. 2023, doi: 10.3390/ijms24043424.

[214] E. Y. Senchenkova *et al.*, "Novel Role for the AnxA1-Fpr2/ALX Signaling Axis as a Key Regulator of Platelet Function to Promote Resolution of Inflammation.," *Circulation*, vol. 140, no. 4, pp. 319–335, Jul. 2019, doi: 10.1161/CIRCULATIONAHA.118.039345.

[215] R. de Jong, G. Leoni, M. Drechsler, and O. Soehnlein, "The advantageous role of annexin A1 in cardiovascular disease.," *Cell Adh Migr*, vol. 11, no. 3, pp. 261–274, May 2017, doi: 10.1080/19336918.2016.1259059.

[216] G. S. D. Purvis, E. Solito, and C. Thiemermann, "Annexin-A1: Therapeutic Potential in Microvascular Disease.," *Front Immunol*, vol. 10, p. 938, 2019, doi: 10.3389/fimmu.2019.00938.

[217] T. G. Walsh, Y. Li, C. M. Williams, E. W. Aitken, R. K. Andrews, and A. W. Poole, "Loss of the exocyst complex component EXOC3 promotes hemostasis and accelerates arterial thrombosis.," *Blood Adv*, vol. 5, no. 3, pp. 674–686, Feb. 2021, doi: 10.1182/bloodadvances.2020002515.

7. References

[218] J. E. Miller *et al.*, "Rare variants in the splicing regulatory elements of EXOC3L4 are associated with brain glucose metabolism in Alzheimer's disease.," *BMC Med Genomics*, vol. 11, no. Suppl 3, p. 76, Sep. 2018, doi: 10.1186/s12920-018-0390-6.

[219] C. Watanabe *et al.*, "Essential Roles of Exocyst Complex Component 3-like 2 on Cardiovascular Development in Mice.," *Life (Basel)*, vol. 12, no. 11, Oct. 2022, doi: 10.3390/life12111730.

[220] T. J. Podor *et al.*, "Vimentin exposed on activated platelets and platelet microparticles localizes vitronectin and plasminogen activator inhibitor complexes on their surface.," *J Biol Chem*, vol. 277, no. 9, pp. 7529–39, Mar. 2002, doi: 10.1074/jbc.M109675200.

[221] F. W. Lam, Q. Da, B. Guillory, and M. A. Cruz, "Recombinant Human Vimentin Binds to P-Selectin and Blocks Neutrophil Capture and Rolling on Platelets and Endothelium.," *J Immunol*, vol. 200, no. 5, pp. 1718–1726, Mar. 2018, doi: 10.4049/jimmunol.1700784.

[222] M. G. White *et al.*, "Expression of mesenchymal and α-cell phenotypic markers in islet β-cells in recently diagnosed diabetes.," *Diabetes Care*, vol. 36, no. 11, pp. 3818–20, Nov. 2013, doi: 10.2337/dc13-0705.

[223] P. S. Thiagarajan *et al.*, "Vimentin is an endogenous ligand for the pattern recognition receptor Dectin-1.," *Cardiovasc Res*, vol. 99, no. 3, pp. 494–504, Aug. 2013, doi: 10.1093/cvr/cvt117.

[224] N. Prévost *et al.*, "Signaling by ephrinB1 and Eph kinases in platelets promotes Rap1 activation, platelet adhesion, and aggregation via effector pathways that do not require phosphorylation of ephrinB1.," *Blood*, vol. 103, no. 4, pp. 1348–55, Feb. 2004, doi: 10.1182/blood-2003-06-1781.

[225] S. Güneş, J. Wu, B. Özyılmaz, R. Deveci Sevim, T. Ünüvar, and A. Anık, "Cooccurring Type 1 Diabetes Mellitus and Autoimmune Thyroiditis in a Girl with Craniofrontonasal Syndrome: Are EFNB1 Variants Associated with Autoimmunity?," *Pharmaceuticals (Basel)*, vol. 15, no. 12, Dec. 2022, doi: 10.3390/ph15121535.

[226] A. Sakamoto *et al.*, "Expression and function of ephrin-B1 and its cognate receptor EphB2 in human atherosclerosis: from an aspect of chemotaxis.," *Clin Sci (Lond)*, vol. 114, no. 10, pp. 643–50, May 2008, doi: 10.1042/CS20070339.

[227] K. Downes *et al.*, "G protein-coupled receptor kinase 5 regulates thrombin signaling in platelets via PAR-1.," *Blood Adv*, vol. 6, no. 7, pp. 2319–2330, Apr. 2022, doi: 10.1182/bloodadvances.2021005453.

[228] B. A. T. Rodriguez *et al.*, "A Platelet Function Modulator of Thrombin Activation Is Causally Linked to Cardiovascular Disease and Affects PAR4 Receptor Signaling.," *Am J Hum Genet*, vol. 107, no. 2, pp. 211–221, Aug. 2020, doi: 10.1016/j.ajhg.2020.06.008.

7. References

[229] L. Wang, M. Shen, F. Wang, and L. Ma, “GRK5 ablation contributes to insulin resistance.,” *Biochem Biophys Res Commun*, vol. 429, no. 1–2, pp. 99–104, Dec. 2012, doi: 10.1016/j.bbrc.2012.10.077.

[230] Z. Shang *et al.*, “A variant of GRK5 is associated with the therapeutic efficacy of repaglinide in Chinese Han patients with type 2 diabetes mellitus.,” *Drug Dev Res*, vol. 79, no. 3, pp. 129–135, May 2018, doi: 10.1002/ddr.21426.

[231] R. Eisman, S. Surrey, B. Ramachandran, E. Schwartz, and M. Poncz, “Structural and functional comparison of the genes for human platelet factor 4 and PF4alt.,” *Blood*, vol. 76, no. 2, pp. 336–44, Jul. 1990.

[232] A. A. Amelot, M. Tagzirt, G. Ducouret, R. L. Kuen, and B. F. Le Bonniec, “Platelet factor 4 (CXCL4) seals blood clots by altering the structure of fibrin.,” *J Biol Chem*, vol. 282, no. 1, pp. 710–20, Jan. 2007, doi: 10.1074/jbc.M606650200.

[233] Z. Cai, M. I. Greene, Z. Zhu, and H. Zhang, “Structural Features and PF4 Functions that Occur in Heparin-Induced Thrombocytopenia (HIT) Complicated by COVID-19.,” *Antibodies (Basel)*, vol. 9, no. 4, Oct. 2020, doi: 10.3390/antib9040052.

[234] Z.-Y. Liu *et al.*, “New perspectives on the induction and acceleration of immune-associated thrombosis by PF4 and VWF.,” *Front Immunol*, vol. 14, p. 1098665, 2023, doi: 10.3389/fimmu.2023.1098665.

[235] I. Ek, S. Thunell, and M. Blombäck, “Enhanced in vivo platelet activation in diabetes mellitus.,” *Scand J Haematol*, vol. 29, no. 2, pp. 185–91, Aug. 1982, doi: 10.1111/j.1600-0609.1982.tb00581.x.

[236] S. P. Levine, J. Lindenfeld, J. B. Ellis, N. M. Raymond, and L. S. Krentz, “Increased plasma concentrations of platelet factor 4 in coronary artery disease: a measure of in vivo platelet activation and secretion.,” *Circulation*, vol. 64, no. 3, pp. 626–32, Sep. 1981, doi: 10.1161/01.cir.64.3.626.

[237] E. Stavrou and A. H. Schmaier, “Factor XII: What does it contribute to our understanding of the physiology and pathophysiology of hemostasis & thrombosis,” *Thromb Res*, vol. 125, no. 3, pp. 210–215, Mar. 2010, doi: 10.1016/j.thromres.2009.11.028.

[238] E. Stavrou and A. H. Schmaier, “Factor XII: what does it contribute to our understanding of the physiology and pathophysiology of hemostasis & thrombosis.,” *Thromb Res*, vol. 125, no. 3, pp. 210–5, Mar. 2010, doi: 10.1016/j.thromres.2009.11.028.

[239] J. Konings *et al.*, “The role of activated coagulation factor XII in overall clot stability and fibrinolysis.,” *Thromb Res*, vol. 136, no. 2, pp. 474–80, Aug. 2015, doi: 10.1016/j.thromres.2015.06.028.

7. References

[240] G. Feugray *et al.*, “Factor XII deficiency evaluated by thrombin generation assay.,” *Clin Biochem*, vol. 100, pp. 42–47, Feb. 2022, doi: 10.1016/j.clinbiochem.2021.11.014.

[241] G. M. Patrassi, R. Vettor, D. Padovan, and A. Girolami, “Contact phase of blood coagulation in diabetes mellitus.,” *Eur J Clin Invest*, vol. 12, no. 4, pp. 307–11, Aug. 1982, doi: 10.1111/j.1365-2362.1982.tb02237.x.

[242] R. L. Nachman and P. C. Harpel, “Platelet alpha2-macroglobulin and alpha1-antitrypsin.,” *J Biol Chem*, vol. 251, no. 15, pp. 4512–21, Aug. 1976.

[243] S. Yoshino *et al.*, “Molecular form and concentration of serum α2-macroglobulin in diabetes.,” *Sci Rep*, vol. 9, no. 1, p. 12927, Sep. 2019, doi: 10.1038/s41598-019-49144-7.

[244] S. L. Harwood *et al.*, “Development of selective protease inhibitors via engineering of the bait region of human α2-macroglobulin.,” *J Biol Chem*, vol. 297, no. 1, p. 100879, Jul. 2021, doi: 10.1016/j.jbc.2021.100879.

[245] J. Lagrange, T. Lecompte, T. Knopp, P. Lacolley, and V. Regnault, “Alpha-2-macroglobulin in hemostasis and thrombosis: An underestimated old double-edged sword.,” *J Thromb Haemost*, vol. 20, no. 4, pp. 806–815, Apr. 2022, doi: 10.1111/jth.15647.

[246] R. Zheng, Y. Zhang, K. Zhang, Y. Yuan, S. Jia, and J. Liu, “The Complement System, Aging, and Aging-Related Diseases.,” *Int J Mol Sci*, vol. 23, no. 15, Aug. 2022, doi: 10.3390/ijms23158689.

[247] B. H. F. Weber, P. Charbel Issa, D. Pauly, P. Herrmann, F. Grassmann, and F. G. Holz, “The role of the complement system in age-related macular degeneration.,” *Dtsch Arztebl Int*, vol. 111, no. 8, pp. 133–8, Feb. 2014, doi: 10.3238/arztebl.2014.0133.

[248] D. Bhavanasi, S. Kim, L. E. Goldfinger, and S. P. Kunapuli, “Protein kinase Cδ mediates the activation of protein kinase D2 in platelets.,” *Biochem Pharmacol*, vol. 82, no. 7, pp. 720–7, Oct. 2011, doi: 10.1016/j.bcp.2011.06.032.

[249] O. Konopatskaya *et al.*, “Protein kinase C mediates platelet secretion and thrombus formation through protein kinase D2.,” *Blood*, vol. 118, no. 2, pp. 416–24, Jul. 2011, doi: 10.1182/blood-2010-10-312199.

[250] J. Trujillo-Viera *et al.*, “Protein Kinase D2 drives chylomicron-mediated lipid transport in the intestine and promotes obesity.,” *EMBO Mol Med*, vol. 13, no. 5, p. e13548, May 2021, doi: 10.15252/emmm.202013548.

[251] W. Mao, N. Lazar, H. van Tilbeurgh, P. M. Loiseau, and S. Pomel, “Minor Impact of A258D Mutation on Biochemical and Enzymatic Properties of Leishmania infantum GDP-Mannose Pyrophosphorylase.,” *Microorganisms*, vol. 10, no. 2, Jan. 2022, doi: 10.3390/microorganisms10020231.

7. References

[252] J. S. Kruszewska, M. Saloheimo, M. Penttilä, and G. Palamarczyk, "Isolation of a Trichoderma reesei cDNA encoding GTP: a-D-mannose-1-phosphate guanyltransferase involved in early steps of protein glycosylation.," *Curr Genet*, vol. 33, no. 6, pp. 445–50, Jun. 1998, doi: 10.1007/s002940050358.

[253] M. M. Lee-Sundlov, S. R. Stowell, and K. M. Hoffmeister, "Multifaceted role of glycosylation in transfusion medicine, platelets, and red blood cells.," *J Thromb Haemost*, vol. 18, no. 7, pp. 1535–1547, Jul. 2020, doi: 10.1111/jth.14874.

[254] E. Mammadova-Bach, J. Jaeken, T. Gudermann, and A. Braun, "Platelets and Defective N-Glycosylation.," *Int J Mol Sci*, vol. 21, no. 16, Aug. 2020, doi: 10.3390/ijms21165630.

[255] C. Reily, T. J. Stewart, M. B. Renfrow, and J. Novak, "Glycosylation in health and disease.," *Nat Rev Nephrol*, vol. 15, no. 6, pp. 346–366, Jun. 2019, doi: 10.1038/s41581-019-0129-4.

[256] S. Heesen, L. Lehle, A. Weissmann, and M. Aebi, "Isolation of the ALG5 locus encoding the UDP-glucose:dolichyl-phosphate glucosyltransferase from Saccharomyces cerevisiae.," *Eur J Biochem*, vol. 224, no. 1, pp. 71–9, Aug. 1994, doi: 10.1111/j.1432-1033.1994.tb19996.x.

[257] J. M. Dyson, A. M. Kong, F. Wiradjaja, M. V Astle, R. Gurung, and C. A. Mitchell, "The SH2 domain containing inositol polyphosphate 5-phosphatase-2: SHIP2.," *Int J Biochem Cell Biol*, vol. 37, no. 11, pp. 2260–5, Nov. 2005, doi: 10.1016/j.biocel.2005.05.003.

[258] J. M. Dyson *et al.*, "SHIP-2 forms a tetrameric complex with filamin, actin, and GPIb-IX-V: localization of SHIP-2 to the activated platelet actin cytoskeleton.," *Blood*, vol. 102, no. 3, pp. 940–8, Aug. 2003, doi: 10.1182/blood-2002-09-2897.

[259] S. Giuriato *et al.*, "SH2-containing inositol 5-phosphatases 1 and 2 in blood platelets: their interactions and roles in the control of phosphatidylinositol 3,4,5-trisphosphate levels.," *Biochem J*, vol. 376, no. Pt 1, pp. 199–207, Nov. 2003, doi: 10.1042/BJ20030581.

[260] M. Paul, K. Golla, and H. Kim, "Gelsolin Modulates Platelet Dense Granule Secretion and Hemostasis via the Actin Cytoskeleton.," *Thromb Haemost*, vol. 123, no. 2, pp. 219–230, Feb. 2023, doi: 10.1055/s-0042-1758800.

[261] J. Zhou, M. Di, and H. Han, "Upregulation of SHIP2 participates in the development of breast cancer via promoting Wnt/β-catenin signaling.," *Onco Targets Ther*, vol. 12, pp. 7067–7077, 2019, doi: 10.2147/OTT.S223422.

[262] M. Rijkers *et al.*, "Monitoring storage induced changes in the platelet proteome employing label free quantitative mass spectrometry.," *Sci Rep*, vol. 7, no. 1, p. 11045, Sep. 2017, doi: 10.1038/s41598-017-11643-w.

7. References

[263] K. MacAulay *et al.*, "Glycogen synthase kinase 3alpha-specific regulation of murine hepatic glycogen metabolism.," *Cell Metab*, vol. 6, no. 4, pp. 329–37, Oct. 2007, doi: 10.1016/j.cmet.2007.08.013.

[264] H. N. Munro, "Iron regulation of ferritin gene expression.," *J Cell Biochem*, vol. 44, no. 2, pp. 107–15, Oct. 1990, doi: 10.1002/jcb.240440205.

[265] N. Zhang, X. Yu, J. Xie, and H. Xu, "New Insights into the Role of Ferritin in Iron Homeostasis and Neurodegenerative Diseases.," *Mol Neurobiol*, vol. 58, no. 6, pp. 2812–2823, Jun. 2021, doi: 10.1007/s12035-020-02277-7.

[266] D. B. Kell and E. Pretorius, "Serum ferritin is an important inflammatory disease marker, as it is mainly a leakage product from damaged cells.," *Metallomics*, vol. 6, no. 4, pp. 748–73, Apr. 2014, doi: 10.1039/c3mt00347g.

[267] K. P. Z. Ferreira *et al.*, "Disease progression and oxidative stress are associated with higher serum ferritin levels in patients with multiple sclerosis.," *J Neurol Sci*, vol. 373, pp. 236–241, Feb. 2017, doi: 10.1016/j.jns.2016.12.039.

[268] M. P. Vulinović, P. Turčić, V. Micek, and M. Ljubojević, "Light and heavy ferritin chain expression in the liver and kidneys of Wistar rats: aging, sex differences, and impact of gonadectomy.," *Arh Hig Rada Toksikol*, vol. 73, no. 1, pp. 48–61, Apr. 2022, doi: 10.2478/aiht-2022-73-3621.

[269] J. Kim *et al.*, "Genome-wide gene and serum ferritin interaction in the development of type 2 diabetes in adults aged 40 years or older.," *Nutr Metab Cardiovasc Dis*, vol. 32, no. 1, pp. 231–240, Jan. 2022, doi: 10.1016/j.numecd.2021.09.028.

[270] M. Mishra and J. F. Ndisang, "A critical and comprehensive insight on heme oxygenase and related products including carbon monoxide, bilirubin, biliverdin and ferritin in type-1 and type-2 diabetes.," *Curr Pharm Des*, vol. 20, no. 9, pp. 1370–91, 2014, doi: 10.2174/13816128113199990559.

[271] K. A. Metwalley, D. M. Raafat, D. M. Tamer, H. S. Farghaly, and G. M. Said, "Ferritin levels in children and adolescents with type 1 diabetes mellitus: relationship with microvascular complications and glycemic control.," *Arch Endocrinol Metab*, vol. 64, no. 6, pp. 720–725, May 2021, doi: 10.20945/2359-3997000000279.

[272] S. A. Apostolidis *et al.*, "Signaling Through FcγRIIA and the C5a-C5aR Pathway Mediate Platelet Hyperactivation in COVID-19.," *Front Immunol*, vol. 13, p. 834988, 2022, doi: 10.3389/fimmu.2022.834988.

[273] M. Banerjee and S. W. Whiteheart, "The ins and outs of endocytic trafficking in platelet functions.," *Curr Opin Hematol*, vol. 24, no. 5, pp. 467–474, Sep. 2017, doi: 10.1097/MOH.0000000000000366.

[274] J. Ramos-Castañeda *et al.*, "Deficiency of ATP2C1, a Golgi ion pump, induces secretory pathway defects in endoplasmic reticulum (ER)-associated degradation and

sensitivity to ER stress.," *J Biol Chem*, vol. 280, no. 10, pp. 9467–73, Mar. 2005, doi: 10.1074/jbc.M413243200.

[275] A. V Fejes *et al.*, "Impact of Escherichia coli K12 and O18:K1 on human platelets: Differential effects on platelet activation, RNAs and proteins.," *Sci Rep*, vol. 8, no. 1, p. 16145, Nov. 2018, doi: 10.1038/s41598-018-34473-w.

[276] E. Eitan *et al.*, "Age-Related Changes in Plasma Extracellular Vesicle Characteristics and Internalization by Leukocytes.," *Sci Rep*, vol. 7, no. 1, p. 1342, May 2017, doi: 10.1038/s41598-017-01386-z.

[277] T. Tesovnik *et al.*, "Extracellular Vesicles Derived Human-miRNAs Modulate the Immune System in Type 1 Diabetes.," *Front Cell Dev Biol*, vol. 8, p. 202, 2020, doi: 10.3389/fcell.2020.00202.

[278] D. W. Freeman *et al.*, "Altered Extracellular Vesicle Concentration, Cargo, and Function in Diabetes.," *Diabetes*, vol. 67, no. 11, pp. 2377–2388, Nov. 2018, doi: 10.2337/db17-1308.

[279] A. Agouni *et al.*, "There Is Selective Increase in Pro-thrombotic Circulating Extracellular Vesicles in Acute Ischemic Stroke and Transient Ischemic Attack: A Study of Patients From the Middle East and Southeast Asia.," *Front Neurol*, vol. 10, p. 251, 2019, doi: 10.3389/fneur.2019.00251.

[280] T. Vajen *et al.*, "Platelet extracellular vesicles induce a pro-inflammatory smooth muscle cell phenotype.," *J Extracell Vesicles*, vol. 6, no. 1, p. 1322454, 2017, doi: 10.1080/20013078.2017.1322454.

[281] L. Wang, J. Zhou, L. Wang, C.-C. Wang, and D. W. Essex, "The b' domain of protein disulfide isomerase cooperates with the a and a' domains to functionally interact with platelets.," *J Thromb Haemost*, vol. 17, no. 2, pp. 371–382, Feb. 2019, doi: 10.1111/jth.14366.

[282] R. D. Pinto, A. R. Moreira, P. J. B. Pereira, and N. M. S. dos Santos, "Two thioredoxin-superfamily members from sea bass (Dicentrarchus labrax, L.): characterization of PDI (PDIA1) and ERp57 (PDIA3).," *Fish Shellfish Immunol*, vol. 35, no. 4, pp. 1163–75, Oct. 2013, doi: 10.1016/j.fsi.2013.07.024.

[283] S. Chichiarelli, F. Altieri, G. Paglia, E. Rubini, M. Minacori, and M. Eufemi, "ERp57/PDIA3: new insight.," *Cell Mol Biol Lett*, vol. 27, no. 1, p. 12, Feb. 2022, doi: 10.1186/s11658-022-00315-x.

[284] S. Parakh *et al.*, "ERp57 is protective against mutant SOD1-induced cellular pathology in amyotrophic lateral sclerosis.," *Hum Mol Genet*, vol. 27, no. 8, pp. 1311–1331, Apr. 2018, doi: 10.1093/hmg/ddy041.

7. References

[285] F. Mahmood *et al.*, "PDIA3: Structure, functions and its potential role in viral infections.," *Biomed Pharmacother*, vol. 143, p. 112110, Nov. 2021, doi: 10.1016/j.biopha.2021.112110.

[286] A. Hettinghouse, R. Liu, and C.-J. Liu, "Multifunctional molecule ERp57: From cancer to neurodegenerative diseases.," *Pharmacol Ther*, vol. 181, pp. 34–48, Jan. 2018, doi: 10.1016/j.pharmthera.2017.07.011.

[287] L. Wang *et al.*, "Platelet-derived ERp57 mediates platelet incorporation into a growing thrombus by regulation of the αIIbβ3 integrin.," *Blood*, vol. 122, no. 22, pp. 3642–50, Nov. 2013, doi: 10.1182/blood-2013-06-506691.

[288] L.-M. Holbrook, N. A. Watkins, A. D. Simmonds, C. I. Jones, W. H. Ouwehand, and J. M. Gibbins, "Platelets release novel thiol isomerase enzymes which are recruited to the cell surface following activation.," *Br J Haematol*, vol. 148, no. 4, pp. 627–37, Feb. 2010, doi: 10.1111/j.1365-2141.2009.07994.x.

[289] C. Schulz *et al.*, "Identification of novel downstream targets of platelet glycoprotein VI activation by differential proteome analysis: implications for thrombus formation.," *Blood*, vol. 115, no. 20, pp. 4102–10, May 2010, doi: 10.1182/blood-2009-07-230268.

[290] Y. Wu, S. S. Ahmad, J. Zhou, L. Wang, M. P. Cully, and D. W. Essex, "The disulfide isomerase ERp57 mediates platelet aggregation, hemostasis, and thrombosis.," *Blood*, vol. 119, no. 7, pp. 1737–46, Feb. 2012, doi: 10.1182/blood-2011-06-360685.

[291] O. Eriksson *et al.*, "Thiol isomerase ERp57 targets and modulates the lectin pathway of complement activation.," *J Biol Chem*, vol. 294, no. 13, pp. 4878–4888, Mar. 2019, doi: 10.1074/jbc.RA118.006792.

[292] D. Stepensky, N. Bangia, and P. Cresswell, "Aggregate formation by ERp57-deficient MHC class I peptide-loading complexes.," *Traffic*, vol. 8, no. 11, pp. 1530–42, Nov. 2007, doi: 10.1111/j.1600-0854.2007.00639.x.

[293] M. Wieczorek *et al.*, "Major Histocompatibility Complex (MHC) Class I and MHC Class II Proteins: Conformational Plasticity in Antigen Presentation.," *Front Immunol*, vol. 8, p. 292, 2017, doi: 10.3389/fimmu.2017.00292.

[294] J. Volz *et al.*, "BIN2 orchestrates platelet calcium signaling in thrombosis and thrombo-inflammation.," *J Clin Invest*, vol. 130, no. 11, pp. 6064–6079, Nov. 2020, doi: 10.1172/JCI136457.

[295] M. J. Sánchez-Barrena *et al.*, "Bin2 is a membrane sculpting N-BAR protein that influences leucocyte podosomes, motility and phagocytosis.," *PLoS One*, vol. 7, no. 12, p. e52401, 2012, doi: 10.1371/journal.pone.0052401.

[296] Y. Yu *et al.*, "Progranulin facilitates the increase of platelet count in immune thrombocytopenia.," *Thromb Res*, vol. 164, pp. 24–31, Apr. 2018, doi: 10.1016/j.thromres.2018.02.137.

7. References

[297] J. Liu *et al.*, "Progranulin aggravates lethal Candida albicans sepsis by regulating inflammatory response and antifungal immunity.," *PLoS Pathog*, vol. 18, no. 9, p. e1010873, Sep. 2022, doi: 10.1371/journal.ppat.1010873.

[298] A. M. Al-Yahya, A. A. Al-Masri, E. A. El Eter, A. Hersi, R. Lateef, and O. Mawlana, "Progranulin inhibits platelet aggregation and prolongs bleeding time in rats.," *Eur Rev Med Pharmacol Sci*, vol. 22, no. 10, pp. 3240–3248, May 2018, doi: 10.26355/eurrev_201805_15087.

[299] H. Qu, H. Deng, and Z. Hu, "Plasma progranulin concentrations are increased in patients with type 2 diabetes and obesity and correlated with insulin resistance.," *Mediators Inflamm*, vol. 2013, p. 360190, 2013, doi: 10.1155/2013/360190.

[300] L. Xu *et al.*, "Serum Levels of Progranulin Are Closely Associated with Microvascular Complication in Type 2 Diabetes.," *Dis Markers*, vol. 2015, p. 357279, 2015, doi: 10.1155/2015/357279.

[301] D. Zhou *et al.*, "PGRN acts as a novel regulator of mitochondrial homeostasis by facilitating mitophagy and mitochondrial biogenesis to prevent podocyte injury in diabetic nephropathy.," *Cell Death Dis*, vol. 10, no. 7, p. 524, Jul. 2019, doi: 10.1038/s41419-019-1754-3.

[302] L. Benussi *et al.*, "Loss of exosomes in progranulin-associated frontotemporal dementia.," *Neurobiol Aging*, vol. 40, pp. 41–49, Apr. 2016, doi: 10.1016/j.neurobiolaging.2016.01.001.

[303] A. E. Arrant *et al.*, "Elevated levels of extracellular vesicles in progranulin-deficient mice and FTD-GRN Patients.," *Ann Clin Transl Neurol*, vol. 7, no. 12, pp. 2433–2449, Dec. 2020, doi: 10.1002/acn3.51242.

[304] A. Kuramasu, M. Wakabayashi, M. Inui, and K. Yanai, "Distinct Roles of Small GTPases Rac1 and Rac2 in Histamine H4 Receptor-Mediated Chemotaxis of Mast Cells.," *J Pharmacol Exp Ther*, vol. 367, no. 1, pp. 9–19, Oct. 2018, doi: 10.1124/jpet.118.249706.

[305] C. Kim and M. C. Dinauer, "Rac2 is an essential regulator of neutrophil nicotinamide adenine dinucleotide phosphate oxidase activation in response to specific signaling pathways.," *J Immunol*, vol. 166, no. 2, pp. 1223–32, Jan. 2001, doi: 10.4049/jimmunol.166.2.1223.

[306] B. Liu *et al.*, "Proteomics Analyses Reveal Functional Differences between Exosomes of Mesenchymal Stem Cells Derived from The Umbilical Cord and Those Derived from The Adipose Tissue.," *Cell J*, vol. 23, no. 1, pp. 75–84, Apr. 2021, doi: 10.22074/cellj.2021.6969.

7. References

[307] T. Bruder-Nascimento *et al.*, "Vascular injury in diabetic db/db mice is ameliorated by atorvastatin: role of Rac1/2-sensitive Nox-dependent pathways.," *Clin Sci (Lond)*, vol. 128, no. 7, pp. 411–23, Apr. 2015, doi: 10.1042/CS20140456.

[308] T. Fløyel *et al.*, "The Rac2 GTPase contributes to cathepsin H-mediated protection against cytokine-induced apoptosis in insulin-secreting cells.," *Mol Cell Endocrinol*, vol. 518, p. 110993, Dec. 2020, doi: 10.1016/j.mce.2020.110993.

[309] M. Fokkelman *et al.*, "Cellular adhesome screen identifies critical modulators of focal adhesion dynamics, cellular traction forces and cell migration behaviour.," *Sci Rep*, vol. 6, p. 31707, Aug. 2016, doi: 10.1038/srep31707.

[310] J. A. Cancelas, A. W. Lee, R. Prabhakar, K. F. Stringer, Y. Zheng, and D. A. Williams, "Rac GTPases differentially integrate signals regulating hematopoietic stem cell localization.," *Nat Med*, vol. 11, no. 8, pp. 886–91, Aug. 2005, doi: 10.1038/nm1274.

[311] J. G. Filep, "Context-dependent signalling in platelets in vascular diseases: ROCK2 around thrombosis.," *Cardiovasc Res*, vol. 113, no. 11, pp. 1267–1269, Sep. 2017, doi: 10.1093/cvr/cvx141.

[312] Y. Takeda *et al.*, "ROCK2 Regulates Monocyte Migration and Cell to Cell Adhesion in Vascular Endothelial Cells.," *Int J Mol Sci*, vol. 20, no. 6, Mar. 2019, doi: 10.3390/ijms20061331.

[313] C. Sapet *et al.*, "Thrombin-induced endothelial microparticle generation: identification of a novel pathway involving ROCK-II activation by caspase-2.," *Blood*, vol. 108, no. 6, pp. 1868–76, Sep. 2006, doi: 10.1182/blood-2006-04-014175.

[314] P.-W. Chen *et al.*, "Elevated Platelet Galectin-3 and Rho-Associated Protein Kinase Activity Are Associated with Hemodialysis Arteriovenous Shunt Dysfunction among Subjects with Diabetes Mellitus.," *Biomed Res Int*, vol. 2019, p. 8952414, 2019, doi: 10.1155/2019/8952414.

[315] L. Liu, L. Tan, J. Lai, S. Li, and D. W. Wang, "Enhanced Rho-kinase activity: Pathophysiological relevance in type 2 diabetes.," *Clin Chim Acta*, vol. 462, pp. 107–110, Nov. 2016, doi: 10.1016/j.cca.2016.09.003.

[316] E. Perez-Costas, E. Y. Fenton, and H. J. Caruncho, "Reelin expression in brain endothelial cells: an electron microscopy study.," *BMC Neurosci*, vol. 16, p. 16, Mar. 2015, doi: 10.1186/s12868-015-0156-4.

[317] V. Martínez-Cerdeño, M. J. Galazo, and F. Clascá, "Reelin-immunoreactive neurons, axons, and neuropil in the adult ferret brain: evidence for axonal secretion of reelin in long axonal pathways.," *J Comp Neurol*, vol. 463, no. 1, pp. 92–116, Aug. 2003, doi: 10.1002/cne.10748.

7. References

[318] W.-L. Tseng *et al.*, "Reelin is a platelet protein and functions as a positive regulator of platelet spreading on fibrinogen.," *Cell Mol Life Sci*, vol. 67, no. 4, pp. 641–53, Feb. 2010, doi: 10.1007/s00018-009-0201-5.

[319] W.-L. Tseng *et al.*, "Impaired thrombin generation in Reelin-deficient mice: a potential role of plasma Reelin in hemostasis.," *J Thromb Haemost*, vol. 12, no. 12, pp. 2054–64, Dec. 2014, doi: 10.1111/jth.12736.

[320] N. S. Gowert *et al.*, "Loss of Reelin protects mice against arterial thrombosis by impairing integrin activation and thrombus formation under high shear conditions.," *Cell Signal*, vol. 40, pp. 210–221, Dec. 2017, doi: 10.1016/j.cellsig.2017.09.016.

[321] I. Krueger *et al.*, "Reelin Amplifies Glycoprotein VI Activation and AlphaIIb Beta3 Integrin Outside-In Signaling via PLC Gamma 2 and Rho GTPases.," *Arterioscler Thromb Vasc Biol*, vol. 40, no. 10, pp. 2391–2403, Oct. 2020, doi: 10.1161/ATVBAHA.120.314902.

[322] X. Xiaoling *et al.*, "TRIM40 ameliorates diabetic retinopathy through suppressing inflammation via Reelin/DAB1 signaling disruption: A mechanism by proteasomal degradation of DAB1.," *Biochem Biophys Res Commun*, vol. 664, pp. 117–127, Jul. 2023, doi: 10.1016/j.bbrc.2023.04.020.

[323] Y. Ding *et al.*, "Loss of Reelin protects against atherosclerosis by reducing leukocyte-endothelial cell adhesion and lesion macrophage accumulation.," *Sci Signal*, vol. 9, no. 419, p. ra29, Mar. 2016, doi: 10.1126/scisignal.aad5578.

[324] L. Calvier *et al.*, "Reelin Depletion Protects Against Atherosclerosis by Decreasing Vascular Adhesion of Leukocytes.," *Arterioscler Thromb Vasc Biol*, vol. 41, no. 4, pp. 1309–1318, Apr. 2021, doi: 10.1161/ATVBAHA.121.316000.

[325] M. S. Hayden and S. Ghosh, "NF-κB in immunobiology.," *Cell Res*, vol. 21, no. 2, pp. 223–44, Feb. 2011, doi: 10.1038/cr.2011.13.

[326] T. Liu, L. Zhang, D. Joo, and S.-C. Sun, "NF-κB signaling in inflammation.," *Signal Transduct Target Ther*, vol. 2, pp. 17023-, 2017, doi: 10.1038/sigtrans.2017.23.

[327] L. M. Beaulieu and J. E. Freedman, "NFkappaB regulation of platelet function: no nucleus, no genes, no problem?," *J Thromb Haemost*, vol. 7, no. 8, pp. 1329–32, Aug. 2009, doi: 10.1111/j.1538-7836.2009.03505.x.

[328] E. Malaver *et al.*, "NF-kappaB inhibitors impair platelet activation responses.," *J Thromb Haemost*, vol. 7, no. 8, pp. 1333–43, Aug. 2009, doi: 10.1111/j.1538-7836.2009.03492.x.

[329] C.-W. Hsia, M.-P. Wu, M.-Y. Shen, C.-H. Hsia, C.-L. Chung, and J.-R. Sheu, "Regulation of Human Platelet Activation and Prevention of Arterial Thrombosis in Mice by Auraptene through Inhibition of NF-κB Pathway.," *Int J Mol Sci*, vol. 21, no. 13, Jul. 2020, doi: 10.3390/ijms21134810.

7. References

[330] L. Rivadeneyra *et al.*, "Regulation of platelet responses triggered by Toll-like receptor 2 and 4 ligands is another non-genomic role of nuclear factor-kappaB.," *Thromb Res*, vol. 133, no. 2, pp. 235–43, Feb. 2014, doi: 10.1016/j.thromres.2013.11.028.

[331] R. Mato-Basalo, M. Morente-López, O. J. Arntz, F. A. J. van de Loo, J. Fafián-Labora, and M. C. Arufe, "Therapeutic Potential for Regulation of the Nuclear Factor Kappa-B Transcription Factor p65 to Prevent Cellular Senescence and Activation of Pro-Inflammatory in Mesenchymal Stem Cells.," *Int J Mol Sci*, vol. 22, no. 7, Mar. 2021, doi: 10.3390/ijms22073367.

[332] F. Hojjati, A. Roointan, A. Gholaminejad, Y. Eshraghi, and Y. Gheisari, "Identification of key genes and biological regulatory mechanisms in diabetic nephropathy: Meta-analysis of gene expression datasets.," *Nefrologia*, Jan. 2023, doi: 10.1016/j.nefroe.2022.06.006.

[333] G. Koike *et al.*, "Genetic mapping and chromosome localization of the rat mitochondrial glycerol-3-phosphate dehydrogenase gene, a candidate for non-insulin-dependent diabetes mellitus.," *Genomics*, vol. 38, no. 1, pp. 96–9, Nov. 1996, doi: 10.1006/geno.1996.0599.

[334] J. Ferrer, M. Aoki, P. Behn, A. Nestorowicz, A. Riggs, and M. A. Permutt, "Mitochondrial glycerol-3-phosphate dehydrogenase. Cloning of an alternatively spliced human islet-cell cDNA, tissue distribution, physical mapping, and identification of a polymorphic genetic marker.," *Diabetes*, vol. 45, no. 2, pp. 262–6, Feb. 1996, doi: 10.2337/diab.45.2.262.

[335] H. Qu *et al.*, "Deficiency of Mitochondrial Glycerol 3-Phosphate Dehydrogenase Exacerbates Podocyte Injury and the Progression of Diabetic Kidney Disease.," *Diabetes*, vol. 70, no. 6, pp. 1372–1387, Jun. 2021, doi: 10.2337/db20-1157.

[336] Y. Zheng *et al.*, "Deficiency of Mitochondrial Glycerol 3-Phosphate Dehydrogenase Contributes to Hepatic Steatosis.," *Hepatology*, vol. 70, no. 1, pp. 84–97, Jul. 2019, doi: 10.1002/hep.30507.

[337] G. R. Dodge *et al.*, "Human clathrin heavy chain (CLTC): partial molecular cloning, expression, and mapping of the gene to human chromosome 17q11-qter.," *Genomics*, vol. 11, no. 1, pp. 174–8, Sep. 1991, doi: 10.1016/0888-7543(91)90115-u.

[338] Q. Ma *et al.*, "Long non-coding RNA screening and identification of potential biomarkers for type 2 diabetes.," *J Clin Lab Anal*, vol. 36, no. 4, p. e24280, Apr. 2022, doi: 10.1002/jcla.24280.

[339] J. DeMari, C. Mroske, S. Tang, J. Nimeh, R. Miller, and R. R. Lebel, "CLTC as a clinically novel gene associated with multiple malformations and developmental delay.," *Am J Med Genet A*, vol. 170A, no. 4, pp. 958–66, Apr. 2016, doi: 10.1002/ajmg.a.37506.

7. References

[340] L. Qi, W. Ge, C. Pan, W. Jiang, D. Lin, and L. Zhang, "Compromised osteogenic effect of exosomes internalized by senescent bone marrow stem cells via endocytoses involving clathrin, macropinocytosis and caveolae.," *Front Bioeng Biotechnol*, vol. 10, p. 1090914, 2022, doi: 10.3389/fbioe.2022.1090914.

[341] R. Lundmark and S. R. Carlsson, "Sorting nexin 9 participates in clathrin-mediated endocytosis through interactions with the core components.," *J Biol Chem*, vol. 278, no. 47, pp. 46772–81, Nov. 2003, doi: 10.1074/jbc.M307334200.

[342] N. Shin *et al.*, "Sorting nexin 9 interacts with dynamin 1 and N-WASP and coordinates synaptic vesicle endocytosis.," *J Biol Chem*, vol. 282, no. 39, pp. 28939–28950, Sep. 2007, doi: 10.1074/jbc.M700283200.

[343] R. Lundmark and S. R. Carlsson, "Expression and properties of sorting nexin 9 in dynamin-mediated endocytosis.," *Methods Enzymol*, vol. 404, pp. 545–56, 2005, doi: 10.1016/S0076-6879(05)04048-6.

[344] O. Pylypenko, R. Lundmark, E. Rasmuson, S. R. Carlsson, and A. Rak, "The PX-BAR membrane-remodeling unit of sorting nexin 9.," *EMBO J*, vol. 26, no. 22, pp. 4788–800, Nov. 2007, doi: 10.1038/sj.emboj.7601889.

[345] S. G. Gychka *et al.*, "Vasa Vasorum Lumen Narrowing in Brain Vascular Hyalinosis in Systemic Hypertension Patients Who Died of Ischemic Stroke.," *Int J Mol Sci*, vol. 21, no. 24, Dec. 2020, doi: 10.3390/ijms21249611.

[346] E. Masselli *et al.*, "ROS in Platelet Biology: Functional Aspects and Methodological Insights.," *Int J Mol Sci*, vol. 21, no. 14, Jul. 2020, doi: 10.3390/ijms21144866.

[347] P. Pignatelli, F. M. Pulcinelli, L. Lenti, P. P. Gazzaniga, and F. Violi, "Hydrogen peroxide is involved in collagen-induced platelet activation.," *Blood*, vol. 91, no. 2, pp. 484–90, Jan. 1998.

[348] W.-J. Lu *et al.*, "Role of a Janus kinase 2-dependent signaling pathway in platelet activation.," *Thromb Res*, vol. 133, no. 6, pp. 1088–96, Jun. 2014, doi: 10.1016/j.thromres.2014.03.042.

[349] D. Chen *et al.*, "JAK/STAT pathway promotes the progression of diabetic kidney disease via autophagy in podocytes.," *Eur J Pharmacol*, vol. 902, p. 174121, Jul. 2021, doi: 10.1016/j.ejphar.2021.174121.

[350] M. Zhu, H. Wang, J. Chen, and H. Zhu, "Sinomenine improve diabetic nephropathy by inhibiting fibrosis and regulating the JAK2/STAT3/SOCS1 pathway in streptozotocin-induced diabetic rats.," *Life Sci*, vol. 265, p. 118855, Jan. 2021, doi: 10.1016/j.lfs.2020.118855.

[351] E. Brandt, F. Petersen, A. Ludwig, J. E. Ehlert, L. Bock, and H. D. Flad, "The beta-thromboglobulins and platelet factor 4: blood platelet-derived CXC chemokines with

divergent roles in early neutrophil regulation.," *J Leukoc Biol*, vol. 67, no. 4, pp. 471–8, Apr. 2000, doi: 10.1002/jlb.67.4.471.

[352] A. Walz and M. Baggiolini, "Generation of the neutrophil-activating peptide NAP-2 from platelet basic protein or connective tissue-activating peptide III through monocyte proteases.," *J Exp Med*, vol. 171, no. 2, pp. 449–54, Feb. 1990, doi: 10.1084/jem.171.2.449.

[353] A. Akkaya Fırat, "Chemokines Effective on Platelet Functions," 2023. doi: 10.5772/intechopen.107183.

[354] A. El-Gedaily, G. Schoedon, M. Schneemann, and A. Schaffner, "Constitutive and regulated expression of platelet basic protein in human monocytes.," *J Leukoc Biol*, vol. 75, no. 3, pp. 495–503, Mar. 2004, doi: 10.1189/jlb.0603288.

[355] G. Sonego, T.-T. M. Le, D. Crettaz, M. Abonnenc, J.-D. Tissot, and M. Prudent, "Sulfenylome analysis of pathogen-inactivated platelets reveals the presence of cysteine oxidation in integrin signaling pathway and cytoskeleton regulation.," *J Thromb Haemost*, vol. 19, no. 1, pp. 233–247, Jan. 2021, doi: 10.1111/jth.15121.

[356] T. Vilboux *et al.*, "A congenital neutrophil defect syndrome associated with mutations in VPS45.," *N Engl J Med*, vol. 369, no. 1, pp. 54–65, Jul. 2013, doi: 10.1056/NEJMoa1301296.

[357] P. Stepensky *et al.*, "VPS 45-associated primary infantile myelofibrosis--successful treatment with hematopoietic stem cell transplantation.," *Pediatr Transplant*, vol. 17, no. 8, pp. 820–5, Dec. 2013, doi: 10.1111/petr.12169.

[358] F. Busonero *et al.*, "A Sardinian founder mutation in glycoprotein Ib platelet subunit beta (GP1BB) that impacts thrombocytopenia.," *Br J Haematol*, vol. 191, no. 5, pp. e124–e128, Dec. 2020, doi: 10.1111/bjh.17090.

[359] G. Berger, J. M. Massé, and E. M. Cramer, "Alpha-granule membrane mirrors the platelet plasma membrane and contains the glycoproteins Ib, IX, and V.," *Blood*, vol. 87, no. 4, pp. 1385–95, Feb. 1996.

[360] S. C. Meyer and J. E. Fox, "Interaction of platelet glycoprotein V with glycoprotein Ib-IX regulates expression of the glycoproteins and binding of von Willebrand factor to glycoprotein Ib-IX in transfected cells.," *J Biol Chem*, vol. 270, no. 24, pp. 14693–9, Jun. 1995, doi: 10.1074/jbc.270.24.14693.

[361] M. E. Quach and R. Li, "Structure-function of platelet glycoprotein Ib-IX.," *J Thromb Haemost*, vol. 18, no. 12, pp. 3131–3141, Dec. 2020, doi: 10.1111/jth.15035.

[362] D. L. Springer *et al.*, "Platelet proteome changes associated with diabetes and during platelet storage for transfusion.," *J Proteome Res*, vol. 8, no. 5, pp. 2261–72, May 2009, doi: 10.1021/pr800885j.

7. References

[363] P. A. McEwan *et al.*, “Quaternary organization of GPIb-IX complex and insights into Bernard-Soulier syndrome revealed by the structures of GPIbβ and a GPIbβ/GPIX chimera.,” *Blood*, vol. 118, no. 19, pp. 5292–301, Nov. 2011, doi: 10.1182/blood-2011-05-356253.

[364] L. Buday, L. Wunderlich, and P. Tamás, “The Nck family of adapter proteins: regulators of actin cytoskeleton.,” *Cell Signal*, vol. 14, no. 9, pp. 723–31, Sep. 2002, doi: 10.1016/s0898-6568(02)00027-x.

[365] M. Lettau *et al.*, “The adapter protein Nck: role of individual SH3 and SH2 binding modules for protein interactions in T lymphocytes.,” *Protein Sci*, vol. 19, no. 4, pp. 658–69, Apr. 2010, doi: 10.1002/pro.334.

[366] M. Alfaidi, M. L. Scott, and A. W. Orr, “Sinner or Saint?: Nck Adaptor Proteins in Vascular Biology.,” *Front Cell Dev Biol*, vol. 9, p. 688388, 2021, doi: 10.3389/fcell.2021.688388.

[367] M. Yue *et al.*, “Misshapen/NIK-related kinase (MINK1) is involved in platelet function, hemostasis, and thrombus formation.,” *Blood*, vol. 127, no. 7, pp. 927–37, Feb. 2016, doi: 10.1182/blood-2015-07-659185.

[368] M. Bender and R. Palankar, “Platelet Shape Changes during Thrombus Formation: Role of Actin-Based Protrusions.,” *Hamostaseologie*, vol. 41, no. 1, pp. 14–21, Feb. 2021, doi: 10.1055/a-1325-0993.

[369] E. Boilard *et al.*, “Platelets amplify inflammation in arthritis via collagen-dependent microparticle production.,” *Science*, vol. 327, no. 5965, pp. 580–3, Jan. 2010, doi: 10.1126/science.1181928.

8. Risk and safety statements

Table: List of hazardous chemicals used in this study according to the Globally Harmonized System of Classification and Labelling of Chemicals (GHS), including GHS hazard and precautionary statements.

Chemicals	GHS symbol	GHS hazard statement	GHS precautionary statements
2-Mercaptoethanol		H301, H302, H310, H311, H314, H315, H317, H318, H331, H332, H336, H361, H373, H400, H410, and H411	P203, P260, P261, P262, P264, P264+P265, P270, P271, P272, P273, P280, P301+P316, P301+P317, P301+P330+P331, P302+P352, P302+P361+P354, P304+P340, P305+P354+P338, P316, P317, P318, P319, P321, P330, P332+P317, P333+P313, P361+P364, P362+P364, P363, P391, P403+P233, P405, and P501
2-Propanol		H225, H319, and H336	P210, P233, P240, P241, P242, P243, P261, P264+P265, P271, P280, P303+P361+P353, P304+P340, P305+P351+P338, P319, P337+P317, P370+P378, P403+P233, P403+P235, P405, and P501
Acetonitrile		H225, H302, H312, H319, and H332	P210, P233, P240, P241, P242, P243, P261, P264, P264+P265, P270, P271, P280, P301+P317, P302+P352, P303+P361+P353, P304+P340, P305+P351+P338, P317, P321, P330, P337+P317, P362+P364, P370+P378, P403+P235, and P501
Ammonium hydrogen carbonate		H302	P264, P270, P301+P317, P330, and P501
Ammonium persulphate		H272, H302, H315, H317, H319, H334, and H335	P210, P220, P261, P264, P264+P265, P270, P271, P272, P280, P284, P301+P317, P302+P352, P304+P340, P305+P351+P338, P319, P321, P330, P332+P317, P333+P313, P337+P317, P342+P316,

8. Risk and safety statements

			P362+P364, P370+P378, P403+P233, P405, and P501
Bromophenol Blue		H312, H319, and H332	P261, P264+P265, P271, P280, P302+P352, P304+P340, P305+P351+P338, P317, P321, P337+P317, P362+P364, and P501
Citric acid		H319, and H335	P261, P264+P265, P271, P280, P304+P340, P305+P351+P338, P319, P337+P317, P403+P233, P405, and P501
Dimethyl sulfoxide		H315, H319, and H335	P261, P264, P264+P265, P271, P280, P302+P352, P304+P340, P305+P351+P338, P319, P321, P332+P317, P337+P317, P362+P364, P403+P233, P405, and P501
Dithiothreitol		H302, H315, H318, H319, and H335	P261, P264, P264+P265, P270, P271, P280, P301+P317, P302+P352, P304+P340, P305+P351+P338, P305+P354+P338, P317, P319, P321, P330, P332+P317, P337+P317, P362+P364, P403+P233, P405, and P501
Formic acid		H314	P260, P264, P280, P301+P330+P331, P302+P361+P354, P304+P340, P305+P354+P338, P316, P321, P363, P405, and P501
Hydrochloric acid		H314, and H331	P260, P261, P264, P271, P280, P301+P330+P331, P302+P361+P354, P304+P340, P305+P354+P338, P316, P321, P363, P403+P233, P405, and P501
Indomethacin		H300, H301, H317, H318, H335, H336, H360, H373, and H413	P203, P260, P261, P264, P264+P265, P270, P271, P272, P273, P280, P301+P316, P302+P352, P304+P340, P305+P354+P338, P317, P318, P319, P321, P330, P333+P313, P362+P364, P403+P233, P405, and P501
Iodoacetamide		H301, H317, H334, and H413	P261, P264, P270, P272, P273, P280, P284, P301+P316, P302+P352, P304+P340, P321, P330, P333+P313, P342+P316, P362+P364, P405, and P501

8. Risk and safety statements

Methanol		H225, H301, H311, H331, and H370	P210, P233, P240, P241, P242, P243, P260, P261, P264, P270, P271, P280, P301+P316, P302+P352, P303+P361+P353, P304+P340, P308+P316, P316, P321, P330, P361+P364, P370+P378, P403+P233, P403+P235, P405, and P501
Prostaglandin E1		H301, and H361	P203, P264, P270, P280, P301+P316, P318, P321, P330, P405, and P501
Sodium chloride		H319	P264+P265, P280, P305+P351+P338, and P337+P317
Sodium deoxycholate		H302, H315, H319, and H335	P261, P264, P264+P265, P270, P271, P280, P301+P317, P302+P352, P304+P340, P305+P351+P338, P319, P321, P330, P332+P317, P337+P317, P362+P364, P403+P233, P405, and P501
Sodium dodecyl sulfate		H228, H302, H315, H318, H319, H332, H335, and H412	P210, P240, P241, P261, P264, P264+P265, P270, P271, P273, P280, P301+P317, P302+P352, P304+P340, P305+P351+P338, P305+P354+P338, P317, P319, P321, P330, P332+P317, P337+P317, P362+P364, P370+P378, P403+P233, P405, and P501
Sodium hydroxide		H314	P260, P264, P280, P301+P330+P331, P302+P361+P354, P304+P340, P305+P354+P338, P316, P321, P363, P405, and P501
Tetramethylethylenediamine		H225, H302, H314, and H332	P210, P233, P240, P241, P242, P243, P260, P261, P264, P270, P271, P280, P301+P317, P301+P330+P331, P302+P361+P354, P303+P361+P353, P304+P340, P305+P354+P338, P316, P317, P321, P330, P363, P370+P378, P403+P235, P405, and P501

9. Appendix

R script for imputing missing data using a randomForest approach

```
#Load libraries
library(randomForest)
library(openxlsx)
library(readxl)
data <- read_excel(file.choose ())
#load my data /transfer it to matrix
data<-readWorkbook("……",rowNames = TRUE)
datamatrix<-as.matrix(data)

#Impute with 100 Trees
RFimputedspikein<-rfImpute(datamatrix,y=NULL,iter=10, ntree=1000)
#Create an output
library(MASS)
write.table(RFimputedspikein, file = "……", append = FALSE, quote = TRUE, sep = " ",
            eol = "\n", na = "NA", dec = ".", row.names = TRUE,
            col.names = TRUE, qmethod = c("escape", "double"),
            fileEncoding = "")
```

9. Appendix

Table 8: List of significantly dysregulated proteins from the platelet proteome of young individuals with diabetes compared to healthy sex- and age-matched controls (p-value < 0.05). Significantly downregulated proteins (at least 1.5-fold less abundant) are shown in blue, and significantly upregulated proteins (at least 1.5-fold more abundant) are shown in red.

	Student's T-test	Difference D_C	T: T: Accession	T: T: Description	T: Gene name
2	0,00468293	-1,81681	Q6UWL2	Sushi domain-containing protein 1	SUSD1
3	0,0123014	-1,75019	Q9P0J7	E3 ubiquitin-protein ligase KCMF1	KCMF1
4	0,044749	-1,68575	P02730	Band 3 anion transport protein	SLC4A1
5	0,0460563	-1,55215	Q6ZU35	Capping protein-inhibiting regulator of actin dynamics	KIAA1211
6	0,018944	-1,3766	P22102	Trifunctional purine biosynthetic protein adenosine-3	GART
7	0,00530976	-1,35229	Q5JWF2	Guanine nucleotide-binding protein G(s) subunit alpha isoforms XLas	GNAS
8	0,0345129	-1,25756	Q02108	Guanylate cyclase soluble subunit alpha-1	GUCY1A3
9	0,00791979	-1,16114	Q6UXV4	MICOS complex subunit MIC27	APOOL
10	0,0377384	-1,07903	Q96JB5	CDK5 regulatory subunit-associated protein 3	CDK5RAP3
11	0,033663	-1,04734	Q96C01	Protein FAM136A	FAM136A
12	0,0238323	-1,03744	P08559	Pyruvate dehydrogenase E1 component subunit alpha, somatic form, mitochondrial	PDHA1
13	0,034439	-1,02257	Q9NR46	Endophilin-B2	SH3GLB2
14	0,0150139	-1,007	Q9UKF7	Cytoplasmic phosphatidylinositol transfer protein 1	PITPNC1
15	0,0475058	-1,00559	P32119	Peroxiredoxin-2	PRDX2
16	0,0244966	-0,964582	P62837	Ubiquitin-conjugating enzyme E2 D2	UBE2D2
17	0,00539739	-0,923136	P07108	Acyl-CoA-binding protein	DBI
18	0,0332384	-0,919325	Q12882	Dihydropyrimidine dehydrogenase [NADP(+)]	DPYD
19	0,0497208	-0,916156	P15924	Desmoplakin	DSP
20	0,0322135	-0,907448	P02545	Prelamin-A/C	LMNA
21	0,0470288	-0,859566	Q9UHL4	Dipeptidyl peptidase 2	DPP7
22	0,0148573	-0,825625	Q15435	Protein phosphatase 1 regulatory subunit 7	PPP1R7
23	0,01415	-0,806981	Q8IWB7	WD repeat and FYVE domain-containing protein 1	WDFY1
24	0,0182432	-0,782279	O95674	Phosphatidate cytidylyltransferase 2	CDS2
25	0,00195928	-0,767026	Q96S97	Myeloid-associated differentiation marker	MYADM
26	0,0314996	-0,689276	P09543	2',3'-cyclic-nucleotide 3'-phosphodiesterase	CNP
27	0,0287897	-0,66915	P05166	Propionyl-CoA carboxylase beta chain, mitochondrial	PCCB
28	0,027929	-0,662444	Q3SXM5	Inactive hydroxysteroid dehydrogenase-like protein 1	HSDL1
29	0,0367989	-0,651111	Q6XQN6	Nicotinate phosphoribosyltransferase	NAPRT
30	0,0348147	-0,626041	P51153	Ras-related protein Rab-13	RAB13
31	0,0151952	0,605567	Q13107	Ubiquitin carboxyl-terminal hydrolase 4	USP4
32	0,00752556	0,615859	Q9C0D9	Ethanolaminephosphotransferase 1	EPT1
33	0,0246657	0,637805	Q7L523	Ras-related GTP-binding protein A	RRAGA
34	0,0338286	0,673894	Q00266	S-adenosylmethionine synthase isoform type-1	MAT1A
35	0,0363618	0,683506	Q96AT9	Ribulose-phosphate 3-epimerase	RPE
36	0,0171719	0,686061	Q04446	1,4-alpha-glucan-branching enzyme	GBE1
37	0,0483095	0,716321	P13727	Bone marrow proteoglycan	PRG2
38	0,000293352	0,726206	Q969X0	RILP-like protein 2	RILPL2
39	0,0402316	0,741792	Q9NRL3	Striatin-4	STRN4
40	0,0119871	0,748505	P14174	Macrophage migration inhibitory factor	MIF
41	0,0326604	0,761564	P07360	Complement component C8 gamma chain	C8G
42	0,0199325	0,797589	Q9Y385	Ubiquitin-conjugating enzyme E2 J1	UBE2J1
43	0,0243825	0,800639	Q6IA86	Elongator complex protein 2	ELP2
44	0,0179322	0,847129	Q8ND30	Liprin-beta-2	PPFIBP2
45	0,0493057	0,86795	Q99501	GAS2-like protein 1	GAS2L1
46	0,0211694	0,894434	Q12805	EGF-containing fibulin-like extracellular matrix protein 1	EFEMP1
47	0,019738	0,91989	Q8IXJ6	NAD-dependent protein deacetylase sirtuin-2	SIRT2
48	0,045078	0,987792	Q12959	Disks large homolog 1	DLG1
49	0,0219405	1,04377	Q9H9E3	Conserved oligomeric Golgi complex subunit 4	COG4
50	0,0269472	1,06008	P03956	Interstitial collagenase	MMP1
51	0,0179767	1,11237	P12074	Cytochrome c oxidase subunit 6A1, mitochondrial	COX6A1
52	0,0456785	1,13379	P02743	Serum amyloid P-component	APCS
53	0,0251038	1,14496	A0A0B4J1U7	Immunoglobulin heavy variable 6-1	IGHV6-1
54	0,00980089	1,20274	P13671	Complement component C6	C6
55	0,043276	1,25264	P08603	Complement factor H	CFH
56	0,0023887	1,2583	O15417	Trinucleotide repeat-containing gene 18 protein	TNRC18

9. Appendix

57	0,00320828	1,27884	O95168	NADH dehydrogenase [ubiquinone] 1 beta subcomplex subunit 4	NDUFB4
58	0,0315621	1,28829	Q14432	cGMP-inhibited 3',5'-cyclic phosphodiesterase A	PDE3A
59	0,0174368	1,35945	O95299	NADH dehydrogenase [ubiquinone] 1 alpha subcomplex subunit 10, mitochondrial	NDUFA10
60	0,0132007	1,42328	Q8IVT5	Kinase suppressor of Ras 1	KSR1
61	0,024601	1,42328	P98082	Disabled homolog 2	DAB2
62	0,031584	1,45278	P00738	Haptoglobin	HP
63	0,0312298	1,45511	P01019	Angiotensinogen	AGT
64	0,0193412	1,54725	P36955	Pigment epithelium-derived factor	SERPINF1
65	0,0403364	1,72379	P35625	Metalloproteinase inhibitor 3	TIMP3
66	0,00136156	1,89291	Q92835	Phosphatidylinositol 3,4,5-trisphosphate 5-phosphatase 1	INPP5D
67	0,0459375	2,34325	P35222	Catenin beta-1	CTNNB1

9. Appendix

Table 9: List of significantly dysregulated proteins from the platelet proteome of middle-aged individuals with diabetes compared to healthy sex- and age-matched controls (p-value < 0.05). Significantly downregulated proteins (at least 1.5-fold less abundant) are shown in blue, and significantly upregulated proteins (at least 1.5-fold more abundant) are shown in red.

	Student's T-test	Difference D_C	T: T: Accession	T: T: Description	T: Gene name
2	0,00391338	-1,49069	Q9BYV8	Centrosomal protein of 41 kDa	CEP41
3	0,0139128	-1,28202	P49840	Glycogen synthase kinase-3 alpha	GSK3A
4	0,00428893	-1,21045	P04083	Annexin A1	ANXA1
5	0,0285471	-1,19659	P30038	Delta-1-pyrroline-5-carboxylate dehydrogenase, mitochondrial	ALDH4A1
6	0,0166462	-1,12769	Q9UHD1	Cysteine and histidine-rich domain-containing protein 1	CHORDC1
7	0,0171399	-1,07993	P02741	C-reactive protein	CRP
8	0,0219906	-1,04135	P31641	Sodium- and chloride-dependent taurine transporter	SLC6A6
9	0,0209245	-1,00874	Q99447	Ethanolamine-phosphate cytidylyltransferase	PCYT2
10	0,0226584	-0,980089	O14523	Phospholipid transfer protein C2CD2L	C2CD2L
11	0,0357095	-0,975899	Q99878	Histone H2A type 1-J	HIST1H2AJ
12	0,0130128	-0,962885	Q14571	Inositol 1,4,5-trisphosphate receptor type 2	ITPR2
13	0,00513347	-0,926569	O00571	ATP-dependent RNA helicase DDX3X	DDX3X
14	0,0130574	-0,921434	P30622	CAP-Gly domain-containing linker protein 1	CLIP1
15	0,0336958	-0,888832	Q17RC7	Exocyst complex component 3-like protein 4	EXOC3L4
16	0,0279917	-0,859008	Q16706	Alpha-mannosidase 2	MAN2A1
17	0,027608	-0,849647	Q9NUI1	Peroxisomal 2,4-dienoyl-CoA reductase [(3E)-enoyl-CoA-producing]	DECR2
18	0,000121832	-0,841085	Q96KG9	N-terminal kinase-like protein	SCYL1
19	0,00163521	-0,79444	Q9Y5J7	Mitochondrial import inner membrane translocase subunit Tim9	TIMM9
20	0,0187896	-0,780411	P49354	Protein farnesyltransferase/geranylgeranyltransferase type-1 subunit alpha	FNTA
21	0,00497264	-0,729367	P35749	Myosin-11	MYH11
22	0,0174839	-0,721113	O14734	Acyl-coenzyme A thioesterase 8	ACOT8
23	0,0414312	-0,710702	Q12882	Dihydropyrimidine dehydrogenase [NADP(+)]	DPYD
24	0,0148389	-0,700076	P08670	Vimentin	VIM
25	0,0033635	-0,694693	Q9H832	Ubiquitin-conjugating enzyme E2 Z	UBE2Z
26	0,00140351	-0,693322	O00399	Dynactin subunit 6	DCTN6
27	0,0329914	-0,687383	P16333	Cytoplasmic protein NCK1	NCK1
28	0,0225957	-0,685381	Q15629	Translocating chain-associated membrane protein 1	TRAM1
29	0,0223696	-0,678438	Q9H5X1	Cytosolic iron-sulfur assembly component 2A	FAM96A
30	0,0298758	-0,674904	P30419	Glycylpeptide N-tetradecanoyltransferase 1	NMT1
31	0,0156277	-0,667836	Q13596	Sorting nexin-1	SNX1
32	0,0343717	-0,664235	Q9Y4W6	AFG3-like protein 2	AFG3L2
33	0,00998551	-0,662844	P98172	Ephrin-B1	EFNB1
34	0,00183198	-0,634996	P34947	G protein-coupled receptor kinase 5	GRK5
35	0,00492485	-0,632964	Q9Y265	RuvB-like 1	RUVBL1
36	0,0319413	-0,632273	P10398	Serine/threonine-protein kinase A-Raf	ARAF
37	0,0331745	-0,623974	Q8IYB5	Stromal membrane-associated protein 1	SMAP1
38	0,0188752	-0,618676	Q9H4A3	Serine/threonine-protein kinase WNK1	WNK1
39	0,0423846	0,588727	Q9NS69	Mitochondrial import receptor subunit TOM22 homolog	TOMM22
40	0,0463182	0,597118	P55212	Caspase-6	CASP6
41	0,00413568	0,602227	P04439	HLA class I histocompatibility antigen, A alpha chain	HLA-A
42	0,041728	0,607767	Q9HBH0	Rho-related GTP-binding protein RhoF	RHOF
43	0,0133641	0,620164	Q5XKP0	MICOS complex subunit MIC13	QIL1
44	0,0128811	0,621598	O14744	Protein arginine N-methyltransferase 5	PRMT5
45	0,0320467	0,641772	P01717	Immunoglobulin lambda variable 3-25	
46	0,0457974	0,650875	Q03591	Complement factor H-related protein 1	CFHR1
47	0,0219447	0,65965	Q6P2E9	Enhancer of mRNA-decapping protein 4	EDC4
48	0,0380286	0,669008	Q08426	Peroxisomal bifunctional enzyme	EHHADH
49	0,0231845	0,676263	Q9UBV8	Peflin	PEF1
50	0,0177404	0,696217	P02776	Platelet factor 4	PF4

9. Appendix

51	0,0476645	0,70742	Q96QR8	Transcriptional activator protein Pur-beta	PURB
52	0,0189897	0,728503	Q9Y2B0	Protein canopy homolog 2	CNPY2
53	0,00129454	0,737127	Q7L5N1	COP9 signalosome complex subunit 6	COPS6
54	0,0161936	0,739505	Q494V2	Cilia- and flagella-associated protein 100	CCDC37
55	0,0131859	0,750037	Q9ULC5	Long-chain-fatty-acid--CoA ligase 5	ACSL5
56	0,040196	0,752615	Q14642	Inositol polyphosphate-5-phosphatase A	INPP5A
57	0,0158058	0,756141	A0A0C4DH72	Immunoglobulin kappa variable 1-6	IGKV1-6
58	0,00386607	0,756209	Q9C0A1	Zinc finger homeobox protein 2	ZFHX2
59	0,040095	0,786579	Q9BZL6	Serine/threonine-protein kinase D2	PRKD2
60	0,0141631	0,79368	P49720	Proteasome subunit beta type-3	PSMB3
61	0,0338818	0,872159	P06312	Immunoglobulin kappa variable 4-1	IGKV4-1
62	0,0191405	0,906288	A0A0C4DH67	Immunoglobulin kappa variable 1-8	IGKV1-8
63	0,00333839	0,918331	Q6PRD1	Probable G-protein coupled receptor 179	GPR179
64	0,0474952	0,928579	O14618	Copper chaperone for superoxide dismutase	CCS
65	0,0244223	0,951254	A6NHR8	Putative protein FAM47D	FAM47DP
66	0,0313204	0,992988	P00748	Coagulation factor XII	F12
67	0,00648225	1,02645	P14209	CD99 antigen	CD99
68	0,0348375	1,02855	P10643	Complement component C7	C7
69	0,0175989	1,06547	P01023	Alpha-2-macroglobulin	A2M
70	0,00530808	1,06874	P08571	Monocyte differentiation antigen CD14	CD14
71	0,00907139	1,09233	P02656	Apolipoprotein C-III	APOC3
72	0,0416574	1,10941	P01593	Immunoglobulin kappa variable 1D-33	
73	0,0202188	1,11129	P63261	Actin, cytoplasmic 2	ACTG1
74	0,00520174	1,17572	Q9HCP0	Casein kinase I isoform gamma-1	CSNK1G1
75	0,0122288	1,1764	P0DOX2	Immunoglobulin alpha-2 heavy chain	
76	0,0255773	1,29426	P02766	Transthyretin	TTR
77	0,0198363	1,39709	A0MZ66	Shootin-1	KIAA1598
78	0,0187129	1,52152	P0DOX7	Immunoglobulin kappa light chain	
79	0,000434979	1,53939	Q15036	Sorting nexin-17	SNX17
80	0,0487623	1,80306	P49770	Translation initiation factor eIF-2B subunit beta	EIF2B2

9. Appendix

Table 10: List of significantly dysregulated proteins from the platelet proteome of old-aged diabetes compared to healthy sex- and age-matched controls (p-value < 0.05). Significantly downregulated proteins (at least 1.5-fold less abundant) are shown in blue, and significantly upregulated proteins (at least 1.5-fold more abundant) are shown in red.

	N: Student's T-test	Difference D_C	T: T: Accession	T: T: Description	T: Gene name
2	0,0129523	-3,1892	O15111	Inhibitor of nuclear factor kappa-B kinase subunit alpha	CHUK
3	0,0028895	-1,78637	Q16204	Coiled-coil domain-containing protein 6	CCDC6
4	0,00252321	-1,14681	Q9NUP1	Biogenesis of lysosome-related organelles complex 1 subunit 4	BLOC1S4
5	0,00350287	-1,07341	Q96IJ6	Mannose-1-phosphate guanyltransferase alpha	GMPPA
6	0,00269622	-1,05638	Q8WW12	PEST proteolytic signal-containing nuclear protein	PCNP
7	0,0123944	-1,00193	O75592	E3 ubiquitin-protein ligase MYCBP2	MYCBP2
8	0,0114613	-0,952214	Q8N766	ER membrane protein complex subunit 1	EMC1
9	0,0274929	-0,926386	Q9Y3A3	MOB-like protein phocein	MOB4
10	0,0350957	-0,915165	O43776	Asparagine--tRNA ligase, cytoplasmic	NARS
11	0,0443199	-0,87382	O15397	Importin-8	IPO8
12	0,0264924	-0,870984	Q9NQT8	Kinesin-like protein KIF13B	KIF13B
13	0,0113246	-0,83369	P35914	Hydroxymethylglutaryl-CoA lyase, mitochondrial	HMGCL
14	0,0240489	-0,790539	O60313	Dynamin-like 120 kDa protein, mitochondrial	OPA1
15	0,0325273	-0,789472	P14209	CD99 antigen	CD99
16	0,0482743	-0,777419	Q9Y673	Dolichyl-phosphate beta-glucosyltransferase	ALG5
17	0,04774	-0,774888	P27708	CAD protein	CAD
18	0,00953773	-0,770515	O15357	Phosphatidylinositol 3,4,5-trisphosphate 5-phosphatase 2	INPPL1
19	0,0365278	-0,761295	P48556	26S proteasome non-ATPase regulatory subunit 8	PSMD8
20	0,0142835	-0,728969	Q9UJ68	Mitochondrial peptide methionine sulfoxide reductase	MSRA
21	0,00954159	-0,701356	Q8NFV4	Protein ABHD11	ABHD11
22	0,0143376	-0,689498	P46976	Glycogenin-1	GYG1
23	0,0444416	-0,673338	Q9UPN3	Microtubule-actin cross-linking factor 1, isoforms 1/2/3/5	MACF1
24	0,0472842	-0,626485	O75150	E3 ubiquitin-protein ligase BRE1B	RNF40
25	0,0151865	0,614289	Q9Y385	Ubiquitin-conjugating enzyme E2 J1	UBE2J1
26	0,0267153	0,618318	O75396	Vesicle-trafficking protein SEC22b	SEC22B
27	0,0363323	0,62235	P98194	Calcium-transporting ATPase type 2C member 1	ATP2C1
28	0,0481494	0,659041	Q2M389	WASH complex subunit 4	KIAA1033
29	0,0433179	0,664114	Q9Y3E5	Peptidyl-tRNA hydrolase 2, mitochondrial	PTRH2
30	0,0152879	0,669937	Q99961	Endophilin-A2	SH3GL1
31	0,0229702	0,687163	P60983	Glia maturation factor beta	GMFB
32	0,000421396	0,689402	Q8IZ81	ELMO domain-containing protein 2	ELMOD2
33	0,0012649	0,706799	P26196	Probable ATP-dependent RNA helicase DDX6	DDX6
34	0,049401	0,727038	P02794	Ferritin heavy chain	FTH1
35	0,0103116	0,731666	Q6NVY1	3-hydroxyisobutyryl-CoA hydrolase, mitochondrial	HIBCH
36	0,0250224	0,736098	P49840	Glycogen synthase kinase-3 alpha	GSK3A
37	0,0185467	0,740508	P50453	Serpin B9	SERPINB9
38	0,0452211	0,745248	Q93050	V-type proton ATPase 116 kDa subunit a1	ATP6V0A1
39	0,0345669	0,824453	Q8NF50	Dedicator of cytokinesis protein 8	DOCK8
40	0,00923516	0,848891	Q99614	Tetratricopeptide repeat protein 1	TTC1
41	0,0100164	0,854295	Q15006	ER membrane protein complex subunit 2	EMC2
42	0,0326907	0,856193	Q9NQP4	Prefoldin subunit 4	PFDN4
43	0,0167156	0,908304	P19652	Alpha-1-acid glycoprotein 2	ORM2
44	0,0356641	0,940365	Q9HB71	Calcyclin-binding protein	CACYBP
45	0,0158929	0,970938	Q9BWD1	Acetyl-CoA acetyltransferase, cytosolic	ACAT2
46	0,0195128	0,989319	Q9Y274	Type 2 lactosamine alpha-2,3-sialyltransferase	ST3GAL6
47	0,0344144	1,00116	O14727	Apoptotic protease-activating factor 1	APAF1
48	0,0442774	1,01326	Q9H8H3	Methyltransferase-like protein 7A	METTL7A
49	0,0308127	1,03976	O15523	ATP-dependent RNA helicase DDX3Y	DDX3Y
50	0,0314736	1,14241	O95202	Mitochondrial proton/calcium exchanger protein	LETM1
51	0,0146686	1,18457	Q96EP5	DAZ-associated protein 1	DAZAP1
52	0,0460036	1,1985	O00154	Cytosolic acyl coenzyme A thioester hydrolase	ACOT7
53	0,0292502	1,42151	Q9NR45	Sialic acid synthase	NANS
54	0,0160015	1,62851	Q8WVC6	Dephospho-CoA kinase domain-containing protein	DCAKD
55	0,0117293	1,9238	Q86TI0	TBC1 domain family member 1	TBC1D1

9. Appendix

Table 11: List of significantly dysregulated proteins from plasma-derived EVs proteome of middle-aged individuals with diabetes compared to healthy sex- and age-matched controls (p-value < 0.05). Significantly downregulated proteins (at least 1.5-fold less abundant) are shown in blue, and significantly upregulated proteins (at least 1.5-fold more abundant) are shown in red.

	Student's T-test	Difference D_C	T: T: Accession	T: T: Description	T: Gene name
2	0,0214516	-2,63991	Q9ULV4	Coronin-1C	CORO1C
3	0,000569079	-1,38476	P30101	Protein disulfide-isomerase A3	PDIA3
4	0,0149642	-1,31833	Q16891	MICOS complex subunit MIC60	IMMT
5	0,0461173	-1,23131	Q9UBW5	Bridging integrator 2	BIN2
6	0,0069204	-1,18299	A0A075B6J9	Immunoglobulin lambda variable 2-18	IGLV2-18
7	0,00441955	-0,964136	P28799	Progranulin	GRN
8	0,0269326	-0,957346	P15153	Ras-related C3 botulinum toxin substrate 2	RAC2
9	0,0206757	-0,931004	A0A075B6I9	Immunoglobulin lambda variable 7-46	IGLV7-46
10	0,0298141	-0,910418	P28065	Proteasome subunit beta type-9	PSMB9
11	0,0382218	-0,90784	A0A0C4DH34	Immunoglobulin heavy variable 4-28	IGHV4-28
12	0,0483166	-0,89287	P01601	Immunoglobulin kappa variable 1D-16	
13	0,0113599	-0,849901	A0A075B6H9	Immunoglobulin lambda variable 4-69	IGLV4-69
14	0,0457566	-0,807772	Q04206	Transcription factor p65	RELA
15	0,0140136	-0,788395	Q01813	ATP-dependent 6-phosphofructokinase, platelet type	PFKP
16	0,036645	-0,767671	O75116	Rho-associated protein kinase 2	ROCK2
17	0,044066	-0,712566	Q9H5X1	Cytosolic iron-sulfur assembly component 2A	FAM96A
18	0,0182503	-0,64207	Q9NVK5	FGFR1 oncogene partner 2	FGFR1OP2
19	0,0122523	-0,595812	P78509	Reelin	RELN
20	0,0387164	0,588534	Q14558	Phosphoribosyl pyrophosphate synthase-associated protein 1	PRPSAP1
21	0,00390669	0,610469	Q9NWV4	CXXC motif containing zinc binding protein	C1orf123
22	0,0316454	0,655855	P47756	F-actin-capping protein subunit beta	CAPZB
23	0,0222481	0,690008	P04040	Catalase	CAT
24	0,016208	0,69358	P02775	Platelet basic protein	PPBP
25	0,0237875	0,729093	Q14974	Importin subunit beta-1	KPNB1
26	0,0158779	0,733691	Q9Y230	RuvB-like 2	RUVBL2
27	0,00837836	0,764579	O60674	Tyrosine-protein kinase JAK2	JAK2
28	0,00954007	0,775884	P0DOX4	Immunoglobulin epsilon heavy chain	
29	0,00678	0,789319	Q15165	Serum paraoxonase/arylesterase 2	PON2
30	0,00640206	0,799217	Q5T013	Putative hydroxypyruvate isomerase	HYI
31	0,0366432	0,799378	Q9BWP8	Collectin-11	COLEC11
32	0,0350359	0,800275	A0A0C4DH36	Probable non-functional immunoglobulin heavy variable 3-38	IGHV3-38
33	0,0221071	0,80258	P04114	Apolipoprotein B-100	APOB
34	0,0318326	0,850439	Q13033	Striatin-3	STRN3
35	0,0021632	0,920041	Q14008	Cytoskeleton-associated protein 5	CKAP5
36	0,000112407	0,964406	Q9NRW7	Vacuolar protein sorting-associated protein 45	VPS45
37	0,0297342	1,00062	P06681	Complement C2	C2
38	0,0323355	1,02221	Q92614	Unconventional myosin-XVIIIa	MYO18A
39	0,0288733	1,09485	Q9Y5X1	Sorting nexin-9	SNX9
40	0,00564645	1,14088	Q13103	Secreted phosphoprotein 24	SPP2
41	0,00911333	1,19414	Q00610	Clathrin heavy chain 1	CLTC
42	0,0342639	1,22011	Q9BVJ7	Dual specificity protein phosphatase 23	DUSP23
43	0,0189538	1,2478	P40227	T-complex protein 1 subunit zeta	CCT6A
44	0,00449068	1,43564	P02656	Apolipoprotein C-III	APOC3
45	0,0293958	1,44045	P43304	Glycerol-3-phosphate dehydrogenase, mitochondrial	GPD2

9. Appendix

Table 12: List of significantly dysregulated proteins from the platelet soluble fraction, along with loosely associated membrane proteins from diabetes platelets compared to healthy controls (p-value < 0.05). Significantly downregulated proteins (at least 1.5-fold less abundant) are shown in blue, and significantly upregulated proteins (at least 1.5-fold more abundant) are shown in red.

	Student's T-test	Difference D_C	T: T: Accession	T: T: Description	T: Gene name
2	0,0432212	-2,62381	Q8WWA1	Transmembrane protein 40	TMEM40
3	0,00745592	-2,32946	Q86UT6	NLR family member X1	NLRX1
4	0,0038573	-2,11032	P55084	Trifunctional enzyme subunit beta, mitochondrial	HADHB
5	0,0465506	-1,97452	Q96BS2	Calcineurin B homologous protein 3	TESC
6	0,0171337	-1,94751	Q14642	Inositol polyphosphate-5-phosphatase A	INPP5A
7	0,0156161	-1,8988	O95674	Phosphatidate cytidylyltransferase 2	CDS2
8	0,0246702	-1,85184	P36542	ATP synthase subunit gamma, mitochondrial	ATP5C1
9	0,0426925	-1,71539	P16284	Platelet endothelial cell adhesion molecule	PECAM1
10	0,039599	-1,67267	P13645	Keratin, type I cytoskeletal 10	KRT10
11	0,0313662	-1,64129	O15269	Serine palmitoyltransferase 1	SPTLC1
12	0,0159887	-1,35763	P13224	Platelet glycoprotein Ib beta chain	GP1BB
13	0,0258319	-1,10741	P05164	Myeloperoxidase	MPO
14	0,00750061	-1,05063	Q96E17	Ras-related protein Rab-3C	RAB3C
15	0,0271769	-1,02663	P14770	Platelet glycoprotein IX	GP9
16	0,000240314	-1,01408	Q92882	Osteoclast-stimulating factor 1	OSTF1
17	0,0220712	-0,968341	Q9Y624	Junctional adhesion molecule A	F11R
18	0,0369567	-0,958553	Q8N573	Oxidation resistance protein 1	OXR1
19	0,030053	-0,919708	Q13043	Serine/threonine-protein kinase 4	STK4
20	0,00460715	-0,887166	Q13103	Secreted phosphoprotein 24	SPP2
21	0,0319739	-0,879748	P56545	C-terminal-binding protein 2	CTBP2
22	0,0392117	-0,866658	Q9UDY2	Tight junction protein ZO-2	TJP2
23	0,0423745	-0,853042	Q4V328	GRIP1-associated protein 1	GRIPAP1
24	0,0207062	-0,853033	Q9NXL6	SID1 transmembrane family member 1	SIDT1
25	0,0353144	-0,834533	Q9UM00	Calcium load-activated calcium channel	TMCO1
26	0,00207401	-0,79536	Q9NX63	MICOS complex subunit MIC19	CHCHD3
27	6,98E-05	-0,785248	Q8N9U0	Tandem C2 domains nuclear protein	TC2N
28	0,00123797	-0,750986	Q9HAV0	Guanine nucleotide-binding protein subunit beta-4	GNB4
29	0,00273479	-0,71951	P00918	Carbonic anhydrase 2	CA2
30	0,00107377	-0,69702	P51570	Galactokinase	GALK1
31	0,00823755	-0,692162	P61086	Ubiquitin-conjugating enzyme E2 K	UBE2K
32	0,0329804	-0,664588	O43852	Calumenin	CALU
33	0,00139086	-0,656695	Q12913	Receptor-type tyrosine-protein phosphatase eta	PTPRJ
34	0,0272794	-0,655164	Q14847	LIM and SH3 domain protein 1	LASP1
35	0,0280832	-0,63483	P00491	Purine nucleoside phosphorylase	PNP
36	0,0338527	-0,625816	P05556	Integrin beta-1	ITGB1
37	0,0106627	0,615675	P01127	Platelet-derived growth factor subunit B	PDGFB
38	0,049993	0,626583	Q96MK2	RIPOR family member 3	FAM65C
39	0,022248	0,627404	P01024	Complement C3	C3
40	0,0360954	0,632128	P01859	Immunoglobulin heavy constant gamma 2	IGHG2
41	0,0418831	0,645734	Q9Y6A5	Transforming acidic coiled-coil-containing protein	TACC3
42	0,0354627	0,656718	P00747	Plasminogen	PLG
43	0,00516652	0,68089	P53680	AP-2 complex subunit sigma	AP2S1
44	0,029983	0,701432	Q9Y6W5	Actin-binding protein WASF2	WASF2
45	0,0259263	0,725609	Q9UHD8	Septin-9	
46	0,00161477	0,830131	Q9Y2A7	Nck-associated protein 1	NCKAP1
47	0,0079465	0,844176	P43250	G protein-coupled receptor kinase 6	GRK6

9. Appendix

48	0,0160467	0,874072	Q9NW15	Anoctamin-10	ANO10
49	0,0417556	0,915885	P21266	Glutathione S-transferase Mu 3	GSTM3
50	0,023044	0,940198	P00751	Complement factor B	CFB
51	0,0332117	0,943385	Q13162	Peroxiredoxin-4	PRDX4
52	0,0409319	0,95885	Q14554	Protein disulfide-isomerase A5	PDIA5
53	0,0154566	1,05244	P0DOX8	Immunoglobulin lambda-1 light chain	
54	0,0300519	1,05583	P0C0L4	Complement C4-A	C4A
55	0,0184754	1,11769	P01860	Immunoglobulin heavy constant gamma 3	IGHG3
56	0,0481125	1,23184	P0C7P3	Protein SLFN14	SLFN14
57	0,0392626	1,37655	P16333	Cytoplasmic protein NCK1	NCK1
58	0,0322541	1,37827	O14817	Tetraspanin-4	TSPAN4
59	0,0187073	1,38097	P00738	Haptoglobin	HP
60	0,00750608	1,40501	O60493	Sorting nexin-3	SNX3
61	0,00530976	1,48733	Q6P1M0	Long-chain fatty acid transport protein 4	SLC27A4
62	0,0494225	1,56782	Q99829	Copine-1	CPNE1
63	0,00333819	2,00259	O75150	E3 ubiquitin-protein ligase BRE1B	RNF40
64	0,0353809	2,23413	P09525	Annexin A4	ANXA4
65	0,0441062	2,74009	P20645	Cation-dependent mannose-6-phosphate receptor	M6PR
66	0,00537941	2,91775	Q13724	Mannosyl-oligosaccharide glucosidase	MOGS
67	0,00556104	3,24464	Q9BVK6	Transmembrane emp24 domain-containing protein	TMED9
68	0,00729369	3,55963	Q969V3	Nicalin	NCLN

10. Acknowledgment

I want to say thank you to everyone who helped me complete this thesis successfully. Firstly, I would like to give my thanks and highest respect to Prof. Dr. Hartmut Schlüter for affording me the opportunity to complete my Ph.D. thesis in his lab, with his direct supervision and support during my work.

Furthermore, I would like to acknowledge my co-supervisor, Dr. Hannah Voß, who has a shining example of a knowledgeable scientist. I am truly thankful for her guidance in both lab work and writing. Additionally, I would like to thank my previous co-supervisor, Dr. Giordano Pula, for his help and initial supervision.

I also extend my gratitude to the members of the Institute for Clinical Chemistry and Laboratory Medicine at UKE for sharing their scientific knowledge and creating a friendly working environment. A special thanks to Dr. Nina Wolska for guiding me through essential experimental techniques during my initial lab period.

I would like to express my appreciation to all of Prof. Schlüter's lab members for their friendly support. Dr. Maria Riedner, Manuela Moritz, Bente Siebels, Bojia Peng, and Thomas Mair, your guidance has been invaluable.

Moreover, I extend my sincere thanks to Dr. Pia Roser and Dr. Salma Wollin for generously providing the clinical samples essential to my research.

Last but not least, I would like to thank my parents and my brother, Koosha, for always supporting me in both my personal life and studies.

11. Declaration

Declaration on oath

I hereby declare that this thesis has been generated by me from my own research and experiments. I have not used other than the acknowledged resources and aids. The submitted written version corresponds to the version on the electronic storage medium. Furthermore, I assure that this work has not been submitted elsewhere as a thesis.

Eidesstattliche Versicherung

Hiermit erkläre ich, dass ich diese Arbeit eigenständig anhand meiner eigenen Forschung und Experimente verfasst habe. Ich habe keine anderen als die anerkannten Quellen und Hilfsmittel verwendet. Die eingereichte schriftliche Version entspricht der Version auf dem elektronischen Speichermedium. Weiterhin versichere ich, dass diese Arbeit noch nicht an anderer Stelle als Abschlussarbeit vorgelegen hat.

Hamburg, 24.11.2023	Rosa Haghiri Limoudehi
Place and Date	Signature